REPORT NO. DOT-TSC-OST-76-57

REVIEW OF DIESEL COMBUSTION
MODELS FOR NOx AND SMOKE EMISSIONS

David Anderton

University of Southampton
Institute of Sound and Vibration Research
Southampton England

OCTOBER 1977

FINAL REPORT

Prepared for

U.S. DEPARTMENT OF TRANSPORTATION
OFFICE OF THE SECRETARY

Office of the Assistant Secretary for Systems
Development and Technology
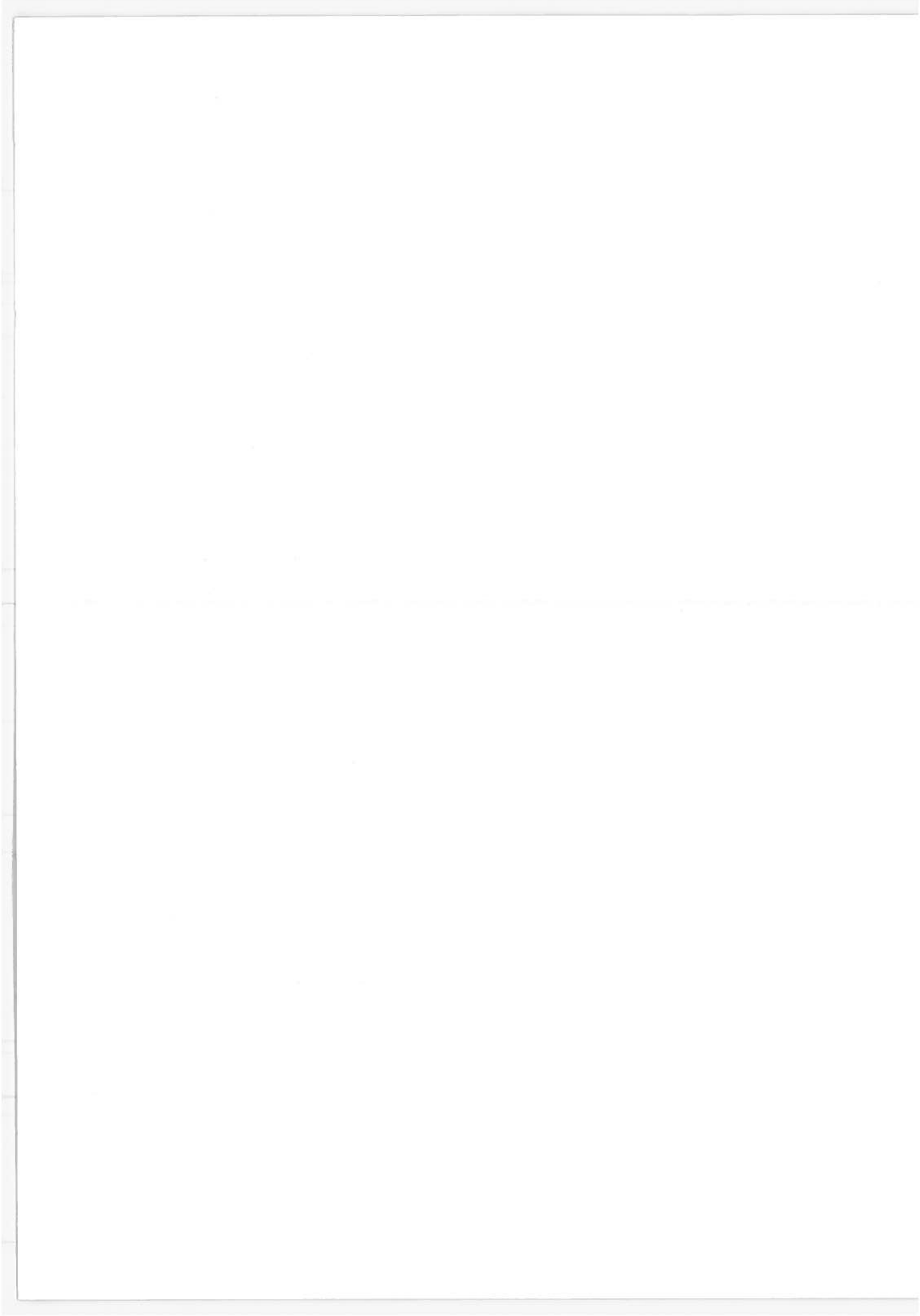Office of Noise Abatement
Washington DC 20590

1. Report No.	2. Government Accession No.	3. Recipient's Catalog No.
DOT-TSC-OST-76-57		

4. Title and Subtitle	5. Report Date
REVIEW OF DIESEL COMBUSTION MODELS FOR NOx AND SMOKE EMISSIONS	October 1977
	6. Performing Organization Code

7. Author's)	8. Performing Organization Report No.
David Anderton	DOT-TSC-OST-76-57

9. Performing Organization Name and Address	10. Work Unit No. (TRAIS)
University of Southampton* Institute of Sound and Vibration Research Southampton England	OS707/R8509
	11. Contract or Grant No.
	DOT-TSC-1101

12. Sponsoring Agency Name and Address	13. Type of Report and Period Covered
U.S. Department of Transportation Office of the Secretary Office of the Assistant Secretary for Systems Development and Technology Office of Noise Abatement Washington DC 20590	FINAL REPORT June-November 1976
	14. Sponsoring Agency Code

15. Supplementary Notes
* Under contract to: U.S. Department of Transporation Transportation Systems Center Kendall Square Cambridge MA 02142

16. Abstract

   A comprehensive reveiw of diesel emissions models is presented together with assessments of the pertinenet fundamental NOx and soot kinetics. The results of diesel emissions experiments carried out at Southampton are also presented and correlations are suggested.

   The review suggest that available emissions models do not incorporate a sufficiently detailed description of the fundamental mixing and chemical kinetic processes occuring in the diesel. They cannot therefore be used predictively. Suggestions are made for model development, fundamental data acquisition and the use of incylinder experimental techniques. The latter are required to obtain data on the flowfield and mixing processes occurring in the diesel combustion chamber.

17. Key Words	18. Distribution Statement
Diesel emissions, smoke emissions, NOx,	DOCUMENT IS AVAILABLE TO THE U.S. PUBLIC THROUGH THE NATIONAL TECHNICAL INFORMATION SERVICE, SPRINGFIELD, VIRGINIA 22161

19. Security Classif. (of this report)	20. Security Classif. (of this page)	21. No. of Pages	22. Price
Unclassified	Unclassified	166	

Form DOT F 1700.7 (8-72)   Reproduction of completed page authorized

PREFACE

This report was performed under contract to the U.S.
Department of Transportation, Transportation Systems Center,
Cambridge MA, by the Institute of Sound and Vibration Research of
the University of Southampton at Southampton, England. It is
part of an outgoing project on diesel engine noise reduction
sponsored by the U.S. Department of Transportation, Office of the
Secretary, Office of Noise Abatement. The subject covered is
NOx and smoke emissions in diesel combustion engines and their
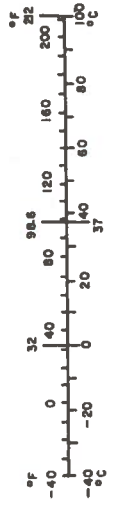relationship to combustion noise.

METRIC CONVERSION FACTORS

Approximate Conversions to Metric Measures

Symbol	When You Know	Multiply by	To Find	Symbol
		LENGTH		
in	inches	2.5	centimeters	cm
ft	feet	30	centimeters	cm
yd	yards	0.9	meters	m
mi	miles	1.6	kilometers	km
		AREA		
in²	square inches	6.5	square centimeters	cm²
ft²	square feet	0.09	square meters	m²
yd²	square yards	0.8	square meters	m²
mi²	square miles	2.6	square kilometers	km²
	acres	0.4	hectares	ha
		MASS (weight)		
oz	ounces	28	grams	g
lb	pounds	0.45	kilograms	kg
	short tons (2000 lb)	0.9	tonnes	t
		VOLUME		
tsp	teaspoons	5	milliliters	ml
Tbsp	tablespoons	15	milliliters	ml
fl oz	fluid ounces	30	milliliters	ml
c	cups	0.24	liters	l
pt	pints	0.47	liters	l
qt	quarts	0.95	liters	l
gal	gallons	3.8	liters	l
ft³	cubic feet	0.03	cubic meters	m³
yd³	cubic yards	0.76	cubic meters	m³
		TEMPERATURE (exact)		
°F	Fahrenheit temperature	5/9 (after subtracting 32)	Celsius temperature	°C
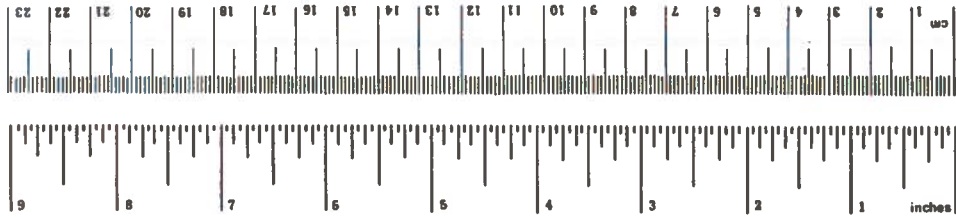
Approximate Conversions from Metric Measures

Symbol	When You Know	Multiply by	To Find	Symbol
		LENGTH		
mm	millimeters	0.04	inches	in
cm	centimeters	0.4	inches	in
m	meters	3.3	feet	ft
m	meters	1.1	yards	yd
km	kilometers	0.6	miles	mi
		AREA		
cm²	square centimeters	0.16	square inches	in²
m²	square meters	1.2	square yards	yd²
km²	square kilometers	0.4	square miles	mi²
ha	hectares (10,000 m²)	2.5	acres	
		MASS (weight)		
g	grams	0.035	ounces	oz
kg	kilograms	2.2	pounds	lb
t	tonnes (1000 kg)	1.1	short tons	
		VOLUME		
ml	milliliters	0.03	fluid ounces	fl oz
l	liters	2.1	pints	pt
l	liters	1.06	quarts	qt
l	liters	0.26	gallons	gal
m³	cubic meters	35	cubic feet	ft³
m³	cubic meters	1.3	cubic yards	yd³
		TEMPERATURE (exact)		
°C	Celsius temperature	9/5 (then add 32)	Fahrenheit temperature	°F

iv

TABLE OF CONTENTS

TABLE OF CONTENTS (CONTINUED)

TABLE OF CONTENTS (CONTINUED)

LIST OF ILLUSTRATIONS

LIST OF ILLUSTRATIONS (CONTINUED)

LIST OF ILLUSTRATIONS (CONTINUED)

LIST OF TABLES

1. INTRODUCTION

1.1. Objectives

The objectives of this report are –

(1) To provide a critical review of the current state of knowledge regarding NO_x (nitrogen oxides) formation relevant to diesel engine combustion and to present some measurements of NO in diesel engine exhaust obtained at Southampton from (mainly) production engines.

(2) To provide a critical review of the current state of knowledge regarding smoke (soot) formation and oxidation relevant to diesel combustion and to present some exhaust smoke measurements obtained at Southampton from a variety of engines.

(3) To provide a critical review of the current state-of-the-art of diesel combustion modelling related to the prediction of the effect of design and operating variables on exhaust smoke and NO_x.

The most pertinent recent reviews which overlap these objectives are the one by Wilson et al (1.1)*, now nearly three years old, and the more comprehensive but less detailed and less critical survey by Henein (1.2). The present report does not consider other undesirable exhaust emissions of the diesel – unburned hydrocarbons, carbon monoxide, aldehydes and other partially oxidised hydrocarbons (including odours) – for two reasons : primarily because no diesel model has yet considered these species in sufficient detail for comparisons between model prediction and observations to be meaningful, and secondarily because Henein's very recent review (1.2) presents all the available experimental evidence of the effect of design and operating variables on these emissions. Omission of these pollutants permits a more detailed examination of the NO_x and smoke problems.

1.2. Organisation and Content of the Report

Section 1.3 provides a summary of the necessary legislative background.

Section 2 reviews the status of our understanding of NO_x kinetics in combustion. Whilst it may be true that the Zeldovich or, better, the expanded Zeldovich mechanism adequately represents the major NO_x formation process in current diesel engines for a wide range of operating conditions, it may no longer be true once NO_x emissions are reduced (or attempts are made to reduce it) significantly below current levels. Then two or three additional mechanisms for the formation of NO_x in combustion systems come into play, resulting in a total of four basic kinetic routes which must be incorporated in any quantitative model of NO_x formation :

(1) Thermal reactions of oxygen and nitrogen – the Zeldovich and expanded Zeldovich mechanisms.

(2) Combustion reactions which produce species in non-equilibrium (excess) concentrations that participate in the thermal nitric oxide mechanism (e.g. the O-atom).

---

* Numbers in parenthesis indicate References, which are listed in Section 7.

(3) Reactions of the fuel and/or fuel decomposition or partial oxidation fragments with nitrogen.

(4) Reactions of fuel-bound nitrogen, or nitrogen containing fuel additives.

To date diesel combustion modellers have incorporated only item (1) of this list. It would be surprising if, in a situation in which diffusion controlled combustion (especially droplet and spray combustion) plays such an important role, routes (2) and/or (3) of the list can be ignored for much longer. Thus Section 2 reviews all four mechanisms and also considers factors affecting the NO/NO_2 ratio.

In addition combustion in all lightweight diesels occurs under highly turbulent conditions. This adds yet another dimension to the problem, that of turbulence combustion interactions. These phenomena are currently the subject of active research effort worldwide and the first indications of their potential importance to the concentrations of the trace species are becoming available. Such effects may certainly be expected to affect the NO_x production in a diesel engine, although it is probably too early for reliable quantitative prediction. The topic is briefly reviewed.

Exhaust NO_x measurements from a range of (mainly) production engines obtained at Southampton are correlated against brake mean effective pressure (BMEP), air-fuel ratio and chamber surface-to-volume ratio. This would appear to be the first attempt to correlate emission data against the latter chamber design feature. An example of NO measurements obtained by in-cylinder sampling is also presented.

Section 3 provides a review of the diesel smoke problem to parallel Section 2. Black smoke (soot) only is considered. Again emphasis is placed on fundamentals, while the one attempt (1.3)* to model diesel smoke to date is considered in some detail.

The possibility that turbulence effects couple with the soot kinetics is just beginning to be considered by some workers (see, for example, Becker and Yamazaki, and Magnussen and Hjertager (1.4) but discussion of this topic is held over to Section 5.

Results of smoke measurements made at Southampton are also presented.

Section 4 presents a critical review of attempts to model diesel combustion and emissions. Six models are considered in some detail and their strengths and weaknesses are indicated. Appendix II summarises other modelling attempts.

* Recently Hiroyasu and Kadota (1.5) have incorporated a similar description in their diesel combustion model.

A general discussion follows in Section 5. The limitations of our understanding of the fundamentals of NO_x and smoke formation are considered in relation to present and future diesel combustion modelling efforts. This leads naturally to recommendations for further work.

The conclusions of the study are listed in Section 6.

1.3. Legislative Background

The introduction of standards limiting the emission of gaseous pollutants and smoke from the exhaust of a compression ignition engine have been due to separate needs in Europe, the U.S.A. and Japan. Standards limiting smoke have been in existence in Europe for nearly ten years whereas they have only recently been introduced in the U.S.A. Legal requirements to limit gaseous pollutants from diesel exhaust were first introduced in the U.S.A. and are expected to become progressively more stringent. Similar standards have been recently announced for Japan whereas such standards do not yet exist in Europe.

1.3.1. <u>Gaseous pollutants legislation</u>: Gaseous emissions limits for diesel engine vehicles were introduced in U.S.A. in 1973 as a follow-on from the spark ignition legislation of the late 1960's. Subsequently proposed more stringent requirements have been modified and their application delayed. The limits, at present and proposed, restricting CO, NO_x and HC are shown in Table 1.1 Ref. (1.6). Diesel emission standards have been introduced in Japan only recently. These are shown in Table 1.2. Gaseous emission standards for diesel engines have yet to be introduced in Europe and U.K.

The methods of assessment of emissions from heavy duty engines (6000 lbs gross vehicle weight and above) in U.S.A. and Japan are similar, although the details and limits are different. A 13-mode E M A (Engine Manufacturers Association) cycle (Figure 1.1) in U.S.A. and 6-mode cycle in Japan is used for steady state operation of the engine at various speeds and loads. The total pollutants emitted are summed, taking into account load factors and driving patterns. No account is taken of the pollutants produced during the transient parts of the engine operation. The pollutants are expressed as g/bhp-h of CO, NO_2 and HC.

For light duty diesel engines (<6000 lbs G. V.W), the method of test is different. The constant volume sampling (C V S) method used is a 'dynamic' cycle which has a pattern of engine operating conditions and weighting factors different from the steady state cycle. In general, the engine test cycle relationship between engine speed and road rated speed is restricted to 70-80% of the engine rated speed. The pollutants are expressed as g/mile.

1.3.2. <u>Smoke legislation</u>: The criteria for limiting smoke from new engines and their method of assessment have been independently developed in Western Europe and U.S.A.

3
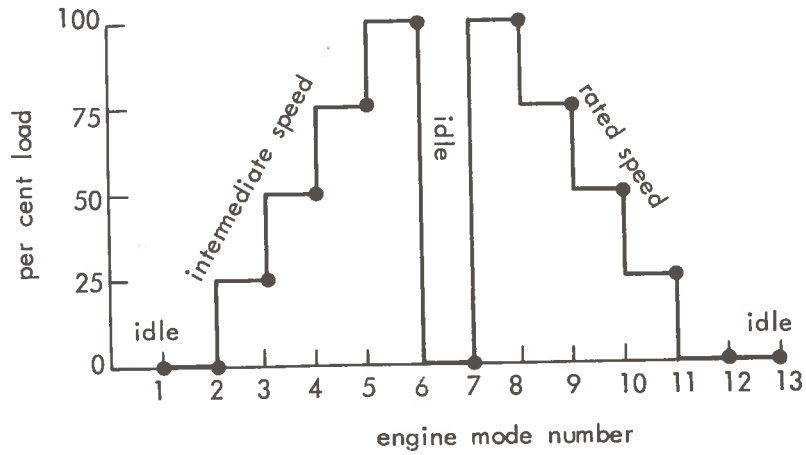
FIGURE 1.1. 13-MODE E.M.A. (ENGINE MANUFACTURERS' ASSOCIATION) DIESEL CYCLE FOR USA.
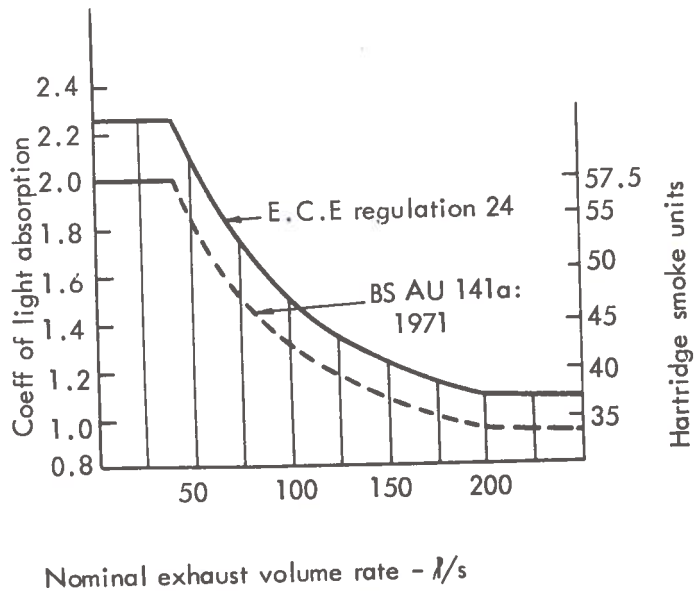
FIGURE 1.2. EXHAUST GAS SMOKE OPACITY REQUIREMENTS FOR EUROPE AND UK.

TABLE 1.1.   PRESENT AND PROPOSED EMISSIONS STANDARDS - DIESEL - U.S.A.

COUNTRY/STATE	CLASS	EFFECTIVE DATE	STATUS	EMISSIONS				UNITS	SMOKE % OPACITY		
				HC	NO_x	$HC+NO_x$	CO		ACCN	LUG	PEAK
U.S. FEDERAL	L.D. VEHICLE (Passenger car or derivative ≤ 12 people)	1976	ENACTED	1.5	3.1	--	15	GMS/MILE	--	--	--
		1977	ENACTED	1.5	2.0	--	15		--	--	--
U.S. FEDERAL	L.D. TRUCK (<6000 lbs G.V.W.)	1976	ENACTED	2.0	3.1	--	20		--	--	--
		1978	ENACTED	1.7	2.3	--	18		--	--	--
U.S. FEDERAL	H.D. VEHICLE ENGINES (>6000 lbs G.V.W.)	1976	ENACTED	--	--	16	40	GMS/BHP HR	20	15	50
		1979	PROPOSED	1.5	--	10	25		20	15	35
U.S. CALIFORNIA	L.D. VEHICLE & TRUCK Passenger car and trucks (≤6000 lbs G.V.W.)	1976	ENACTED	0.9	2.0	--	9	GMS/MILE	--	--	--
U.S. CALIFORNIA	MEDIUM DUTY TRUCK (6001-8500 lbs G.V.W.)	1978	PROPOSED	0.9	2.3	--	17	GMS/MILE	--	--	--
U.S. CALIFORNIA	HEAVY DUTY ENGINE (>6000 lbs G.V.W.)	1976	ENACTED	--	--	10	25	GMS/BHP HR	--	--	--
		1977	ENACTED	0.0	7.5	--)	25		--	--	--
		1979	PROPOSED	1.0	4.0	--	25		--	--	--

TABLE 1.2   DIESEL EMISSIONS STANDARDS IN JAPAN (Ref. 1.6)

CLASS	EFFECTIVE DATE	STATUS	Smoke[a]	$\frac{CO^b}{ppm}$	$\frac{HC^b}{ppm}$	$\frac{NO_x^b}{ppm}$
HEAVY DUTY and LIGHT DUTY DIESELS	Smoke 1974 Gaseous Emissions 1975	ENACTED	50% Equivalent 5 Bosch Units	980 (790)	670 (510)	1000 (770) = D.I.Engines 590 (450) = I.D.I. "

( ) = Average Values

a = Free acceleration test

b = Hot cycle of six modes lasting 3 minutes as shown below

Running Mode	Engine rev/min	Load Factor	Weighting Factor
1	idling		0.355
2	40% rated speed	100%	0.071
3	40% " "	25%	0.059
4	60% " "	100%	0.107
5	60% " "	25%	0.122
6	80% " "	75%	0.286

(a) European Position

Until recently, various European countries had separate requirements for smoke emission in the exhaust. Their differing standards and methods of assessment are now being rationalised. The present levels required by the E.C.E. Regulation 24 (1.7) are shown in Figure 1.2. The limit values of exhaust gas opacity applicable in the U.K. are shown in Table 1.3. These are based on steady state full load smoke limits measured on an engine test bed over a usable speed range (45-100 % of the rated engine speed). The method of test is by sampling a part of the total exhaust which is analysed by an optical obscuration meter. The legal limits are quoted in terms of the coefficient of light absorption. The Hartridge smoke meters used in the U.K. can be easily recalibrated to correspond to the coefficient of light absorption from the Beer-Lambert Law.

(b) United States Position

The federal smoke control standards have been introduced only recently. A direct visibility measurement with a simulated load operation has been chosen for monitoring purposes. Full flow of the exhaust is tested for smoke and the test cycle simulates idling condition, full load acceleration and 'lugging' mode on an engine dynamometer. The rates of acceleration and deceleration are closely defined, as is the length and diameter of the exhaust pipe. The diameter of the exhaust pipe is related to engine power in steps (i.e. 2" diameter up to 100 b.h.p., 5" diameter above 300 b.h.p).

For the same specified obscuration, the smoke density is reduced on a logarithmic scale as the engine size increases. This is similar in effect to E.C.E. and B.S.I. regulations. The effect of the exhaust pipe on the correlation of full flow measurements (U.S.P.H.S.) and sampling flow measurements (Hartridge smoke meter) is shown in Figure 1.3 (Ref. 1.9). Only two smoke limits are specified, i.e. 20% obscuration during acceleration and 15% during lugging mode. These limits are less stringent than those of B.S.I. and E.C.E. regulations as can be seen from Figure 1.4 (Ref. 1.8).

TABLE 1.3   SMOKE LIMITS FOR AUTOMOTIVE DIESELS – UNITED KINGDOM

Limit Values of Exhaust Gas Opacity Applicable in the Engine Tests at Steady Speed

G Nominal flow	k Absorption coefficient	G Nominal flow	k Absorption coefficient
l/s	m^{-1}	l/s	m^{-1}
⩽42	2.00	120	1.20
45	1.91	125	1.17
50	1.82	130	1.15
55	1.75	135	1.15
60	1.68	140	1.11
65	1.61	145	1.09
70	1.56	150	1.07
75	1.50	155	1.05
80	1.46	160	1.04
85	1.41	165	1.02
90	1.38	170	1.01
95	1.34	175	1.00
100	1.31	180	0.99
105	1.27	185	0.97
110	1.25	190	0.96
115	1.22	195	0.95
		⩾200	0.93
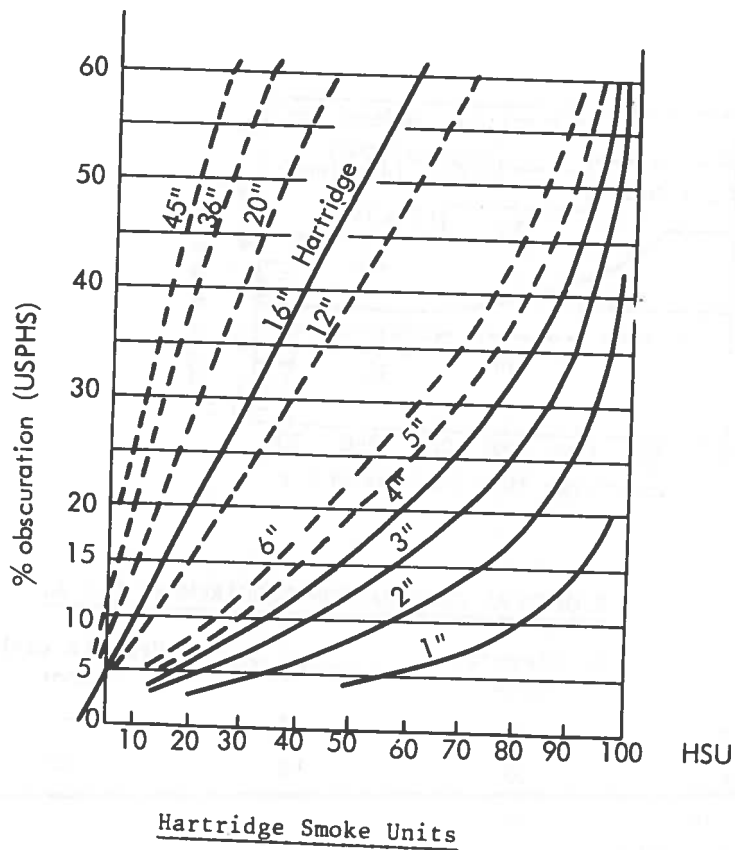
FIGURE 1.3.   CORRELATION ON HARTRIDGE SMOKE UNITS (HSU) AND UNITED STATES PUBLIC HEALTH SERVICES (US PHS) SMOKE METER.   EXHAUST PIPE DIAMETER EFFECT.

Figure plot axes: Hatridge smoke units (left, 0–90), Bosch smoke units (right, 0.5–6), Normal gas flow l/s (= rated h.p.) (bottom, 0–300).

Legend within plot:
- U.S.A. federal limits (lugging mode) — dashed
- BS.AU. 141a limits — solid
- 2in stack, 3in, 4in, 5in
- 15% 1974
- 5% in future
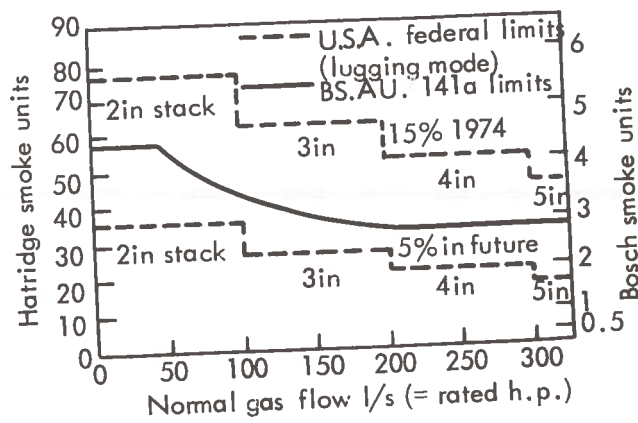
% OPTICAL OBSCURATION REQUIREMENT U.S.A.

	Acceleration Mode	Lugging Mode	Peak in either Mode
1973	40	20	--
1974	20	15	50
1979 (proposed)	20	15	35

FIGURE 1.4. COMPARISON OF BRITISH STANDARD AND US FEDERAL REQUIREMENTS FOR SMOKE LIMITS.

2.   <u>NO$_x$ IN DIESELS</u>

2.1. <u>Review of Chemical Kinetics of NO$_x$ Production in Combustion.</u>

Nitric oxide (NO) is the predominant oxide of nitrogen emitted by combustion devices. In addition, under some operating conditions, significant amounts of nitrogen dioxide (NO$_2$) may also be emitted. This review will therefore be concerned with the reaction mechanisms for the formation and destruction of both NO and NO$_2$ in the context of diesel combustion. The formation and destruction of NO and NO$_2$ in combustion generally has recently been well reviewed by Bowman (2.1).

2.1.1 <u>Model A for NO Production and Removal</u>. A principal source of NO in the combustion of conventional fuels is the oxidation of atmospheric nitrogen (N$_2$) by the hot combustion products. This process has been studied extensively (2.1 and references therein). For lean and near-stoichiometric fuel-air mixtures the principal reactions governing the formation of NO from N$_2$ are

$$O + N_2 \;\rightleftharpoons\; NO + N \qquad\qquad (2.1)$$

$$N + O_2 \;\rightleftharpoons\; NO + O \qquad\qquad (2.2)$$

as originally proposed by Zeldovich (2.2). Reactions (2.1) and (2.2) are commonly referred to as the Zeldovich mechanism. Rate coefficient expressions for these reactions have been proposed by Baulch et al (2.3) as a result of a critical review of the published data.

Under some conditions the reaction

$$N + OH \;\rightleftharpoons\; NO + H \qquad\qquad (2.3)$$

may contribute to the NO production (2.4); this is especially likely in near stoichiometric and fuel-rich conditions. Reactions (2.1) to (2.3) are sometimes referred to as the extended Zeldovich mechanism. Bowman (2.1) has recently reviewed the published rate data for the extended Zeldovich mechanism and Table 2.1 is taken from his paper.

With the addition of a reaction relating H and OH

$$O + OH \;\rightleftharpoons\; O_2 + H \qquad\qquad (2.4)$$

which is assumed to be equilibrated, and applying a steady state approximation for the N atom concentration, the local NO formation rates may be written

$$\frac{d\,[NO]}{dt} \;=\; 2\,k_1\,[O]\,[N_2]\left(\frac{1 - [NO]^2/K\,[O_2]\,[N_2]}{1 + K_1\,[NO]/k_2\,[O_2] + k_3\,[OH]}\right) \qquad (2.5)$$

where K is the equilibrium constant for the process N$_2$ + O$_2$ $\rightleftharpoons$ 2 NO.

TABLE 2.1. EXTENDED ZELDOVICH NO FORMATION MECHANISM (FROM BOWMAN (2.1))

Reaction	Rate constant (cm³/mole·sec)	Temperature range (K)	Uncertainty	Ref.
(1) $O+N_2 \rightarrow NO+N$	$7.6 \times 10^{13} \exp[-38,000/T]$	2000–5000	2	2.3
(−1) $N+NO \rightarrow N_2+O$	1.6×10^{13}	300–5000	±20% at 300 K, 2 2000–5000 K	2.3
(2) $N+O_2 \rightarrow NO+O$	$6.4 \times 10^9 T \exp[-3150/T]$	300–3000	±30% 300–1500 K, 2 at 3000 K	2.3
(−2) $O+NO \rightarrow O_2+N$	$1.5 \times 10^9 T \exp[-19,500/T]$	1000–3000	±30% at 1000 K, 2 at 3000 K	2.3
(3) $N+OH \rightarrow NO+H$	1.0×10^{14}	300–2500	±80%	2.1
(−3) $H+NO \rightarrow OH+N$	$2.0 \times 10^{14} \exp[-23,650/T]$	2200–4500	2	2.28, 2.29, 2.74

12

With known values for the rate coefficients (Table 2.1), calculation of the local NO formation rate requires the local temperature and local concentrations ([ ]) of O_2, N_2, O and OH as input.

An alternative form of equation (2.5) is sometimes employed in engine calculations (2.4), and is

$$\frac{d(NO)}{dt} = \frac{2M_{NO}}{\rho} (1 - \alpha^2) \frac{R_1}{1 + \alpha K} \tag{2.5a}$$

where $\alpha = [NO] / [NO]_e$,

$$K = \frac{R_1}{R_2 + R_3} ,$$

$$R_1 = k_1 [NO]_e [N]_e,$$

$$R_2 = k_2 [O_2]_e [N]_e,$$

$$R_3 = k_3 [OH]_e [N]_e,$$

$$(\ ) = \text{mass fraction},$$

$$M_{NO} = \text{molecular weight of NO}$$

$$\rho = \text{local density}$$

The formation rate of NO can be obtained in terms of $[NO]$, T, p and equivalence ratio, plus known rates and equilibrium concentrations, $[\ ]_e$, involving N, O_2, OH and NO.

A frequently used and often adequate approximation is to consider NO production to be slow compared to the main bimolecular flame reactions. In this approximation the NO production is essentially decoupled from the principal combustion reactions, and the latter are assumed to be equilibrated in the post-combustion zone. The NO formation rate is then calculated using equilibrium values of the temperature and of the O_2, N_2, O and OH concentrations.

Most of the recent experimental studies of laboratory flames (2.5 - 2.7) support the foregoing description of NO formation in the post combustion zone. Of particular importance is the strong dependence of the formation rate on the temperature; Sarofim and Flagan (2.8) have indicated that, typically, the rate doubles for every 40 K increase in temperature in the neighbourhood of 2000 K.

Occasionally three further reactions involving N_2O are added to the above 3-reaction scheme. Some workers (2.9) have postulated additional NO production via formation of nitrous oxide (N_2O). The N_2O then reacts with O to give NO via

$$N_2O + O \rightleftharpoons 2 NO \tag{2.5b}$$

with possible alternative routes

$$N_2O + O \quad \rightleftharpoons \quad N_2 + O_2$$

and

$$N_2O + H \quad \rightleftharpoons \quad N_2 + OH$$

To date there has been little evidence that this additional mechanism is of importance under spark ignition engine conditions (2.4) and it has been shown not to apply in high temperature flames (2.10). It is, however, possible it could play a small role in lower temperature fuel-lean combustion, as shown by some recent calculations (2.11).

2.1.2. <u>Effects of chemical non-equilibrium in combustion on NO production and removal</u>:   Following Fenimore's work (2.6) drawing attention to an additional source of NO formation in the flame zone, a number of laboratory studies have explored and confirmed the effect (2.12 - 2.17). The enhanced NO formation rate in the flame zone, frequently referred to as 'prompt' NO has been shown to be attributable to a number of effects. In the combustion zone NO formation rates significantly larger than would be predicted using reactions (2.1) - (2.3), have been observed under some conditions. Of particular significance is the observation, confirmed by a number of workers (2.14 - 2.17), that the amount of NO formed in the combustion zone increases as the equivalence ratio, $\emptyset$, increases. The greatest difference between observation and the prediction of the simplified mechanism occurs in fuel-rich hydrocarbon-air mixtures.

The validity of the simplified mechanism in the combustion zone depends upon proper assignment of values for the concentrations of the radical species. Equilibrium values for these concentrations are certainly incorrect in the combustion zone. Some studies (2.10, 2.14, 2.18 - 2.20) have indicated that the enhanced NO production was attributable to the overshoot of radical concentrations, particularly O and OH, as the combustion in zone and quantitative prediction of the NO production rate was claimed when the observed, nonequilibrium, values of the concentrations were used in conjunction with the simplified mechanism (2.1) - (2.3). In these circumstances, therefore, the proper prediction of the NO production, which is now partly coupled to the combustion reactions, requires simultaneous integration of the NO rate equation with the rate equations for the combustion process. Unfortunately detailed and accurate models of hydrocarbon combustion are unavailable for all but the simplest hydrocarbon (methane). Approximate models have been developed (2.21) for some of the higher hydrocarbons, but almost all are not designed to predict accurately the radical concentrations important in the NO mechanism.

An alternative - and simpler - approach to the prediction of the nonequilibrium radical concentrations in the flame zone, is to employ the partial equilibrium approximation (2.22) for the radical species. The essence of the partial equilibrium approximation is that whilst the concentrations of the individual species are not those found at equilibrium, the ratios of concentrations among the species are those given by the equilibrium expressions at the local temperature and pressure. A number of the differential equations can then be replaced by algebraic equations.

Measurements of the concentration of the appropriate stable species
will then give the concentrations of the required radical species (O and
OH in particular). This approach appears to provide satisfactory
results for lean and slightly rich hydrocarbon - air flames.

Not all observations of NO production in combustion systems appear
to be explained in terms of the Zeldovich (or extended Zeldovich)
mechanism and the appropriate nonequilibrium radical concentrations.

In fuel-rich hydrocarbon combustion there appears to be a greater need
for some additional mechanism to explain the observed NO formation rate in
the flame zone, where the partial equilibrium approach significantly
underestimates the NO production (2.6, 2.15, 2.23). Reactions of the
type

$$CH + N_2 \rightleftharpoons HCN + N \qquad (2.6)$$

$$C + N_2 \rightleftharpoons CN + N \qquad (2.7)$$

followed by

$$HCN, CN \rightarrow NH_3 \qquad (2.31),$$

have been invoked to provide an enhanced N-atom concentration, the N-atoms
subsequently producing NO via reaction (2.3). Support for this mechanism
comes from recent experimental studies (2.16, 2.17), while small traces
of HCN and NH_3 have long been known to occur in hydrocarbon combustion and
engine exhausts. Whether reactions (2.6) and (2.7) constitute the correct
mechanism, or whether the formation of intermediate amine compounds
(NH , NH_2, NH_3) is necessary is beyond the scope of the present discussion
(but see Section 2.1.3). It should be noted, however, that observed O-atom
concentrations can exceed partial equilibrium estimates in fuel-rich hydrocarbon
combustion (2.24), although not sufficiently to explain the observed NO
formation rates.

2.1.3. <u>Additional effects due to fuel-bonded nitrogen</u>: The previous
two sections have been concerned with the fixation of atmospheric nitrogen (N_2)
to form NO. An additional source of NO occurs if the fuel contains bonded
nitrogen (as amines, pyridines etc). All naturally occurring fossil
hydrocarbon fuels contain such compounds, in some cases to more than 1 per cent
by weight. Fortunately, from the transport engine standpoint, such
nitrogenous species are retained and concentrated in the higher boiling
fractions (distillable oils etc). However, nitrogen-containing fuel
additives are sometimes used to increase the cetane number of the fuel (2.25).

No complete mechanistic model is currently available to describe the
oxidation of fuel nitrogen (sometimes called 'organic nitrogen') to form NO.
Both Fenimore (2.26) and de Soete (2.27) have proposed phenomenological
mechanisms in which the fuel-nitrogen, N_f, is first pyrolysed to a (usually)
simpler nitrogen-containing intermediate NI. NI is not normally specified,
but is presumed to be one or more of the species HCN, CN, NH_3, NH_2, NH , N
and/or other small molecular fragments containing N. The intermediate NI
then reacts either with an oxygen-containing species Ox to produce NO or
with NO, another NI species or some other reducing species containing bonded-N,
to give N_2. Schematically these possibilities may be represented as

$$N_f \rightarrow NI \quad \begin{cases} + O_x \rightarrow NO + \dots & (2.8a) \\ + NO(NI) \rightarrow N_2 + \dots & (2.8b) \end{cases}$$
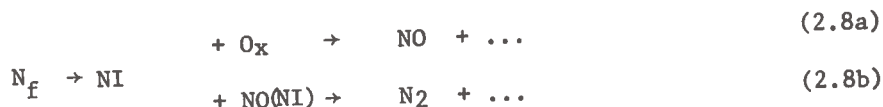
The subject of NO formation from fuel-nitrogen is still an active research topic (2.6, 2.7, 2.28-2.30) and much of the literature is still speculative. It is worth drawing attention, however, to the possibility of fuel-nitrogen species removing NO from combustion systems under certain conditions (reaction 2.8b), (2.31)). Schemes involving only one elementary reaction to control the NO have been proposed (2.32).

Many of the chemical reactions which will be necessary to account for the fomation of NO from fuel-nitrogen will be the same as those postulated in the previous section to account for NO formation from the products of reactions between hydrocarbon fragments and molecular nitrogen.

The reaction mechanism (2.8) has formed the basis of the only semi-quantitative attempts to date to model fuel-nitrogen conversion to NO (2.32). The evidence is that such modelling must involve coupling between the combustion and NO formation processes.

2.1.4. <u>NO$_2$ and the NO/NO$_2$ ratio</u>: The nitric oxide produced in combustion may subsequently react with oxygen-containing species to give the peroxide, NO$_2$. At the flame temperatures occurring in typical combustors equilibrium concentrations of NO$_2$ should be very small. In unpremixed combustors, such as the gas turbine, NO$_2$ measurements indicate that NO$_2$/NO ratios considerably in excess of equilibrium are sometimes observed near the flame zone in the primary region. A similar situation might be postulated for the diesel.

The significance of such NO$_2$ observations is difficult to determine. There are at least three problems associated with any basic understanding. First there is concern regarding the origin of NO$_2$ measured from probe samples; it could have been formed by surface catalysis in the probe as the sample is cooled (2.33). The concentration obtained is known in some cases to depend on the analytical technique employed (e.g. chemiluminescent and non-dispersive ultraviolet methods may disagree (2.34); probes may show NO$_2$ as much as a factor of 2-5 higher than 'in situ' optical techniques applied to aircraft gas turbines - U.S. DOT/NASA Upper Atmosphere Program Bulletin 76-1, p4, January 1976). In addition there is an unfortunate combination of fast reactions and shifting equilibrium associated with the NO/NO$_2$ interconversion. This is partly illustrated in Figure 2.1 which shows how the NO$_2$/(NO+NO$_2$) equilibrium ratio in air varies with temperature and pressure. In unmixed situations, such as occur in diesels and gas turbines, there is evidently scope for local thermochemical conditions near the flame zone to favour NO$_2$ for part of the engine operating envelope and/or part of the engine cycle.

Further complexity must be admitted to the picture when it is noted that large NO$_2$/NO ratios have been observed near the flame zone of premixed near-stoichiometric methane-air flames (2.35, 2.36) and in fuel-lean (CO+H$_2$)-air and ethylene-air flames (2.39) with apparent conversion of the NO$_2$ back to NO further downstream, provided the temperature remains sufficiently high (2.37). A reaction involving the hydroperoxyl radical has been postulated (2.35)

16
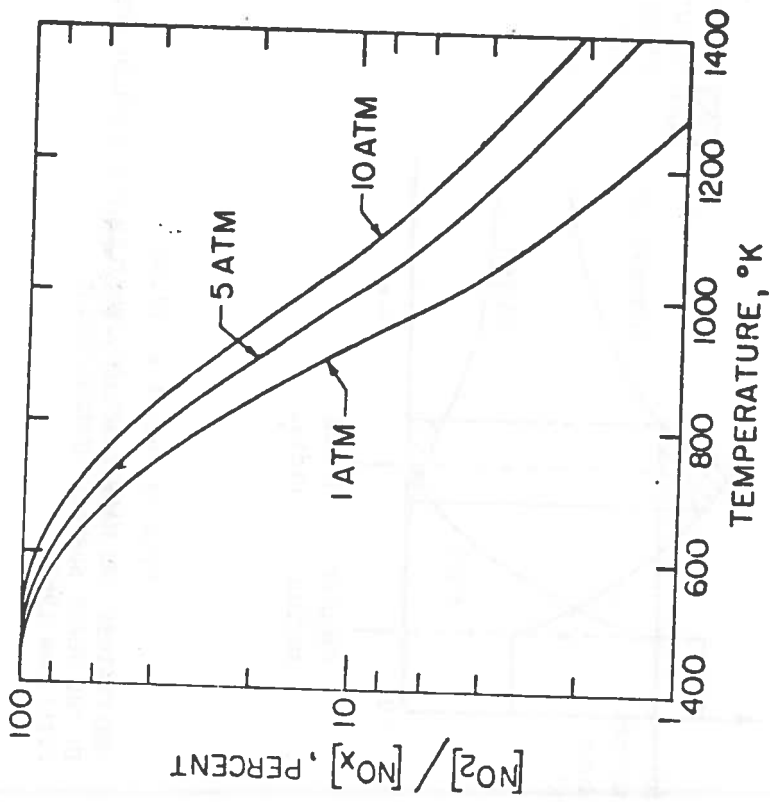
From Laurendeau (2.4)

FIGURE 2.1 EQUILIBRIUM DISTRIBUTION OF NO AND NO_2 IN AIR

NO formation would
occur in this region
where high temperature
and O_2-content overlap.

Temperature

Oxygen

r →

flame
radius

Fuel

droplet
radius

0

Threshold
NO-formation
Temperature
($\sim 2000^\circ$K)
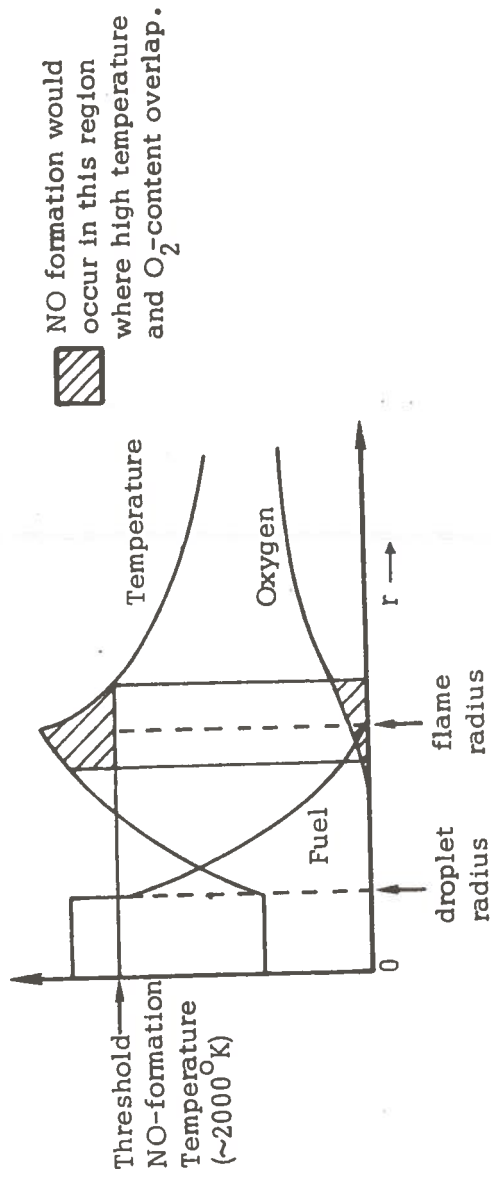
From Wilson et al (2.56)

FIGURE 2.2 TEMPERATURE AND MASS FRACTION PROFILES FOR BURNING FUEL DROPLET
IN THE FLAME SURFACE APPROXIMATION
(Williams 1965)

$$NO + HO_2 \rightarrow NO_2 + OH \tag{2.9}$$

which is known to be fast at room temperature. Such a mechanism for NO_2 production might be dubbed "prompt" NO_2. The NO_2 is then removed via

$$NO_2 + O \rightarrow NO + O_2 \tag{2.10}$$

A mechanism involving reactions (2.9) and (2.10) might account for the observed excess NO_2 from the primary zone of gas turbine combustors and from diesels under low-load conditions, provided that suitable mechanisms exist to 'freeze' the NO_2 thus formed. It has been proposed that such 'freezing' mechanisms can be provided by turbulent mixing (2.38, 2.39), which rapidly cool the NO_2 formed near the combustion zone and thus quenches reaction (2.10).

The fast reactions involving NO_2 and their significance during NO decomposition and NO_2 formation have recently been reviewed by Laurendeau (2.40).

2.2. Fluid Mechanical-Chemical Kinetic Coupling

2.2.1. Effects of composition and temperature fluctuations on NO production:
In the last few years interest in the interactions between turbulence and chemical kinetics, including the effects of the turbulent fluctuations, has been growing rapidly. Some of this interest has been focussed on the prediction of NO in turbulent premixed (2.41) and diffusion (2.42, 2.43) flames. It is not intended, in this report, to enter into a detailed discussion of this subject area which has been reviewed recently by several authors (2.42, 2.44-2.48). A brief summary of some of the more important factors must suffice.

In a turbulent reacting flow it is not sufficient (2.48) to express the mean reaction rate for the ith reaction in terms of mean composition and mean temperature, such as

$$\overline{w}_i = \kappa (\overline{A})(\overline{B}) ,$$

where κ is a reaction parameter containing the temperature and (A) and (B) are mass fractions of the species A and B involved in the reaction. The foregoing widely used approximation can lead to errors of many orders of magnitude in some circumstances. An example of such circumstances is the turbulent diffusion flame. Two important contributions to the overall description of the reaction rate may be identified in a turbulent mixing and reacting flow which are absent in laminar and time-averaged descriptions. They are

(i) the effect of composition fluctuation covariance terms on the reaction rate: such covariance (correlation) terms can be either positive or negative; and

19

(ii)   the effect of temperature fluctuations on the reaction rate through the rate coefficient (i.e. $\bar{k} \neq k(\bar{T})$, because of the exponential temperature dependence of the rate coefficient k). Both (i) and (ii) can contribute, individually or in combination, to the chemical source term. They may thereby modify the rate of NO (or any other species) production or removal.

To date no attempt has been made to incorporate terms modelling these features in descriptions of diesel engine combustion behaviour. The nearest approach is the attempt to predict NO in a stratified charge engine using a two-turbulent-equation model by Bellan and Sirignano (2.49). Whether or not the effects will prove significant in practical engine conditions remains to be seen. In a study of turbulent premixed flames simulating gas turbine combustors, Semerjian and Vranos (2.50) found NO_x formation rates in the reaction zone far exceeded those found in the post flame region. It was also found that the maximum formation rate was much higher in turbulent than in laminar flames. Kent and Bilger have indicated (2.43) that correlations of NO in turbulent jet hydrogen diffusion flames show a rich shift; production of NO is most rapid on the rich side of stoichiometric. In addition they claim that production of NO has a $Re^{-\frac{1}{2}}$ dependence on the turbulence Reynolds number. Such behaviour appears to be attributable to the effects of turbulence on the O-atom super-equilibrium, although a completely satisfactory theory is still awaited. It is projected, however, that these effects should be weaker in hydrocarbon flames.

Another recent development in our ability to describe turbulent flows, with potentially significant implications for engine combustion phenomena, is in our understanding of the coherent character of certain structures within the flow (2.51, 2.52). Unfortunately these new concepts are not yet ready for application to complex problems.

Finally, C.I. engine models are awaiting the incorporation of unsteady hydrodynamic effects. Possible routes include that suggested by Spalding as part of the now defunct Battelle combustion research proposal of two or more years ago.

2.2.2. NO$_x$ production in two-phase combustion: A special case of hydrodynamic-chemical kinetic interaction arises in droplet and spray combustion. The implications for NO_x production are briefly summarised here. The extent to which, in typical diesel combustion, the fuel burns as single droplets with surrounding flames or as an evaporating spray enveloped by a turbulent gaseous diffusion flame is still uncertain (2.53). Both combustion modes are undoubtedly present. Some evidence (2.54) suggests that spray flames at atmospheric pressure are similar to gaseous diffusion flames in all essential respects, including NO_x formation. This conclusion needs confirmation under conditions representativ of highly turbulent, high pressure, in-cylinder combustion.

Droplet combustion has been reviewed by Williams (2.55). Figure 2.2 (2.56) illustrates the gross features of the reaction zone around a single droplet. Unfortunately, even for the simplest situation - the steady

20

vaporisation and combustion of a constant radius, constant temperature droplet with convection effects neglected – agreement between experimental and theoretical results is poor. The lack of agreement is attributable, firstly, to the absence of experiments in which buoyance effects can genuinely be neglected, and secondly, to the inclusion of simplifying assumptions in the theoretical modelling which result in the omission of effects known to influence the combustion properties (2.57). Nitric oxide is known to be formed in laminar diffusion flames around hydrocarbon drops burning in air (2.58). The NO_x index (mass NO_x formed per unit mass of fuel burned) increases with increasing drop size, some workers (2.59) suggesting a square-law dependence. Although there is some disagreement in the literature (2.57, 2.60, 2.61) the latest evidence suggests that prediction of the NO production rate is a factor of two or more less than observation for a single, steady-burning hydrocarbon droplet of 1.2 mm diameter (2.57). The reasons for this disagreement may be several, and may include inaccuracies in the transport and chemical kinetic properties, invalid assumptions regarding equilibrium oxygen concentrations and the use of steady-state N-atom concentration in the prediction of the nitric oxide (2.57). In addition the experimental data shows that fuel pyrolysis and partial oxidation products exist between the evaporating fuel and the flame zone. Such molecular species may be an indication of the ability of the system to form fuel-bonded nitrogen in the rich zone of the flame and so enhance NO production.

It is evident that considerable development of theoretical models of nitric oxide formation in two-phase combustion is still required. Not until such models exist is it worth employing descriptions of nitric oxide production in two-phase combustion as sub-units in the prediction of NO_x emissions from diesel combustion.

2.3. Exhaust NO_x Measurements at Southampton

2.3.1. **Data considered**: Research activities at the I.S.V.R. and the Department of Aeronautics and Astronautics have included studies of diesel combustion and pollutant formation (2.62, 2.66). Results of some of the investigations are presented and discussed.

2.3.2. **Engine test details**: Table 2.2 shows the details of engines tested. With the exception of one engine, all engines were multicylinder power units for automotive application. The exception was a single cylinder engine for stationary use. All the engines were standard production units except engine B which was a commercial engine with an unmatched turbo-charger fitted to increase the engine air intake pressure. This experimental engine produced the same power as the standard commercial engine.

Except for single cylinder engine H, all the engines were tested according to the 13-mode EMA cycle, shown in Figure 1.1. Single cylinder engine H was tested for exhaust emissions at one speed and various loads.

2.3.3. **Results and discussion**: Exhaust nitric oxide from the engines tested is shown in Figures 2.3-2.5. In Figure 2.3, the nitric

21

TABLE 2.2.   DETAILS OF ENGINES TESTED AT SOUTHAMPTON

Engine	Stroke	Induction	No. of Cylinders	Capacity/ Cylinder Litres	Compression Ratio	Power Output BHP.
A	4	N.A.	6	1.36	17:1	145
B	4	Lightly T/C Unmatched	6	1.36	17:1	145
C	4	T/C Matched	6	1.36	15.5:1	195
D	4	N.A.	6	0.90	17:1	92
E	2	T/C Matched	8	1.16	17:1	350
F	4	N.A.	8	0.96	17.5:1	185
G	4	N.A. – I.D.I	4	.56	23:1	60
H	4	N.A.	1	.553	16.5:1	5

TABLE 2.3.   DETAILS OF COMBUSTION SURFACE AND VOLUME FOR THE ENGINES TESTED AT SOUTHAMPTON

ENGINE	COMBUSTION BOWL AREA in^2	AREA OF PISTON TOP LAND – in^2	AREA OF CYLINDER HEAD in^2	TOTAL AREA in^2	COMBUSTION VOLUME in^3	AREA/VOLUM $(in)^{-1}$
A	8.47	10.71	16.950	36.150	5.747	6.29
B	8.49	10.71	16.950	36.150	5.208	6.941
C	8.49	10.71	16.950	36.150	5.208	6.941
D	5.483	9.521	12.863	27.867	3.438	8.106
E	5.594	2.845	14.186	22.626	4.438	5.098
F	4.547	9.349	16.381	30.277	3.561	8.502
G	3.280	9.965	9.809	23.054	1.655	13.930
COMPRESSION RATIO						
14:1*	21.01	15.488	23.78	60.278	11.0	5.48
17:1*	10.48	15.488	23.78	49.748	8.93	5.571

*   Engine data from reference 2.69
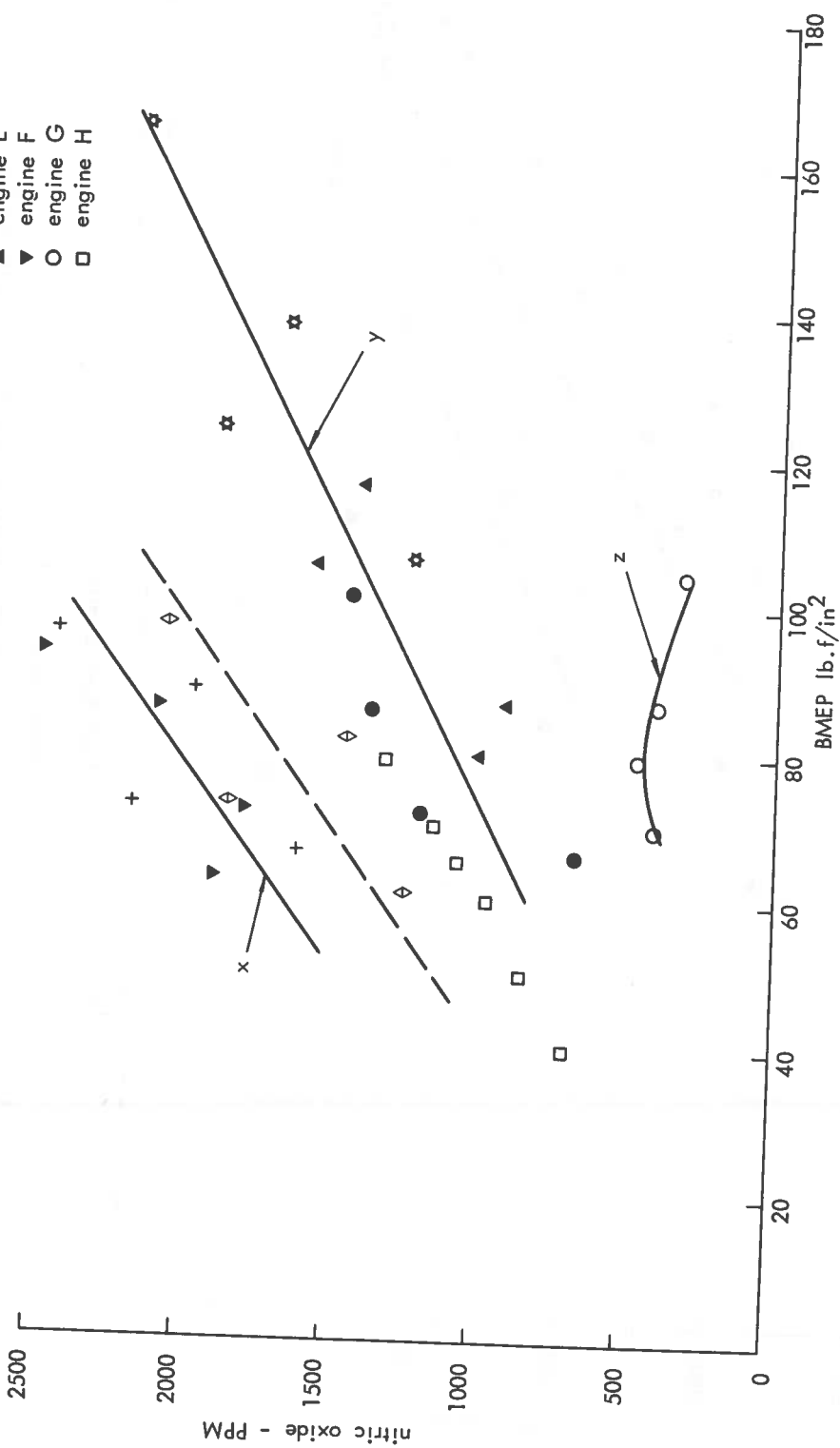
FIGURE 2.3. NITRIC OXIDE (PPM) AGAINST B.M.E.P. (LB_F/IN^2) FOR ENGINES TESTED AT SOUTHAMPTON
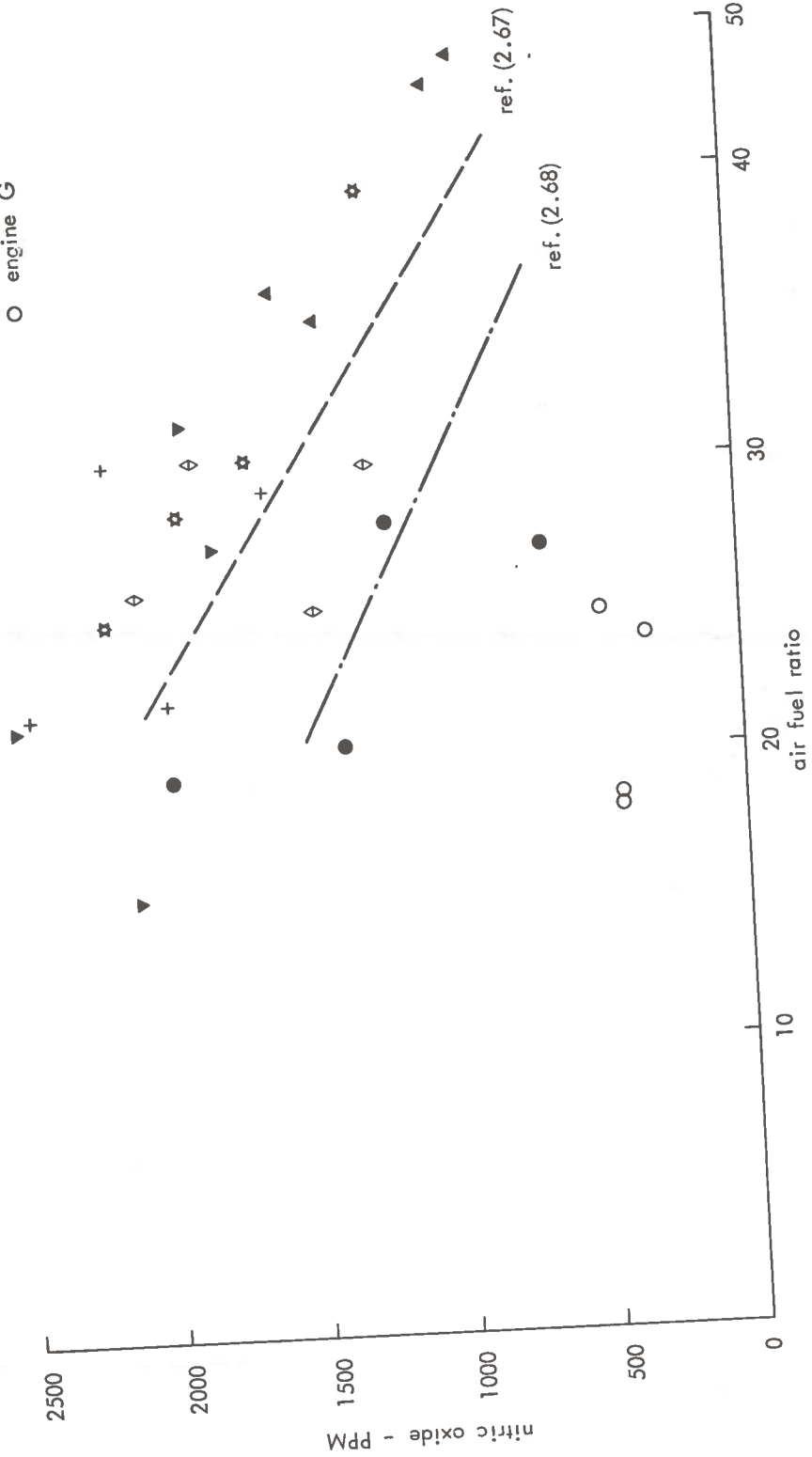
(From Table 2.2).

FIGURE 2.4. NITRIC OXIDE (PPM) AGAINST AIR-FUEL RATIO FOR ENGINES TESTED AT SOUTHAMPTON
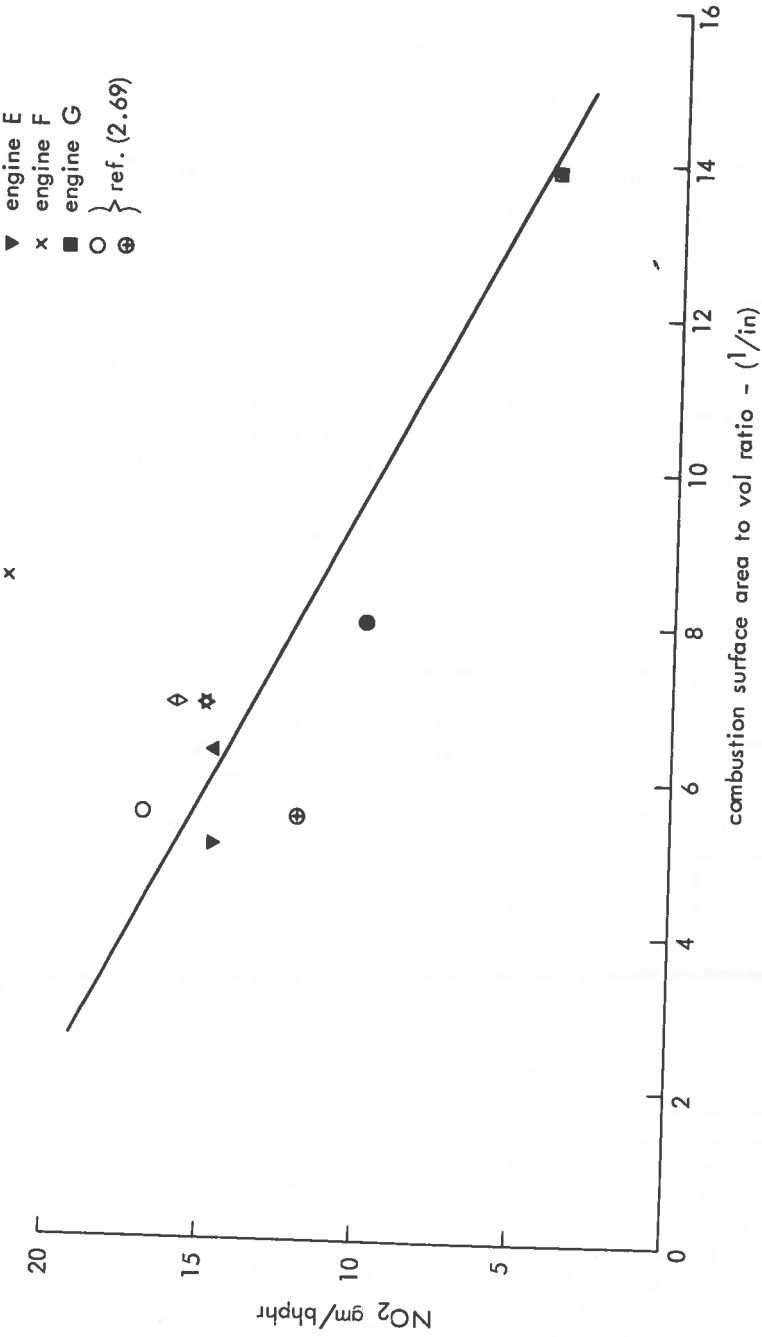
(From Table 2.2).

FIGURE 2.5 NITROGEN DIOXIDE (G/BHP-HR) AGAINST SURFACE-TO-VOLUME RATIO FOR
ENGINES TESTED AT SOUTHAMPTON

(From Tables 2.2 and 2.3)

oxide (ppm) is plotted against Brake Mean Effective Pressure (lbf/in^2) developed by the engines. For the multicylinder engines, the BMEP developed at the intermediate speed and rated speed for 75% and 100% load only is plotted. It can be seen that there is a large spread of nitric oxide levels for the various engines. However, despite this scatter, a general trend of increase of nitric oxide with BMEP can be seen (Figure 2.3) for all the engines tested except engine G (I.D.I). Naturally-aspirated engines C and F show the highest NO levels and rate of increase of NO with BMEP, represented by the line, X. The unmatched turbocharged experimental engine, B (represented by the line Y) shows lower levels of NO than a similar naturally aspirated engine, C, although the rate of increase of NO is practically the same as engine C. Naturally aspirated engines, D, H, as well as matched turbocharged engines A and E show even lower NO levels. The rate of increase of NO with respect to BMEP (represented by line Z) is also lower than the other direct injection engines tested (i.e. engines, B, C and F). The indirect injection engine G, shows considerably lower peak NO level (between $\frac{1}{3}$ and $\frac{1}{5}$ of that from equivalent direct injection types). The NO levels do not follow the pattern of increase with BMEP as seen for the other engines tested, in fact the levels show a slight reduction with BMEP.

In Figure 2.4 nitric oxide (ppm) level is shown against overall air-fuel ratio measured during the tests. From the scatter of points, it can be seen that NO levels increase as the air-fuel ratio approaches 20:1 for all engines except G. For engine G, the NO level remains unaffected between the air-fuel ratios 18:1 to 25:1. The effects of air-fuel ratio on nitric oxide reported by other investigators (Ref. 2.67, 2.68) are also shown in Figure 2.4. Their results show similar effects in terms of nitric oxide increase and rate of increase to that shown in the present investigation.

For the engines tested on the 13-mode EMA cycle, oxides of nitrogen as NO_2 (g/bhp/hr) are shown in Figure 2.5 against engine combustion surface-to-volume ratio. The combustion surface area for the D.I. engines tested was obtained by summing of the areas of the combustion bowl in the piston, the top land of the piston and the cylinder head facing the piston. For the I.D.I. engine G, the swirl chamber surface and the throat area represented the combustion bowl (compared with the D.I. combustion bowl). Details of the individual areas are given in Table 2.3. Surface-to-volume ratio was calculated on the same basis from the piston details given in reference 2.69 and is also presented in the table. Most of the data points for the engines fall between 5-9 combustion surface-to-volume ratios. A line through the points shows a reduction of NO_2 as the surface-to-volume ratio increases.

It can be seen that the indirect injection engine has an advantage over direct injection diesel engines for exhaust NO levels. The reasons for this advantage are not yet well understood although various mechanisms affecting these have been suggested. Figure 2.5 shows a possible mechanism, i.e. larger combustion surface-to-volume ratio may limit overall bulk gas temperature because of the larger heat transfer area of the combustion chamber. It has also been suggested that due to the fuel-rich combustion in an indirect injection engine, not enough oxygen may be available for NO formation, although bulk gas temperatures would be high. As the combustion products expand into the main chamber where excess O_2 and N_2 are available for combination, the temperature of the bulk gas would be too low to support rapid NO formation.

26

The NO levels [reported as NO_2 (g/bhp-hr)] for the other direct injection engines were not significantly scattered except for engine D which shows lower NO_2 levels at a higher surface-to-volume ratio. The differences in exhaust NO (ppm) for the direct injection engines shown in Figure 2.3 are probably due to differences in injection characteristics, air-fuel mixing and swirl in the naturally aspirated designs as well as differences introduced by turbocharging of the engines. Tests in which NO was added to the air intake are discussed in association with the Backhouse-Raine model in Section 4.

Finally some data is presented in Figures 2.6 and 2.7 showing typical results of in-cylinder sampling for NO and CO (2.71). An I.D.I. engine was used in these tests and the plots show a sequence of samples taken over many cycles. The cylinder configuration with the sampling valve in its wall position (2 mm into the cylinder) is shown inset in Figure 2.7. The poppet sampling valve was designed and developed at the I.S.V.R. (2.65). The necessary requisite of reaction quenching is achieved by water cooling the sample line right up to the poppet face. The valve is operated by an auxiliary fuel injector. Sampling times of less than 5^oC.A. can be achieved easily at engine speeds of 1000 rev/min. It has been operated for a number of hours, sampling from various positions in an I.D.I. engine cylinder.

The noteworthy features of the test data are the indications (Figure 2.6) of an initial spike in the NO history at $\sim 4^o$ A.T.D.C, which coincides with the time at which the flamefront passes the sampling point, followed by a gradual build-up in NO concentration to a peak at about 20° A.T.D.C. Comparison with the history of CO at the same sampling point is revealing. The sequential peaks of CO (Figure 2.7) correspond exactly to the swirl frequency in the cylinder. If the CO is formed in the flame front and nowhere else then such a picture is to be expected if the flow (vortex) remains coherent. The fact that no such cyclic picture emerges from the NO data is suggestive that, as might be expected, the bulk of the NO is formed in the post-flame gases in this engine.

Almost all present production engines can meet the current federal limits without significant modification. It is now well documented that I.D.I. engines produce lower nitric oxide and hydrocarbon levels than D.I. engines. (2.70, 2.72). Future lower limits would make oxides of nitrogen the most difficult pollutant to control without some sacrifice of power and specific fuel consumption.

It has been suggested (2.73) that for smaller engines (<0.8ℓ/cylinder), operating over a wide speed range, an I.D.I. combustion system is to be preferred and for a larger engine (>1.2ℓ/cylinder), the D.I. combustion system gives as low HC + NO_2 emission as an I.D.I. engine. An I.D.I. combustion system will, however, carry a fuel economy penalty which could be at least 10% compared with a D.I. system.

It is expected that an engine that meets 4 g/bhp h NO_2 and 0.8 g/bhp h HC on the EMA cycle will meet the 1977 U.S. Federal Lightweight standards of 2g/mile NO_2 and 0.41 g/mile HC (2.73).
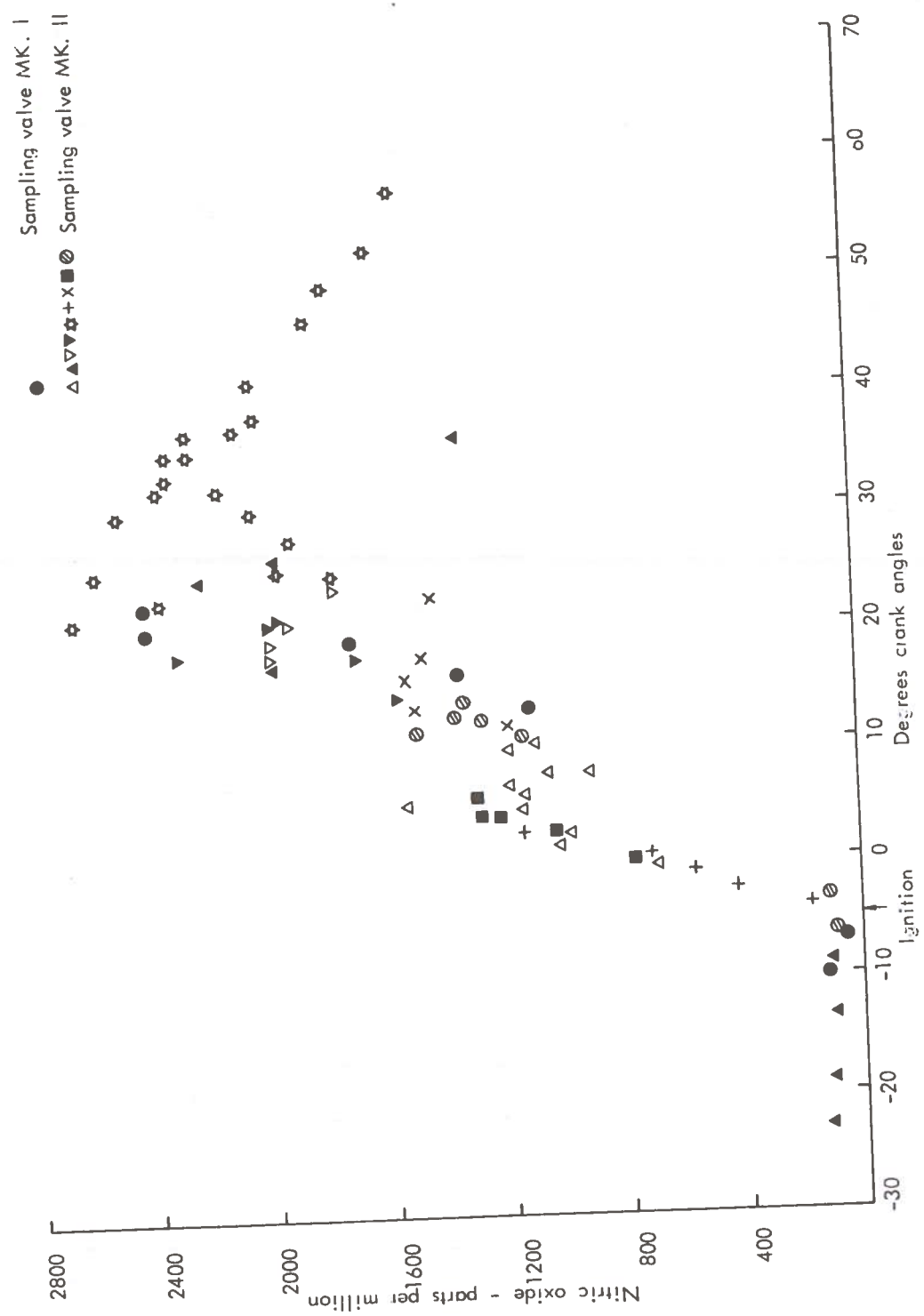
FIGURE 2.6.   IN-CYLINDER SAMPLING FROM AN IDI ENGINE: NITRIC OXIDE (PPM)
AGAINST ENGINE CRANK ANGLE (DEGREES)

28
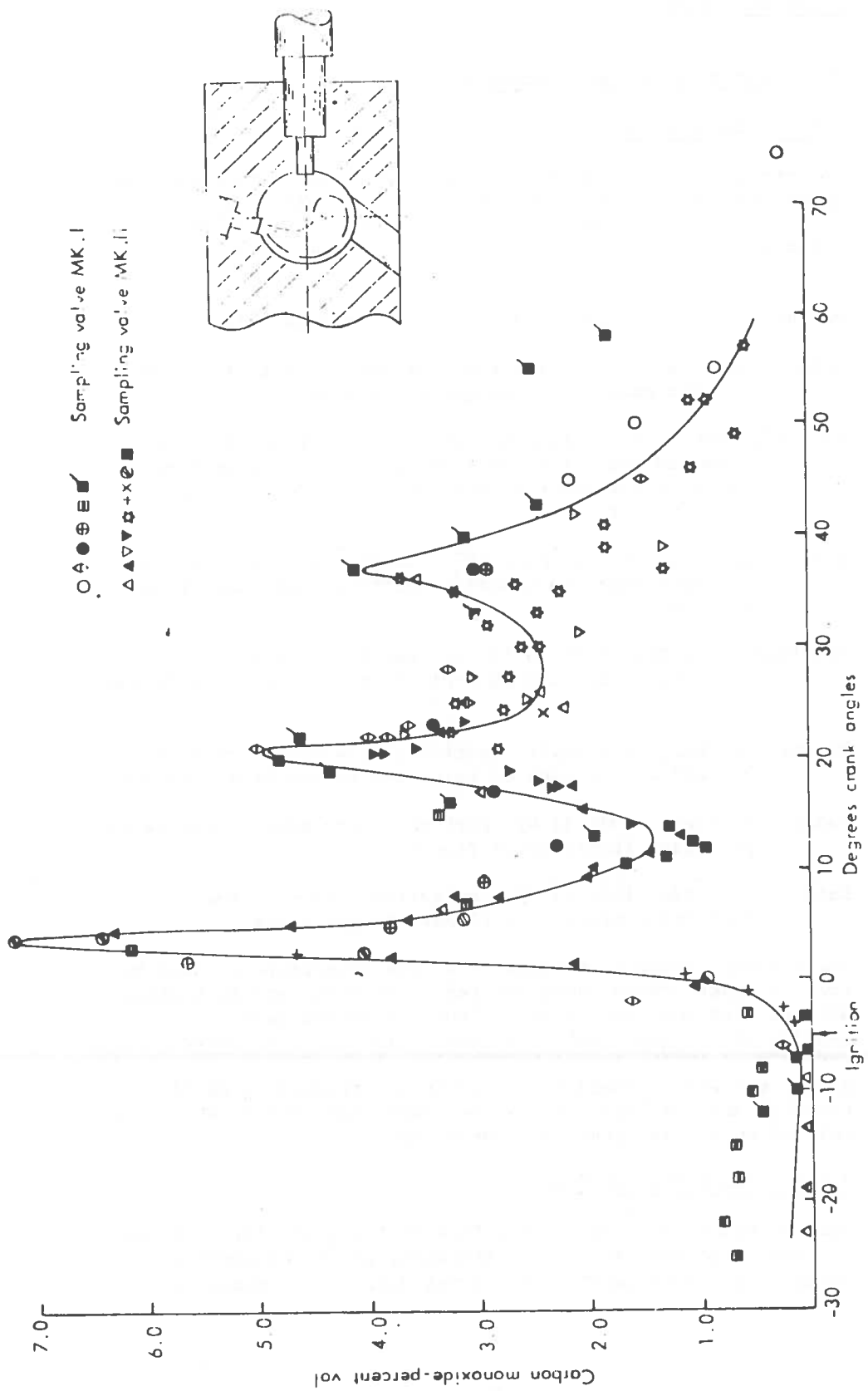
FIGURE 2.7. IN-CYLINDER SAMPLING FROM AN IDI ENGINE: CARBON MONOXIDE (VOLUME PERCENT) AGAINST ENGINE CRANK ANGLE (DEGREES)

29

3. SMOKE IN DIESELS

3.1 Processes of Soot Formation

3.1.1 Introduction

An extensive review of the processes of carbon formation from gases was compiled by Palmer and Cullis in 1965 (3.1). Some of the more recent reviews covering various aspects of carbon formation are:

Homann, 1967 (3.2) carbon formation in premixed flames.

Homann, 1970 (3.3) covering the same subject matter as the earlier paper, and brought up to date.

Feugier, 1969 (3.4) in French, covers soot formation in both premixed and diffusion flames, physical properties of soot, influence of pressure, temperature, fuel additives etc.

Gaydon and Wolfhard, 3rd Edn. 1970 Chapter 8 (3.5) covering the same aspects as earlier editions and brought up to date.

McArragher and Tan, 1972 (3.6) reviews the literature on soot formation at high pressure and biased towards the Diesel.

Broome and Khan, 1973 (3.7) specifically a review of soot formation processes of relevance to the Diesel engine.

Palmer and Seery, 1973 (3.8) part of a more general review on pollutant formation in flames.

Lahaye and Prado, 1974 (3.9) a selective review of the nucleation process in flames and pyrolysis.

The present review is restricted to the literature related to the dry black type of soot emitted by Diesels, and most noticeable at high load conditions. Thus the authors have considered 'cenospheres' of carbon, which are very large particles ($\sim 10^7$Å), formed by cracking of the fuel in the liquid phase, and which should not occur in a correctly adjusted Diesel; nor are 'blue' or 'white' smoke considered, which are emitted only under transient conditions.

3.1.2 Composition of Soot

Soot as exhausted from a combustion system generally contains at least 1 percent by mass of hydrogen, giving an empirical formula of approximately C_8H. X-ray diffraction measurements

and electron microscopy have been used to determine the following data on the structure of carbon black (produced by pyrolysis) and soot particles (3.1, 3.7):

Sheets (termed 'platelets' by Broome and Khan (3.7)) containing approximately 100 carbon atoms (of the basic type existing in ideal graphite), with a length and breadth of 20 - 30Å, build up into crystallites. Each crystallite consists of 5 to 10 platelets lying parallel to one another, the inter-layer spacing being 3 to 5% larger than that of graphite. A particle is made up of a large number (10^3 to 10^4) of crystallites randomly packed, but oriented with their planes generally parallel to the particle surface. The particles, which are roughly spherical, have diameters in the range 20 to 6000Å, but 50 to 500Å are more typical figures. These particles may then agglomerate to form chain-like aggregates at later stages of the combustion process, the aggregates being from 1000Å to 10 microns (10^5Å) in size.

It has often been noted that the outer appearance of soot particles formed in the gas phase is similar whether produced by pyrolysis, in diffusion flames, or in premixed flames (3.1) (3.2). This can be illustrated by the following two examples.

Recent work (Vuk et al 1976 (3.10)) has demonstrated that the soot sampled from the exhaust gases of a Diesel engine at high exhaust gas temperatures consist of aggregates of spherical particles. The particles range in size from 100 to 800Å in diameter, with a mean size of approximately 260Å. These roughly spherical particles form aggregates consisting of from 1- 4000 particles. The aggregates are from 100Å (one particle) to 30μm in size.

In publications dealing with carbon black, particle sizes are frequently quoted as specific surface areas (defined as the surface area per unit mass of material) (e.g. Knorre et al 1972 (3.11)). This can be converted to a surface mean particle diameter by assuming that the particles are spherical, and that the soot density is known. Thus specific surface area,

$$S = \frac{\pi d^2 \cdot 6}{\pi d^3 \cdot \rho_s} = \frac{6}{d \cdot \rho_s} \qquad m^2/gm. \qquad (3.1)$$

where d = surface mean particle diameter (m.)

and ρ_s = soot particle density (gm./m^3.).

The density of soot is variously quoted at between 1.6 and 2.0 gm./cm^3. Taking an average value of ρ_s = 1.8 gm./cm^3. we obtain

$$S \simeq \frac{3.3 \times 10^{-6}}{d} \qquad m^2/gm. \qquad (3.2)$$

31

Typical values for the specific surface areas of carbon blacks (Knorre, 1972 (3.11)) are 80 to 110 m.^{2}/gm., which by equation (3.2) give surface mean diameters of 420 to 300Å.

3.1.3 Influence of Chemical and Physical Factors on Carbon Formation

Molecular Structure

Early experiments to determine the tendency of a fuel to form carbon in diffusion flames were carried out by measuring the height of the flame at which soot formation first occurs (Minchin, 1935 (3.12), Clarke et al, 1946 (3.13)). In the laminar case, the height of the flame is dependent upon the fuel flow rate. Results of this type of experiment are shown in figure 3.1 and indicate that in most cases the tendency of an homologous series to form carbon decreases with increasing molecular weight. A notable exception is the paraffin series, although in this case the tendency to form carbon changes very little.

More recently, Meier Zu Kocker, 1972 (3.14, 3.15) has attempted to correlate the molecular structure of the fuel with soot forming tendencies in turbulent diffusion flames by introducing a dimensionless "characteristic fuel number" (BKZ), dependent upon the carbon to hydrogen weight ratio and the mean boiling point of the fuel. Thus

$$BKZ = \ln(\nu \cdot \nu_{min}) + \frac{T_s}{T_{s,min}} \quad , \quad (3.3)$$

where ν = C/H weight ratio of the fuel,
     T_s = mean boiling point of the fuel,
and subscript 'min' refers to a reference fuel, chosen as pentane (ν_{min} = 5, $T_{s,min}$ = 310K). An example of the correlation obtained in two different types of diffusion flame is shown in figure 3.2.

In general, it appears that the C/H ratio is one of the principal factors controlling the tendency to carbon formation. Compactness of the molecule and unsaturation, however, also increase the tendency to carbon formation in diffusion flames.

In premixed flames, a useful measure of the carbon forming tendency of a fuel is the atomic O/C ratio at which carbon formation just occurs. Carbon is not expected to form, under equilibrium conditions, from mixtures in which there is more than sufficient oxygen to convert all the carbon to CO (i.e. O/C >1) (ref.3.16). However, in practice, carbon formation is frequently observed in mixtures considerably weaker than this.

A systematic study of the influence of molecular structure on carbon formation was undertaken by Street and Thomas, 1955 (3.17)
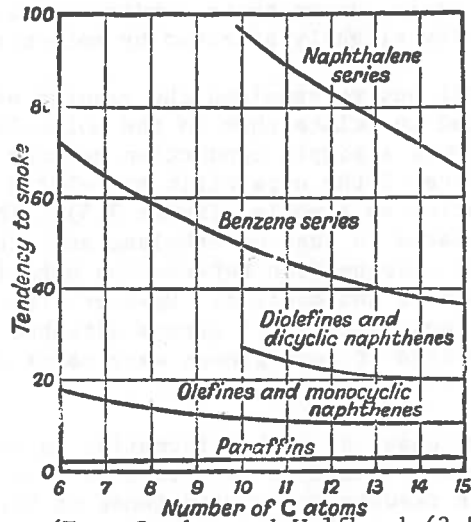
(From Gaydon and Wolfhard (3.5))

FIGURE 3.1 TENDENCY OF VARIOUS FUELS TO SMOKE WHEN BURNT AS A LAMINAR DIFFUSION FLAME
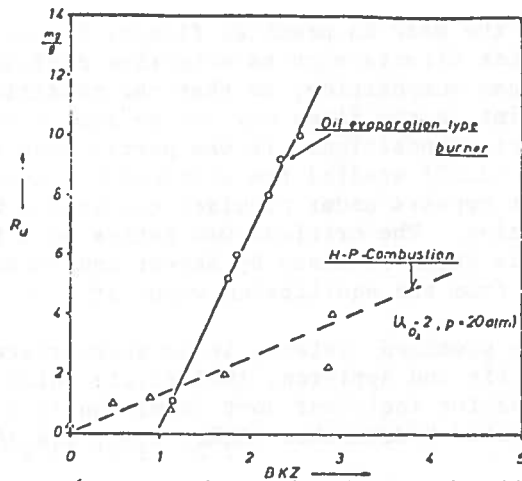
(From Gaydon and Wolfhard (3.5))

FIGURE 3.2 SOOT CONCENTRATION VS. FUEL NUMBER, BKZ, FOR TWO TYPES OF DIFFUSION FLAME

Fuel	Mean critical air/fuel ratio by weight	λ, mixture strength. Actual air as fraction of stoichiometric	λ for O/C=1, i.e. theoretical carbon point	O/C at actual carbon point
Ethane	9·7	0·60	0·285	2·1
Propane	10·1	0·64	0·300	2·1
n-pentane	10·4	0·68	0·313	2·2
n-octane	10·8	0·72	0·320	2·2
Acetylene	6·4	0·48	0·40	1·20
Ethylene	8·1	0·55	0·33	1·67
Benzene	9·3	0·70	0·40	1·75
Ethyl alcohol	6·0	0·66	0·167	2·5
Acetaldehyde	4·3	0·55	0·20	1·9
Diethyl ether	6·4	0·58	0·25	2·0

(From Gaydon and Wolfhard (3.5))

FIGURE 3.3 ONSET OF CARBON LUMINOSITY IN SELECTED PREMIXED FUEL-AIR FLAMES

33

in a premixed bunsen-type burner. A selection of their results is given in figure 3.3, and in figure 3.4. For paraffins the critical air-fuel ratio, under their conditions, lies between 10 and 11 and is only slightly affected by molecular weight.

Daniels, 1960 (3.18) has re-examined the results of Street and Thomas and attempted to relate them to the molecular structure of the fuel. He found a simple connection between the behaviour of individual members of the n-paraffin and olefin series, and between the two series as a whole (figure 3.5). The behaviour of acetylene is related to that of ethylene and ethane, and there appears to be a connection between the behaviour of benzene and that of n-paraffins and olefins. However, the relationship did not extend to fuels with alkyl groups attached to the benzene, which would be expected if such groups were parts of aliphatic molecules.

Further work on the onset of carbon formation in premixed flames has been carried out by Fenimore et al., 1956 (3.19). Whilst the trends of their results agree with those of Street and Thomas as regards the effect of molecular structure, the critical O/C ratios obtained are somewhat higher.

With reference to the work in premixed flames, Homann, 1967 (3.2) has pointed out that effects such as selective diffusion can modify the local gas composition, so that the condition for soot formation at a point in the flame may not be simply related to the initial mixture composition. It was partly with this in mind that Wright, 1969 (3.20) studied the critical O/C atom ratios at which carbon first appears under premixed conditions with intense recirculation. The critical O/C ratios were found to be 10 - 20% lower than those obtained by Street and Thomas, but were still far removed from the equilibrium value of 1.0.

In connection with premixed systems, it is appropriate to mention the work of Radcliffe and Appleton, 1971 (3.21) which determined critical O/C ratios for incipient soot formation in a limited number of shock-heated hydrocarbon (C_2H_2, C_2H_4, C_2H_6)/oxygen/ argon mixtures.

Temperature

A change of flame temperature has a complex effect on the soot released from flames, as it affects both the formation and oxidation processes.

In diffusion flames, the effect of temperature is difficult to deduce, since the general method employed to adjust the flame temperature is by the addition of diluents to the fuel or combustion stream. The interpretation of the results is thus complicated by the fact that the diluent may itself be affecting the reaction mechanisms.

Dearden and Long, 1968 (3.22), in studying laminar diffusion flames of ethylene and propane, added a variety of species to the fuel

34
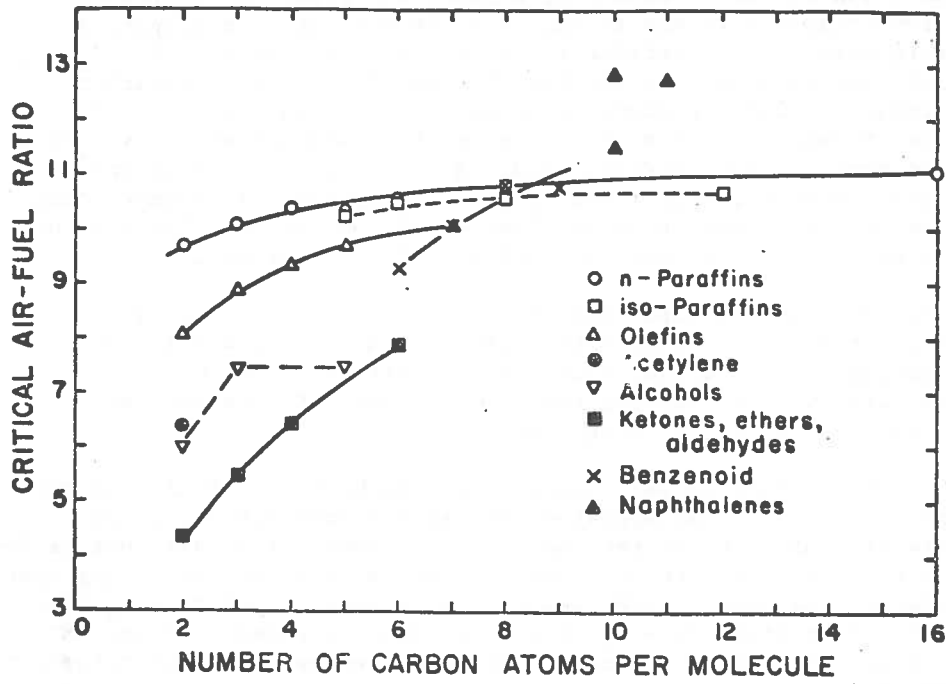
From Palmer and Cullis (3.1)

FIGURE 3.4.   CRITICAL AIR:FUEL RATIO FOR CARBON FORMATION IN PREMIXED FLAMES
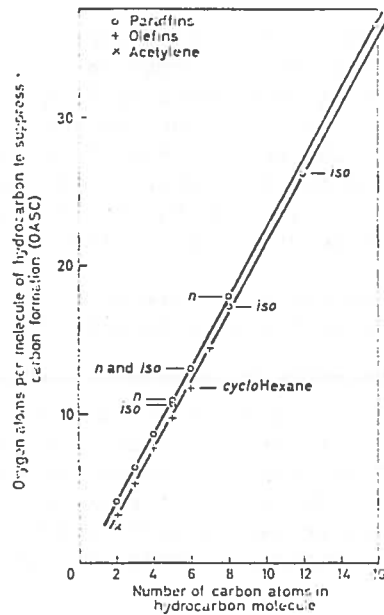
From Daniels (3.18)

FIGURE 3.5.   SUPPRESSION OF CARBON IN PREMIXED FLAMES OF PARAFFINS, OLEFINS AND ACETYLENE

35

and oxidant streams in order to determine the effect of flame temperature on the sooting rates. With the exception of oxygen addition to the propane fuel stream, the result of increased flame temperature was to increase the sooting rate (figure 3.6). This should be compared with the finding of Wright, 1974 (3.23), that adding oxygen to the fuel stream of several hydrocarbon diffusion flames produced a marked increase in the level of soot formation. This effect was most pronounced with unsaturated and aromatic hydrocarbons, and least pronounced with saturated ones. However, Wright interprets his experiments as suggesting that oxygen promotes polymerization of the fuel to high molecular weight soot precursors, and not as a thermal effect.

Dearden and Long also found that the sooting rate increased for both of the fuels they investigated with an increase in the 'oxygen index' (oxygen flow/oxygen + diluent flow) of the combustion 'air' supply, the rate falling off, however, at higher values of the oxygen index.

McLintock, 1968 (3.24), measured the smoke point (fuel flow rate at which soot first appeared) of laminar ethylene diffusion flames, when the 'oxygen index' of the combustion 'air' was varied. He found very different trends of the smoke point, depending upon whether the oxygen index was varied by keeping constant O_2 flow rate or constant $N_2 + O_2$ flow rate, and concluded that the results indicated the complex effect of temperature and transport properties.

Near the threshold of soot formation, higher temperature appears to suppress soot formation in premixed flames, whereas for very rich mixtures it may increase the amount of soot formed.

Street and Thomas (3.17) found that raising the flame temperature shifted the threshold for carbon formation to slightly richer mixtures. Similar results were found by Wright (3.20) in the study of premixed combustion with intense recirculation (figure 3.7), and in the shock tube work of Radcliffe and Appleton (3.21) (figure 3.8). Note that at the higher temperatures obtained by Radcliffe and Appleton, they were able to attain mixtures richer than $O/C = 1$ before the onset of carbon formation.

For mixtures richer than the soot threshold, Macfarlane et al., 1964 (3.25) found a marked increase in soot deposition at increased temperature.

Gaydon and Wolfhard (3.5) suggest that near the threshold, higher temperature probably decreases soot formation because it has a greater effect on the competing oxidation process than on the soot formation process. In very rich mixtures, however, the competing oxidation will be less important and the high temperature will accelerate the now dominant pyrolysis reactions.

Diluents

Palmer and Cullis, 1965 (3.1) state that the effect of diluents (by which is meant gases added in relatively large amounts) is

From Dearden
and Long (3.22)

Legend:
- ○ Ethylene 'standard flame'
- ▽——▽ ethylene with oxygen as additive to fuel
- △ ethylene with acetylene as additive to fuel
- × ethylene with hydrogen as additive to fuel
- + ethylene with nitrogen as additive to fuel
- □—□ ethylene flames in 'air' of various oxygen indices
- ● propane 'standard flame'
- ▼——▼ propane with oxygen as additive to fuel
- ▲——▲ propane with acetylene as additive to fuel
- ■——■ propane flames in 'air' of various oxygen indices

FIGURE 3.6.   SOOTING RATES OF VARIOUS DIFFUSION FLAMES VS. MAXIMUM FLAME
TEMPERATURES

From Wright (3.20)
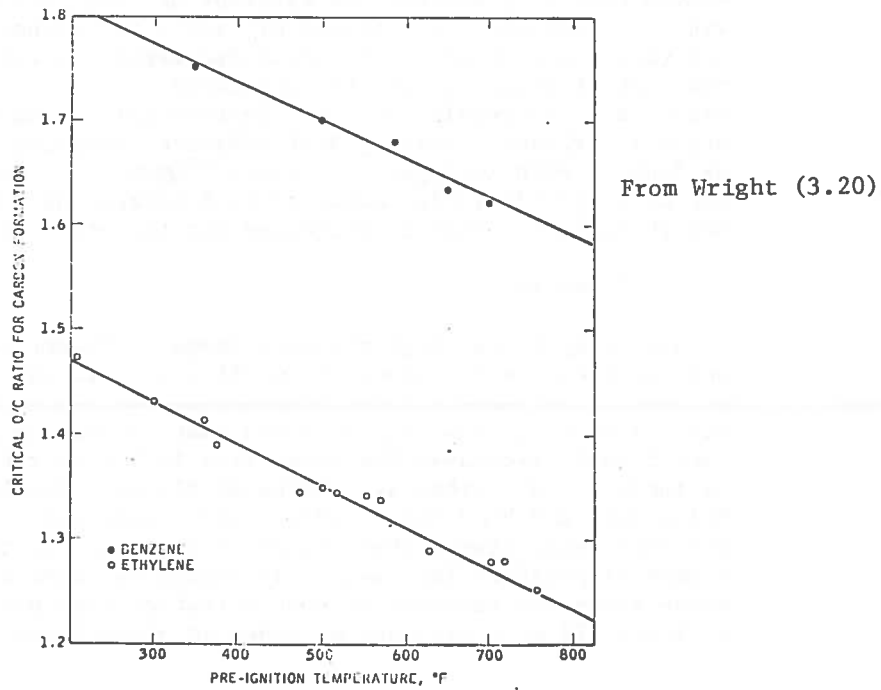
FIGURE 3.7.   INFLUENCE OF PRE-HEATING COMBUSTIBLE MIXTURE ON THE THRESHOLD FOR
CARBON FORMATION IN A WELL-STIRRED REACTOR

37

generally to suppress carbon formation in diffusion flames. As mentioned previously, experimental results must be interpreted with care since the use of diluents will usually affect the temperature.

The effect of 'inert' diluents (N_2, Ar and He) in the fuel and in the combustion 'air' stream has been investigated by McLintock, 1968 (3.24), who found that they were more efficient as soot suppressors when added to the fuel stream than when added to the oxidant stream. He also noted the high efficiency of CO_2 and H_2O as suppressors of soot formation when used as fuel diluents (figure 3.9), and attributed this to their ability to influence the oxidative reactions.

Related to this is the work of Sjögren, 1972 (3.26) on the influence of diluents in the combustion air surrounding large droplets burning individually. If these droplets burn with an envelope flame, soot formation is many times higher than if they burn with a wake flame. In order to extinguish the envelope flame, the relative velocity between the droplet and air must exceed a certain critical velocity. Sjögren found that this critical velocity is a function of oxygen concentration in the combustion air, and that it falls to zero if the oxygen concentration is reduced to 14 - 16%, with N_2 as diluent. With CO_2 as diluent, the critical extinction velocity falls to zero at 17 - 18% O_2. He suggests that this could be responsible for the marked effect which recirculation has in industrial furnaces on soot formation.

With reference to premixed combustion, Street and Thomas (3.17) showed that with benzene and kerosene as fuels, dilution of air with N_2 increases the critical O/C ratio for carbon formation and enrichment of air with oxygen decreases the ratio. However the work of Wright (3.20) has indicated that the influence of diluents is extremely complex. He used helium, nitrogen and argon as diluents, working with ethylene, propylene and benzene as fuels. With nitrogen as diluent (figure 3.10) he found that the critical O/C ratio increased with benzene as fuel (cf. Street and Thomas), but that it decreased for the other two fuels.

Pressure

Generally speaking, high pressure seems to favour soot formation and low pressure to reduce it in diffusion flames.

Schalla et al., 1954 (3.27), found that increasing pressure considerably decreased the smoke free fuel flow rate (figure 3.11) in laminar hydrocarbon-air diffusion flames. Similarly, Holderness and Macfarlane, 1973 (3.28), have shown that in turbulent kerosene spray flames there is an increase in the total soot formed as pressure increases. It should be noted that in both of these works the increase in soot formation with pressure appears to level off at a pressure of order 10 atmospheres.

From Radcliffe and Appleton (3.21)
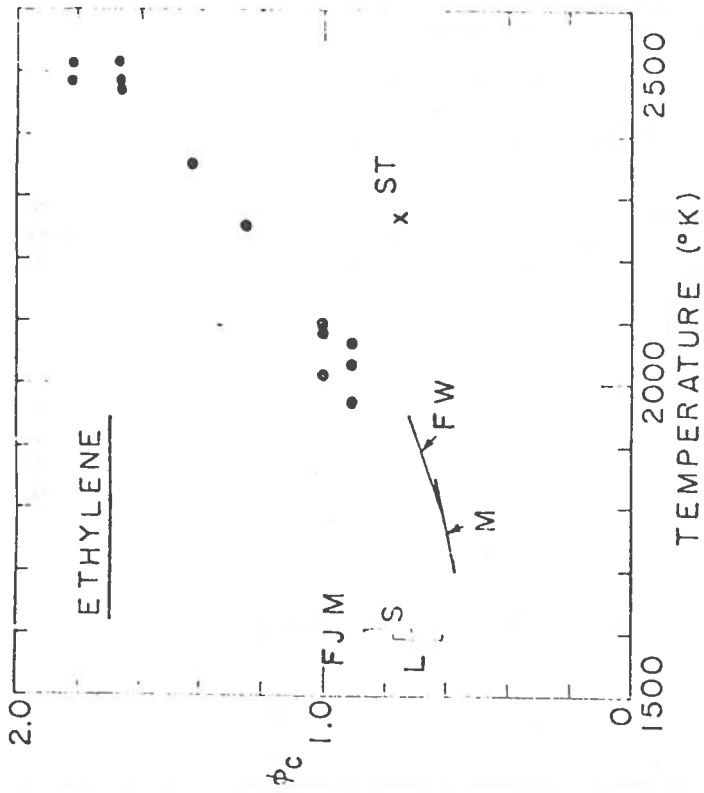
FIGURE 3.8. INFLUENCE OF TEMPERATURE ON THE THRESHOLD FOR CARBON FORMATION

N.B. ϕ_c = CRITICAL ATOMIC C:O RATIO

SYMBOLS;

    ●   SHOCK–TUBE RESULTS OF RADCLIFFE AND APPLETON (1971)

    ST   STREET AND THOMAS (1955)

    FJM   FENIMORE ET AL. (1956) ON TWO BURNERS, OF 1.6 cm (S) and 3.2 cm (L) DIAMETER

    M   MILLIKAN (1962)

    FW   FLOSSDORF AND WAGNER (1967)

39
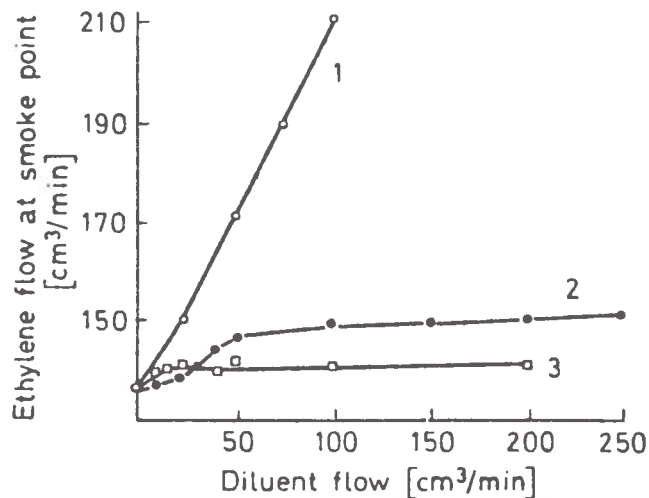
From McLintock (3.24)

FIGURE 3.9. VARIATION OF SMOKE POINT ON ADDITION OF DILUENTS TO
FUEL STREAM OF AN ETHYLENE-AIR DIFFUSION FLAME
    CURVE 1, CARBON DIOXIDE
    CURVE 2, ARGON OR NITROGEN
    CURVE 3, HELIUM

	Diluent			
Fuel	He	N_2	Ar	Oxygen
Ethylene	1.32	1.43	1.53	20%
	1.30	1.44	1.16	30%
Propylene	1.33	1.42	1.67	20%
	1.28	1.51	1.37	30%
Benzene	1.51	1.75	1.93	20%
	1.44	1.72	1.80	30%

From Wright (3.20)

FIGURE 3.10. EFFECT OF DILUENTS ON THE CRITICAL O:C RATIO FOR CARBON FORMATION

The work of Fenimore et al., 1956 (3.19), in premixed flames
suggests that as pressure is increased, the greater is the
oxygen to carbon ratio required to suppress carbon formation.
However, Gaydon and Wolfhard (3.5) have indicated that this
effect may be due to burner quenching, and that for a true
comparison the burner diameter and flow rate should have been
increased at the lower pressures. The work of Bonne and
Wagner, 1965 (3.29) on laminar flames, and of Macfarlane et al.,
1964 (3.30), on both laminar and turbulent flames indicate that
there is practically no change in the threshold mixture strength
at which soot appears (figure 3.12) as pressure increases. Once
carbon is set free, however, Macfarlane et al. (3.28, 3.30) found
a marked increase in the amount of soot released with pressure
(figure 3.13), and suggested an index of proportionality between
the soot formation ratio, S (soot formed/total carbon in fuel),
and pressure of the form

$$S \propto p^{2.5} \text{ or } p^3$$

(3.4)

up to a pressure of about 20 atm. However, they state that
further increase in pressure is not expected to continue this
trend.

3.1.4 Mechanisms of Soot Formation

Starting from a hydrocarbon fuel molecule with, in the Diesel
case, or order 12 – 30 carbon atoms, and roughly twice that
number of hydrogen atoms, we must account for the formation of
soot particles with about 10^5 carbon atoms, and much fewer
hydrogen atoms.

Five processes controlling the formation of soot from gaseous
hydrocarbons can be distinguished:

1) Gas phase reaction;

2) Nucleation;

3) Heterogeneous particle growth;

4) Coagulation;

5) Oxidation.

Gas Phase Reactions

During the course of reactions forming soot there are many purely
gas phase reactions occurring. Most of these reactions occur
even if conditions are not favourable for the formation of solid
carbon. Gas phase reactions are responsible for the formation of
soot precursors during the induction period prior to nucleation
of a solid (or liquid) phase, and are also responsible for the
generation of the gas phase species involved in surface growth of

41

From Palmer and
Cullis (3.1)
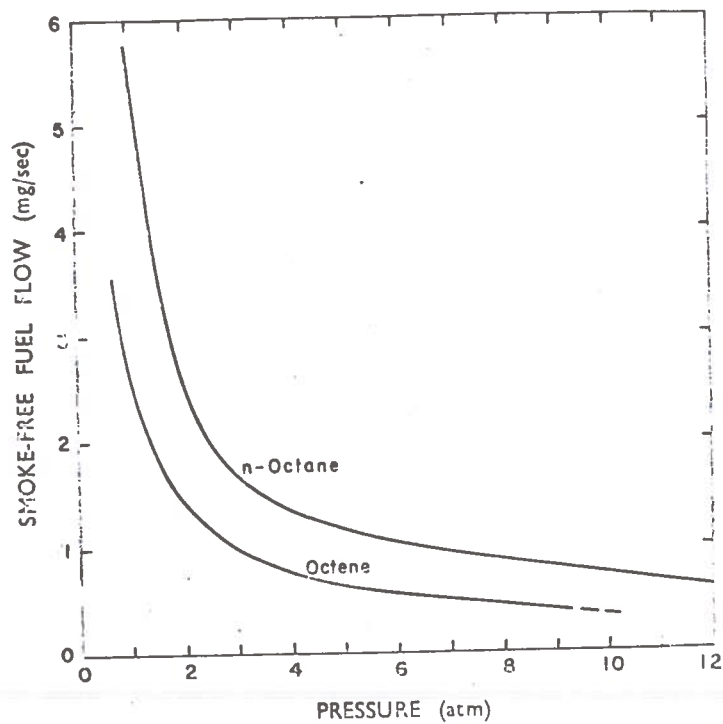
FIGURE 3.11.   VARIATION IN SMOKE-FREE FUEL FLOW WITH PRESSURE FOR TWO FUELS
BURNING AS DIFFUSION FLAMES IN AIR
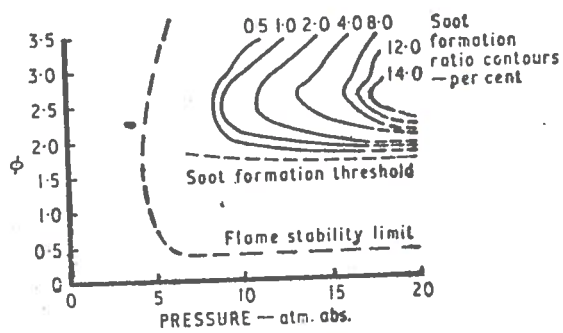
From Macfarlane and Holderness (3.25)

FIGURE 3.12.   SOOT FORMATION DATA FOR PREMIXED HEXENE-AIR FLAMES AT HIGH PRESSURES

ϕ = equivalence ratio($\dfrac{\text{fuel-air ratio of mixture}}{\text{stoichiometric fuel-air ratio}}$)

Soot formation ratio = $\dfrac{\text{soot}}{\text{total carbon in fuel}}$

soot particles. Gas phase reactions also include oxidation
processes, possibly removing soot precursors, and gas phase
species which would otherwise participate in surface growth
of the carbon particles.

Jensen, 1974 (3.31), in an attempt to model the detailed
processes of soot formation from methane in an isothermal,
pyrolysis situation has proposed the following gas phase
reaction mechanism:

(1) CH_4 $\rightleftharpoons$ $CH_3 + H$

(2) $CH_4 + H$ $\rightleftharpoons$ $CH_3 + H_2$

(3) $CH_3 + CH_3$ $\rightleftharpoons$ C_2H_6

(4) C_2H_5 $\rightleftharpoons$ $C_2H_4 + H$

(5) $C_2H_4 + H$ $\rightleftharpoons$ $C_2H_3 + H_2$

(6) $C_2H_3 + M$ $\rightleftharpoons$ $C_2H_2 + H + M$

(7) $C_2H_2 + H$ $\rightleftharpoons$ $C_2H + H_2$

(8) $C_2H + H$ $\rightleftharpoons$ $C_2 + H_2$
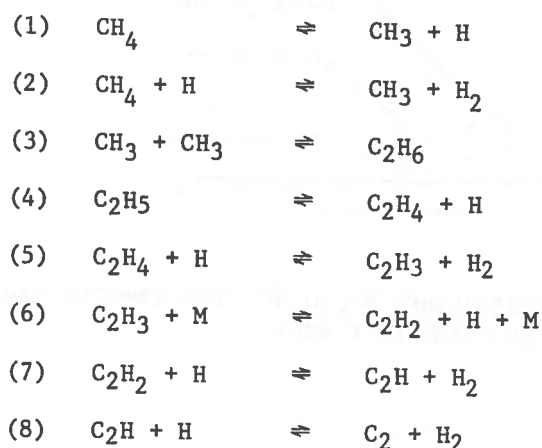
Jensen has estimated the uncertainty in the rate coefficients
of some of the reactions to be a factor of 30, and in the case
of reaction (8), a factor of 100.

Other authors (e.g. Gardiner et al. 1974 (3.32)) have proposed
different pyrolysis schemes and, of course, when gas phase oxidation
processes are included, the number of elementary reactions
involved increases. Thus Bowman, 1974 (3.33), has considered
30 reactions (figure 3.14) in an attempt to model methane
oxidation in shock tubes, and this scheme omits many of the
reactions which Gardiner and Jensen consider to be of importance
in the pyrolysis situation.

Nucleation

Many experiments in shock tubes, both with (Gosling, 1974 (3.34),
Radcliffe and Appleton, 1971 (3.21), and without (Aten and
Greene, 1961 (3.35), Hooker, 1949 (3.36), Jones, 1975 (3.37))
oxygen present, and in rich premixed flames (Homann, 1970 (3.3),
D'Alessio et al. 1972 (3.38), Howard, 1968 (3.39)) have shown
the existence of an induction period, however defined, between
the initiation of reaction and the first detection of soot or
its precursors. This indicates the need for something different
to the original fuel molecule to be present before soot can be
formed. In the past (e.g. Porter, 1952 (3.40)), much effort has
been spent in trying to identify one basic reaction mechanism
involving a particular precursor. It now seems evident however,
that many routes are possible, depending on the physical and
chemical conditions prevailing. Broome and Khan, 1973 (3.7) have
developed a much simplified version (figure 3.15) of a diagram

43
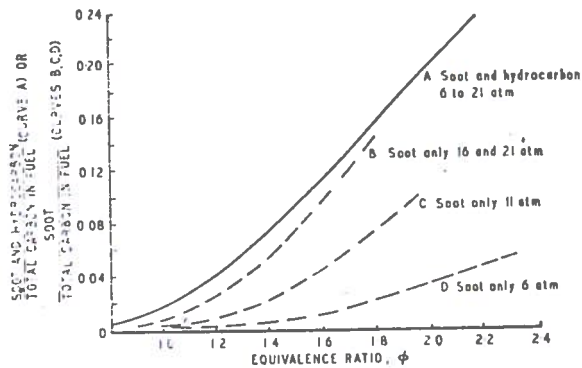
FIGURE 3.13.   VARIATION WITH EQUIVALENCE RATIO OF TOTAL UNBURNT CARBON COMPOUNDS
AND OF SOOT AT HIGH PRESSURES IN PREMIXED FLAMES

	Reaction	Rate constant, k_f*
1.	$CH_4+M \rightarrow CH_3+H+M$	$2 \times 10^{17} \exp(-44\,500/T)$
2.	$CH_4+OH \rightarrow CH_3+H_2O$	$6 \times 10^{14} \exp(-6\,290/T)$
3.	$CH_4+H \rightarrow CH_3+H_2$	$2.24 \times 10^4 T^3 \exp(-4\,400/T)$
4.	$CH_4+O \rightarrow CH_3+OH$	$2.1 \times 10^{13} \exp(-4\,560/T)$
5.	$H_2+OH \rightarrow H+H_2O$	$2.9 \times 10^{14} \exp(-5\,530/T)$
6.	$O+H_2 \rightarrow H+OH$	$3.2 \times 10^{14} \exp(-7\,540/T)$
7.	$H+O_2 \rightarrow O+OH$	$2.2 \times 10^{14} \exp(-8\,450/T)$
8.	$OH+OH \rightarrow O+H_2O$	$5.5 \times 10^{13} \exp(-3\,520/T)$
9.	$CO+OH \rightarrow CO_2+H$	$4.0 \times 10^{12} \exp(-4\,030/T)$
†10.	$CO+O+M \rightarrow CO_2+M$	$5.9 \times 10^{15} \exp(-2\,060/T)$
11.	$H+OH+Ar \rightarrow H_2O+Ar$	$8.4 \times 10^{21} T^{-2}$
12.	$H+OH+H_2O \rightarrow H_2O+H_2O$	$1.4 \times 10^{23} T^{-2}$
†13.	$O_2+Ar \rightarrow O+O+Ar$	$7.9 \times 10^{19} \exp(-52\,770/T)$
†14.	$H_2+Ar \rightarrow H+H+Ar$	$2.2 \times 10^{14} \exp(-48\,300/T)$
15.	$CH_3+O \rightarrow H_2CO+H$	1×10^{14}
16.	$CH_3+O_2 \rightarrow H_2CO+OH$	2×10^{10}
†17.	$CH_3+OH \rightarrow H_2CO+H_2$	4×10^{12}
18.	$H_2CO+O \rightarrow HCO+OH$	$5 \times 10^{13} \exp(-2\,300/T)$
19.	$H_2CO+OH \rightarrow HCO+H_2O$	$5.4 \times 10^{14} \exp(-3\,170/T)$
20.	$H_2CO+H \rightarrow HCO+H_2$	$1.35 \times 10^{13} \exp(-1\,890/T)$
21.	$HCO+O \rightarrow CO+OH$	1×10^{14}
22.	$HCO+OH \rightarrow CO+H_2O$	1×10^{14}
23.	$HCO+H \rightarrow CO+H_2$	2×10^{14}
24.	$HCO+M \rightarrow CO+H+M$	$5 \times 10^{13} \exp(-9\,570/T)$
25.	$H_2CO+M \rightarrow HCO+H+M$	$4 \times 10^{13} \exp(-18\,500/T)$
26.	$H+HO_2 \rightarrow OH+OH$	$2.5 \times 10^{14} \exp(-950/T)$
27.	$H+O_2+M \rightarrow HO_2+M$	$1.5 \times 10^{15} \exp(500/T)$
†28.	$C_2H_6 \rightarrow CH_3+CH_3$	$8 \times 10^{16} \exp(-4\,500/T)$
†29.	$C_2H_6+O \rightarrow C_2H_5+OH$	$4 \times 10^{13} \exp(-3\,280/T)$
†30.	$HCO+O_2 \rightarrow CO+HO_2$	$4.2 \times 10^{13} \exp(-7\,200/T)$

* Units: cm, cal, °K, mole, sec.   † Reaction not included in final mechanism.

From Bowman (3.33)
FIGURE 3.14.   SUGGESTED REACTION SCHEME FOR METHANE OXIDATION IN SHOCK–TUBE
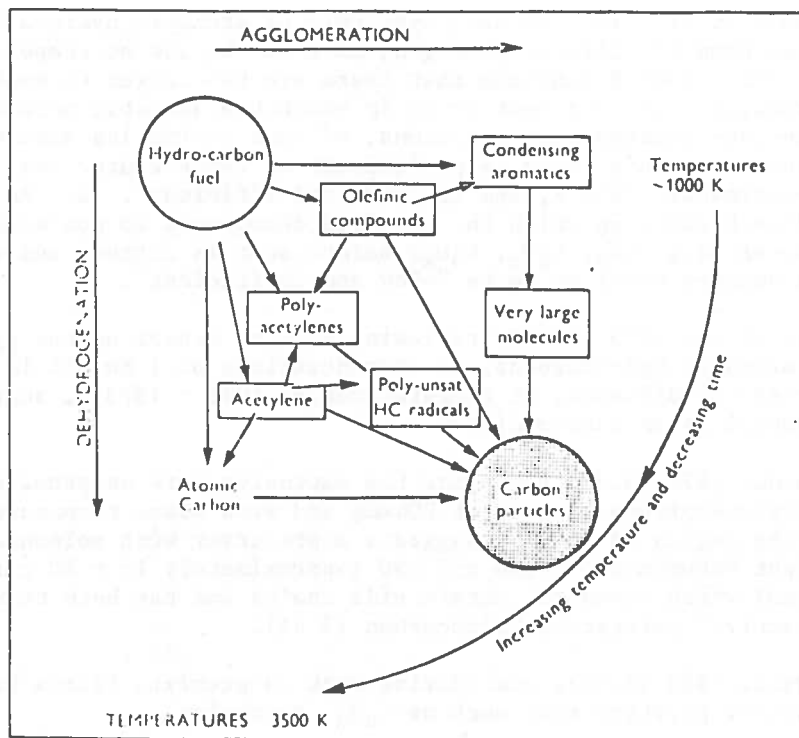
From Broome and Khan (3.7)

FIGURE 3.15. HIGHLY SIMPLIFIED SCHEME OF REACTIONS INVOLVED IN THE FORMATION
OF CARBON FROM HYDROCARBON FUELS

by Street and Thomas, 1955 (3.17) indicating some of the many possible routes to solid carbon.

Broome and Khan have attempted to introduce the temperature of the process as a decisive factor in controlling the reaction route to carbon, but many other factors seem to be equally important. The following is an attempt to give a brief summary of some of the more recent literature on species which have been proposed as soot precursors:

Jensen, 1974 (3.31); isothermal pyrolysis of methane at temperatures of 1400 – 1600 K, suggests C_2 or C_2H.

Prado and Lahaye, 1975 (3.41); pyrolysis of benzene ($\frac{1}{4}$% to 10%) diluted in nitrogen at temperatures from 1323 to 1723 K and reaction times from 0.03 to 6 sec., suggest polynuclear aromatic molecules.

Graham et al., 1975 (3.42); pyrolysis of aromatic hydrocarbons (less than 1%) diluted in argon, in a shock tube at temperatures of 1600 – 2300 K conclude that there are two routes to soot formation. 1) A direct route in which the aromatic molecule undergoes condensation reactions, without losing its aromatic structure. This route is predominant at temperatures less than approximately 1800 K, and is "fast and efficient". 2) An indirect route in which the molecule decomposes to non-aromatic species (e.g. CH_x, C_2H_x, C_3H_x) before soot is formed, and which the authors consider to be "slow and inefficient".

Virk et al, 1973 (3.43); reviewing work by others on the pyrolysis of aromatic hydrocarbons, at concentrations of 1 to 35% in a variety of diluents, at temperatures of 1073 – 1373 K, suggest diphenyl as an intermediate.

Homann, 1970 (3.3); reviewing his extensive work on premixed acetylene-oxygen flames, at 20mmHg and with flame temperatures in the region of 2000 K, suggests a precursor with molecular weight between about 150 and 550 (approximately 15 – 40 carbon atoms) which seems to contain side chains and has been termed a "reactive" polycyclic hydrocarbon (3.44).

Howard, 1968 (3.39); considering work on premixed flames has proposed positive ions such as C_nH_n as nuclei.

Place and Weinberg, 1966 (3.45); studying the effects of applied electric fields on carbon formation in diffusion flames, concluded that positive flame ions can act as nuclei.

Jessen and Gaydon, 1968 (3.46); premixed acetylene-oxygen flames at atmospheric pressure and high temperatures (>3000 K) suggest C_2 radicals may serve as nuclei.

D'Alessio et al.,1974 (3.47); premixed methane-oxygen flames at atmospheric pressure, with flame temperatures of 1700 K, suggest tentatively benzene and polyacetylenes as intermediates to soot.

Tesner et al, 1971 (3.48); laminar acetylene diffusion flames with flame temperatures of 1900 - 2000 K, has suggested that the radical C_2 is the nucleus for soot particles.

Tesner, 1973 (3.49); in a general consideration of soot formation, suggests that nuclei may be of two types, namely either complex unsaturated polymer molecules, or simple radicals.

In spite of the continuing debate about what may or may not act as an initial nucleus for carbon formation, several authors have attempted to quantify the nucleation process on a semi-empirical basis (e.g. Tesner et al, 1971 (3.48), Gilyazetdinov, 1970 (3.50), Hooker, 1949 (3.36)). For example Gosling et al., 1973 (3.34), 1974 (3.51), from shock tube experiments on the pyrolysis of various hydrocarbons at temperatures of 1350 - 2300 K, pressures of 1 - 14 bar, and hydrocarbon concentrations of $\frac{1}{2}\%$ - 10% with argon as diluent, have suggested a relation of the form

$$\Delta\tau \propto \frac{1}{\rho_{HC}} \cdot \exp\left(\frac{E^*}{RT}\right), \qquad (3.5)$$

where $\Delta\tau$ = "induction time" for particle formation,

ρ_{HC} = hydrocarbon density

and E^* = apparent activation energy of the process.

Typical values quoted for E^* are 162.0 and 135.3 kJ/mole for acetylene and kerosene vapour respectively, at a total pressure of 10 - 14 bar, and about 2000°K.

Heterogeneous Particle Growth

Once soot particles are present, growth of these particles occurs by the assimilation of suitable gas phase molecules upon collision of the molecules with the particle surface. As with the particle nucleation process, many suggestions have been made concerning the identity of the gas phase molecules participating in growth reactions.

Many authors have shown (e.g. Tesner, 1959 (3.52), Dugwell and Foster, 1973 (3.53), Magaril, 1974 (3.54)) that growth of a carbon surface can be observed at lower temperatures than carbon can be spontaneously precipitated as a dispersion in the same system. Tesner, 1961 (3.55) has also shown that once soot nuclei are present in sufficient concentration, the formation of new nuclei is suppressed, as the potential soot precursors are preferentially consumed by growth on the existing nuclei. From these and similar observations, the general conclusion is that the activation energy of the growth process is less than that for the nucleation process.

Thus, for example, in attempting to model the formation of carbon black by the thermal decomposition of hydrocarbon stock (e.g. fuel oil) in a flow of products of complete combustion at temperatures of 1600 - 2100 K, Gilyazetdinov, 1972 (3.56) has suggested an apparent activation energy for nucleation of 383 kJ/ mole, and for growth, of 105 kJ/mole.

47

The growth process has also been studied by Foster and co-workers (3.53, 3.57), in an attempt to relate the rate of surface-growth of soot particles to the conditions of the system. They have deduced a relation of the form:

$$\dot{m}_f = 1.0 \times 10^2 \;.n.\gamma.\; \exp\, (-42300/RT)\; gm.cm^{-2}.sec^{-1}, \qquad (3.6)$$

where γ = mole fraction of hydrocarbons in the gas phase bearing n carbon atoms, with n > 3.

Coagulation

The process of particle coagulation is the result of particle - particle collisions. The important factors which determine the rate of coagulation are: particle number density, particle size (and size distribution), temperature and pressure -(all of which influence the probability of collision), and the shape and structure of particles (which influence the probability of sticking).

If the coagulation process is assumed to occur due to Brownian motion of the particles only (i.e. neglecting hydrodynamic, electrical, gravitational or other forces), and the sticking probability is unity, then the rate of particle coagulation is given by the Smoluchowski formula (Fuchs, ch.7, 1964 (3.58));

$$\frac{dN}{dt} = -cN^2 \quad particles \:/\: cm^3 \; sec., \qquad (3.7)$$

where N is the number of particles present per cubic centimetre, and c is the coagulation rate coefficient (cm^3/part.sec.). Many authors have considered soot particle coagulation to be controlled by this expression, and have deduced the value of the coagulation rate coefficient from kinetic considerations.

Thus Fenimore and Jones, 1969 (3.59) have suggested

$$c = 2\sigma^2 \; (\frac{\pi RT}{M})^{\frac{1}{2}}, \qquad (3.8)$$

where σ = particle diameter

and M = "molecular weight" of the particle.

Similar relationships have been used by Gilyazetdinov, 1972 (3.60), Jensen, 1974 (3.31), and Samkhan et al. 1971 (3.61).

Graham et al., 1973 (3.62) have developed a theory of carbon particle coagulation, the rate being given by equation (3.7), but including the effect of enhancement of the collision rate due to dispersive forces in the coagulation rate coefficient. Thus in their model

$$c = (\frac{1}{8})^{\frac{1}{2}} \; (\frac{3}{4} \; \frac{kT}{\rho_s})^{\frac{1}{2}} \; \alpha G' \; \bar{d}^{\frac{1}{2}}, \qquad (3.9)$$

48

where $\bar{d}$ = mean particle diameter,

ρ_s = soot particle density,

k = Boltzmann's constant,

T = Temperature,

α = a function of the particle size distribution assumed (= 6.55 for a self preserving distribution (3.63)),

and G' = dispersion force factor ($\sim$ 2.5).

Howard, 1968 (3.39), however, has developed a model based on the assumption that inter-particle electrostatic forces will control the particle coagulation process.

Oxidation

Oxidation processes will affect soot formation in two ways: 1) the gas phase, oxidation reactions may remove the precursors of carbon nuclei or the growth species, and 2) heterogeneous combustion of soot particles by surface reactions with gas phase species. The first of these processes has been considered earlier, and the present section deals only with the heterogeneous process. Figure 3.16 is an attempt to indicate the range of interest for soot oxidation in the diesel engine.

It is generally accepted (Essenhigh et al., 1965 (3.64)) that the rates of these reactions will be kinetically controlled, since particle sizes in the reaction zone are less than those at which diffusion becomes important.

Several authors (e.g. Park and Appleton, 1973 (3.65), Appleton, 1973 (3.66), Wright, 1974 (3.67)) have shown that the surface oxidation rates for soot and for pyrolytic and other forms of graphite are the same, so that use can be made of the large amount of data which is available in the carbon black literature.

The gas phase species which it has been suggested can take part in the oxidation reactions include O_2, O, OH, CO_2, and H_2O. The relative importance of these species in the oxidation of pyrolytic graphite and in the combustion of soot has been the subject of many studies.

Appleton, 1973 (3.66) has applied the semi-empirical expression proposed by Nagle and Strickland-Constable, 1962 (3.68) for the oxidation of graphite to the results of shock-tube experiments on the oxidation of soot. He has concluded that this expression is suitable for estimating soot oxidation rates in practical combustion systems. The Nagle and Strickland-Constable formula for the surface oxidation rate of carbon is;

$$ w = M_c \cdot x \cdot \left[\frac{k_A \, p_{O_2}}{(1 + k_z \, p_{O_2})} \right] + M_c \cdot k_B \cdot p_{O_2} \, (1 - x) \quad \text{gm.cm}^{-2}.\text{sec}^{-1} $$

$$(3.10)$$

where M_c = molecular weight of carbon,

p_{O_2} = partial pressure of oxygen, atm.,
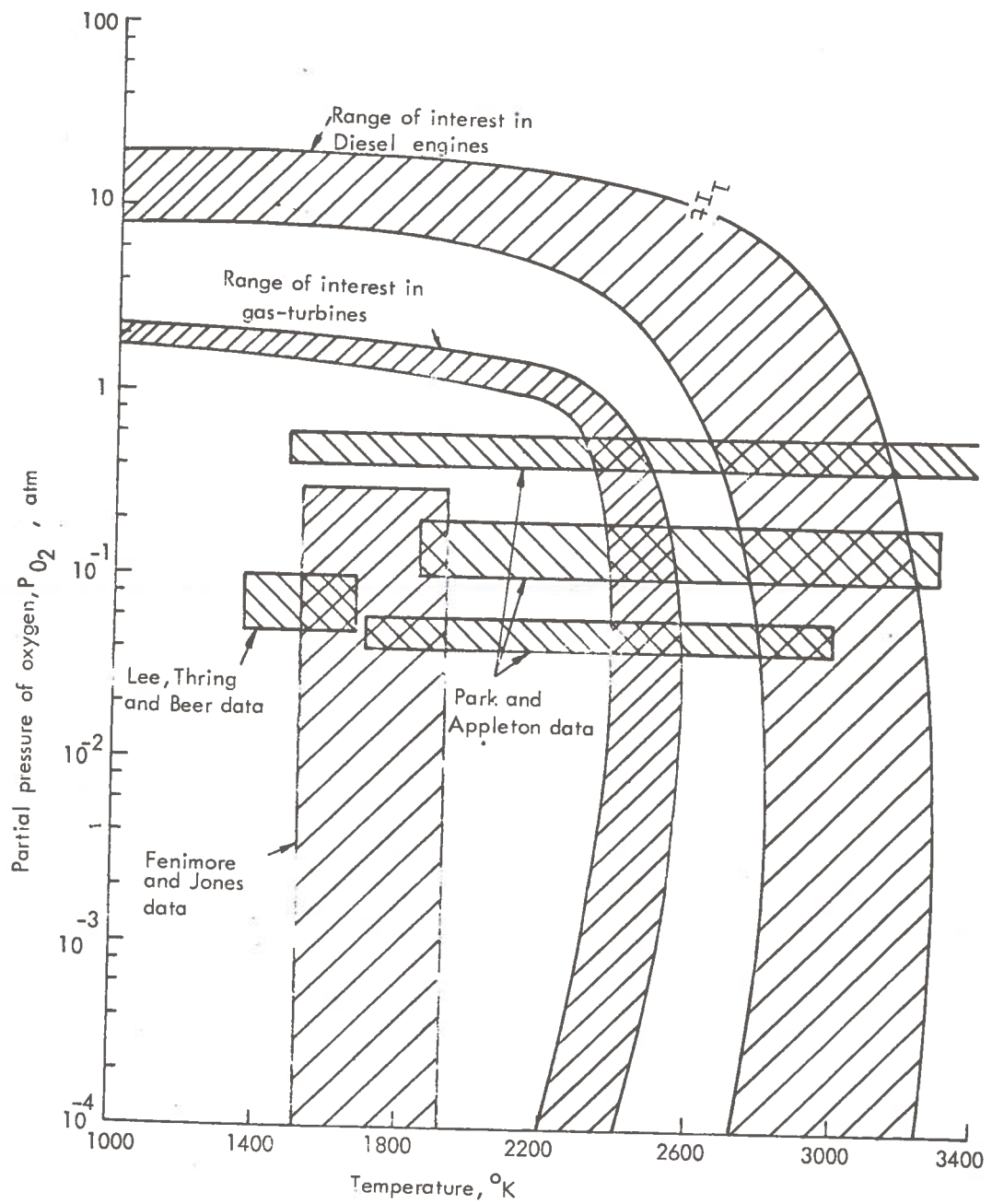
(Based on Appleton (3.66) with additional data
incorporated)

FIGURE 3.16.   COMPARISON OF REGIMES IN WHICH SOOT OXIDATION RATE MEASUREMENTS
HAVE BEEN MADE, WITH THE RANGE OF OPERATING CONDITIONS FOR A GAS–TURBINE
AND DIESEL

$$k_A = 20 \exp(-30,000/RT) \text{ gm.cm}^{-2}.\text{sec}^{-1}.\text{atm}^{-1},$$

$$k_B = 4.46 \times 10^{-3} \exp(-15,200/RT) \text{ gm.cm}^{-2}.\text{sec}^{-1}.\text{atm}^{-1},$$

$$k_z = 21.3 \exp(-4,100/RT) \text{ atm}^{-1},$$

$$x = \left[1 + \frac{k_T}{P_{O_2} \cdot k_B} \right]^{-1},$$

and $k_T = 1.51 \times 10^5.\exp(-97,000/RT) \text{ gm.cm}^{-2}.\text{sec}^{-1}.$

Figure 3.17 shows the complex way in which this function varies with temperature and oxygen partial pressure.

Wright, 1974 (3.67), in studying the oxidation of soot by O atoms at low pressures and temperatures, has also shown that the rates of oxidation of soot, of pyrolytic graphite and of a vitreous carbon are about the same in the range studied (figure 3.18).

The work by Lee et al., 1962 (3.69) on soot oxidation in a laminar hydrocarbon diffusion flame over a limited range of temperature and pressure suggested a rate of surface oxidation of the following form,

$$w = 1.085 \times 10^4.P_{O_2}. \exp(-39,300/RT). T^{-\frac{1}{2}} \text{ gm.cm}^{-2}.\text{sec}^{-1}$$

(3.11)

Recent work by Feugier, 1972 (3.70) and 1974 (3.71) on soot oxidation under similar conditions to those of Lee et al., at temperatures of 2000 - 2300 K has shown that the formula of Nagle and Strickland-Constable can correlate the results.

Broome and Khan, 1973 (3.7) state that the activation energy for the carbon/carbon dioxide and carbon/water vapour reactions are roughly similar and are both much higher than that of the carbon/ oxygen reaction. Thus Tesner and Tsibulevsky, 1967 (3.72) from experiments on acetylene diffusion flames have deduced a soot oxidation rate due to CO_2 of

$$w = 1.15 \times 10^5.P_{CO_2} \exp(-75,000/RT) \text{ gm.cm.}^{-2}\text{sec.}^{-1} \quad (3.12)$$

Donnet et al., 1971 (3.73) have studied the relative rates of reaction of CO_2, H_2O and O_2 with isotropic graphite at temperatures of 1100 - 1200 K. They found that at 1100 K the rate of the C-O_2 reaction was approximately 2500 times that of the C-CO_2 and C-H_2 reactions. The ratio of the rates is strongly temperature dependent, however, and at 1200 K the C-O_2 reaction was only about 1200 times that of the C-CO_2 reaction.

The work of Golovina and Samsonov, 1971 (3.74) on the effect of elevated pressure (1 to 30 atm.) and temperature (1400 to 3400 K)
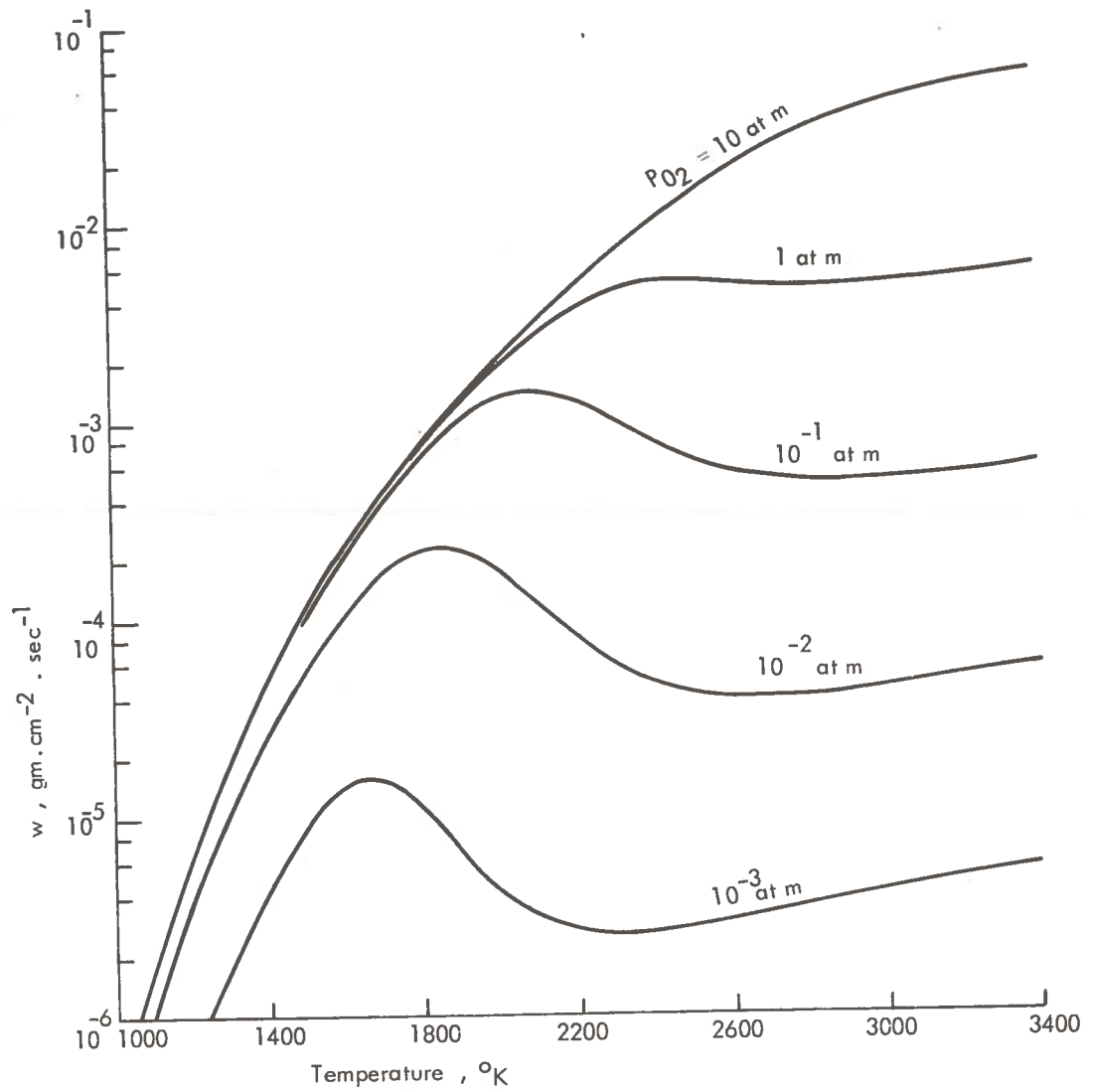
(From Ref. 3.68)

FIGURE 3.17. GRAPHITE SURFACE OXIDATION RATE BY O_2 VS TEMPERATURE AS GIVEN BY THE FORMULA OF NAGLE AND STRICKLAND–CONSTABLE
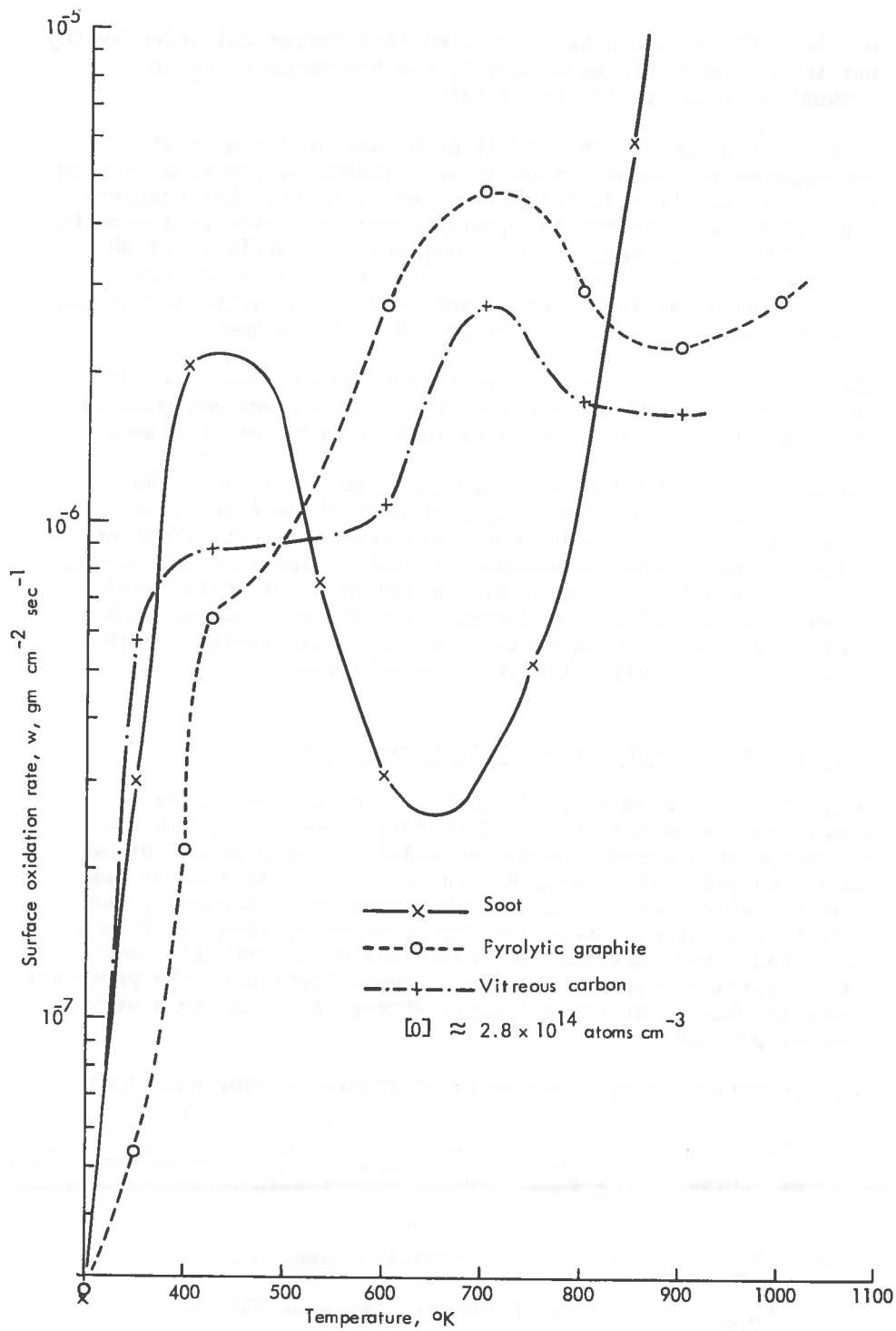
(After Wright (3.67))

FIGURE 3.18. EXPERIMENTALLY MEASURED EFFECT OF TEMPERATURE ON THE RATE OF OXIDATION OF VARIOUS CARBONS BY OXYGEN ATOMS, (O)≃2.8 x 10^{14} atoms.cm.$^{-3}$

on the $C-CO_2$ reaction has indicated that carbon oxidation by CO_2 may be of comparable magnitude to the oxidation by O_2 in combustion products (figure 3.19).

Fenimore and Jones, 1967 (3.75) have suggested that soot consumption in flames can occur as a result of reaction with OH radicals. Appleton (3.66) has argued, however, that Fenimore and Jones's results may be equally consistent with oxidation by O_2. It has been indicated that although the activity of OH radicals is high, their concentration is low at equivalence ratios weak of stoichiometric, and so their contribution to the overall soot oxidation process is likely to be small.

The works of Rosner and Allendorf, 1968 (3.76) and of Wright, 1974 (3.67) have also indicated that oxygen atoms may play an important role in the removal of soot in hydrocarbon flames.

Dalzell et al., 1970 (3.77) and Magnussen, 1974 (3.78) have studied the light scattered by soot in turbulent acetylene diffusion flames, and have concluded that the soot oxidation relations determined in laminar diffusion flames do not account for their results. Dalzell has suggested a qualitative model in which eddies of soot-containing gas mix with oxygen-rich eddies, and the soot particles then burn very rapidly with a typical particle half life of 7.4×10^{-3} sec.

3.2 Models of Soot Formation in Diesel Engines

Only the work of Khan et al. (3.79, 3.80) has attempted to investigate soot formation and removal processes within the framework of a Diesel combustion model. (A very recent Diesel emissions model (Hiroyasu, H. and Kadota, T, SAE 760129) has also included soot formation. The processes considered, and resulting equations used, are very similar to those of Khan et al., though the empirical constants are of course different). Their approach represents a gross simplification of the processes involved, but is at least a first attempt to treat this very complex problem.

Soot formation is represented by an Arrhenius type equation:

$$\left(\frac{dm_s}{dt}\right)_{form.} = C_s \frac{V_u}{V_{NTP}} \cdot \Phi_u^{\,n} \cdot P_u \cdot \exp\left[\frac{-E_s}{R_oT_u}\right] \text{gm/m}^3 \text{ sec.} \quad (3.13)$$

where V_u = volume of soot formation zone, m^3,

V_{NTP} = volume of cylinder contents at NTP, m^3,

P_u = partial pressure of unburned fuel, kN/m^2,

Φ_u = local unburned equivalence ratio for soot formation zone,

R_o = universal gas constant, cal/gm.mole ^oK,

54
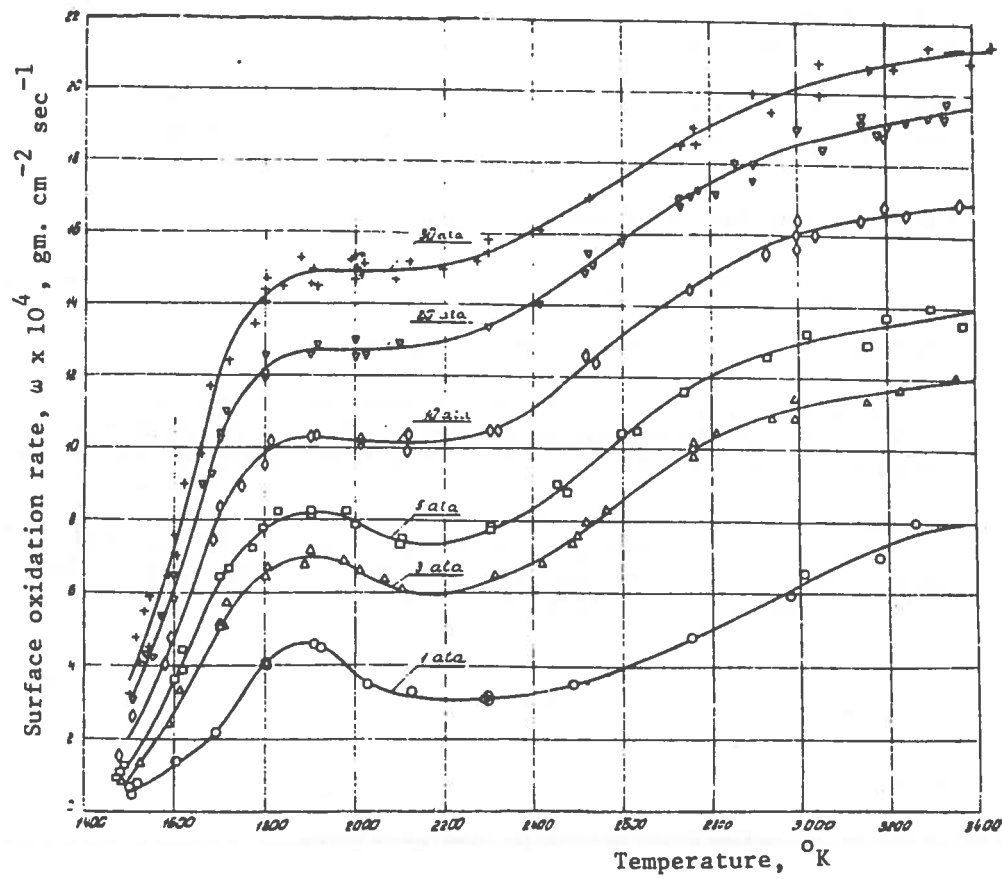
(From Golovina and Samsonov (3.74))

FIGURE 3.19. EXPERIMENTALLY MEASURED GRAPHITE SURFACE OXIDATION RATE BY CO_2 VS. TEMPERATURE AND TOTAL PRESSURE $(P_{CO2} = \frac{1}{2}pTot)$

$$T_u \quad = \quad \text{temperature of soot formation zone, } {}^\circ K$$

$$C_s \quad = \quad \text{soot formation pre-exponential constant, mg/Nm.s.}$$

and $\quad E_s \quad = \quad$ activation energy for soot formation, cal/mole.

A value of E_s = 40,000 cal/mole was determined from a series of engine experiments in which the cycle temperature was varied while holding other conditions constant (3.81). Similarly, experimental data that gave large changes in the Φ_u history were used to determine a value of the exponent n = 3. The value of the constant C_s was determined by matching the calculated soot in the exhaust with the experimentally determined soot in exhaust for a series of test conditions.

It must be noted that the above equation (3.13) implies homogeneous soot formation, i.e. it is assumed not to depend on soot particle size or number density.

After formation the soot is assumed to exist in the form of spherical particles of 250 $\overset{\circ}{A}$ diameter which then undergo coagulation and combustion (3.80).

Particle coagulation is assumed to obey the equation

$$\frac{dN}{dt} \quad = \quad {}^-C_{coag.} \; N^2 \tag{3.14}$$

where N = particle number density (part./cm^3).

The constant C_{coag} was chosen to fit experimental results at one engine test condition, and is assumed constant throughout the coagulation period with the value 1.4×10^{-4} cm^3/part.sec.(3.82).

Generally in coagulation theory, the coagulation coefficient, C_{coag}, is assumed to be a function of particle size and temperature. Thus by analogy to the kinetic theory (Fenimore and Jones, 1969 (3.59), Samkhan et al., 1971 (3.61));

$$C_{coag} \quad = \quad 2\sigma^2 \quad (\frac{\pi \; R_o T}{M})^{\frac{1}{2}} \quad \text{cm}^3/\text{part.sec.} \tag{3.15}$$

where σ = particle diameter (cm.)

$\quad$ M = molecular weight of the particle,

$$= \quad \frac{\pi}{6} \quad \sigma^3 \; . \; N_A . \rho_s \; \text{(gm/gm.mole)}$$

$\quad N_A$ = Avogadro's number (6.023×10^{23} gm.mole^{-1})

and $\quad \rho_s$ = soot density ($\sim$ 2 gm/cm^3).

For a particle of diameter, $\sigma = 250$ Å, and temperature 1500 K, equation (3.15) gives $C_{coag} = 2.5 \times 10^{-9}$ cm^3/part.sec., and for $\sigma = 10^5$ Å, and temperature 1500 K, $C_{coag} = 1.6 \times 10^{-8}$. Thus the constant value used by Khan et al. is many times larger than theoretical estimates based on the assumption of stagnant conditions, and Brownian collisions. Khan et al. (3.80) have suggested that the high value of the coefficient obtained from engine results is due to high air velocities and turbulence effects within the engine cylinder.

Soot particle combustion is assumed to occur as a surface oxidation process, at a rate given by (3.80, 3.82)

$$\left(\frac{dm_s}{dt}\right)_{oxid.} = C_{ox} \frac{\pi \sigma^2}{T^{\frac{1}{2}}} \exp\left(\frac{-E_{ox}}{R_o T}\right) . P_{O_2} \quad gm/cm^2 sec.$$

(3.16)

where σ = soot particle diameter, cm.,

T = local temperature, °K,

P_{O_2} = local partial pressure of oxygen (atm.)

E_{ox} = activation energy for soot combustion (cal./mole)

and C_{ox} = soot oxidation constant (gm.°K$^{\frac{1}{2}}$/atm.sec.cm^2).

This expression is based on the work of Lee, Thring and Beer (3.69) for soot oxidation in rich, laminar hydrocarbon flames. The activation energy, $E_{ox} = 39300$ cal/mole, is taken from the work of Lee, but Khan has used a value of $C_{ox} = 7.5 \times 10^4$ instead of Lee's value of 1.085×10^4 for the pre-exponential constant. This value of C_{ox} (= 7.5×10^4 gm.°K$^{\frac{1}{2}}$/atm.sec.cm^2) was determined from experiments in which Diesel exhaust soot was recirculated through a motored cylinder, and the weight loss of soot measured (3.80).

However, as discussed in section 3.1.4.e, the validity of a simple Arrhenius equation to describe soot oxidation is doubtful (Appleton, 1973 (3.66)). Appleton has suggested that the Nagle and Strickland-Constable formula (eqn. 3.10) is more suitable for estimating soot oxidation rates in practical combustion systems. Figure 3.20 is a comparison of the soot oxidation rate given by eqn.(3.10) and (3.11). As can be seen, the Lee, Thring and Beer equation (3.11) gives an oxidation rate very much larger than the Nagle and Strickland-Constable formula at high temperatures, and also at low temperatures ($\sim$ 1500 K) and high oxygen partial pressures (1-10atm).

It must also be noted that in reference (3.80) in which Khan determined the pre-exponential constant, C_{ox}, the particle size upon which the calculations were based was the diameter of the coagulated soot from the Diesel exhaust ($\sim$ 6000 to 11000 Å). Since these coagulated particles are likely to consist of chains or agglomerates of much smaller particles ($\sim$200 to 500 Å), it is felt that it was unrealistic to base calculations on the coagulate diameter.
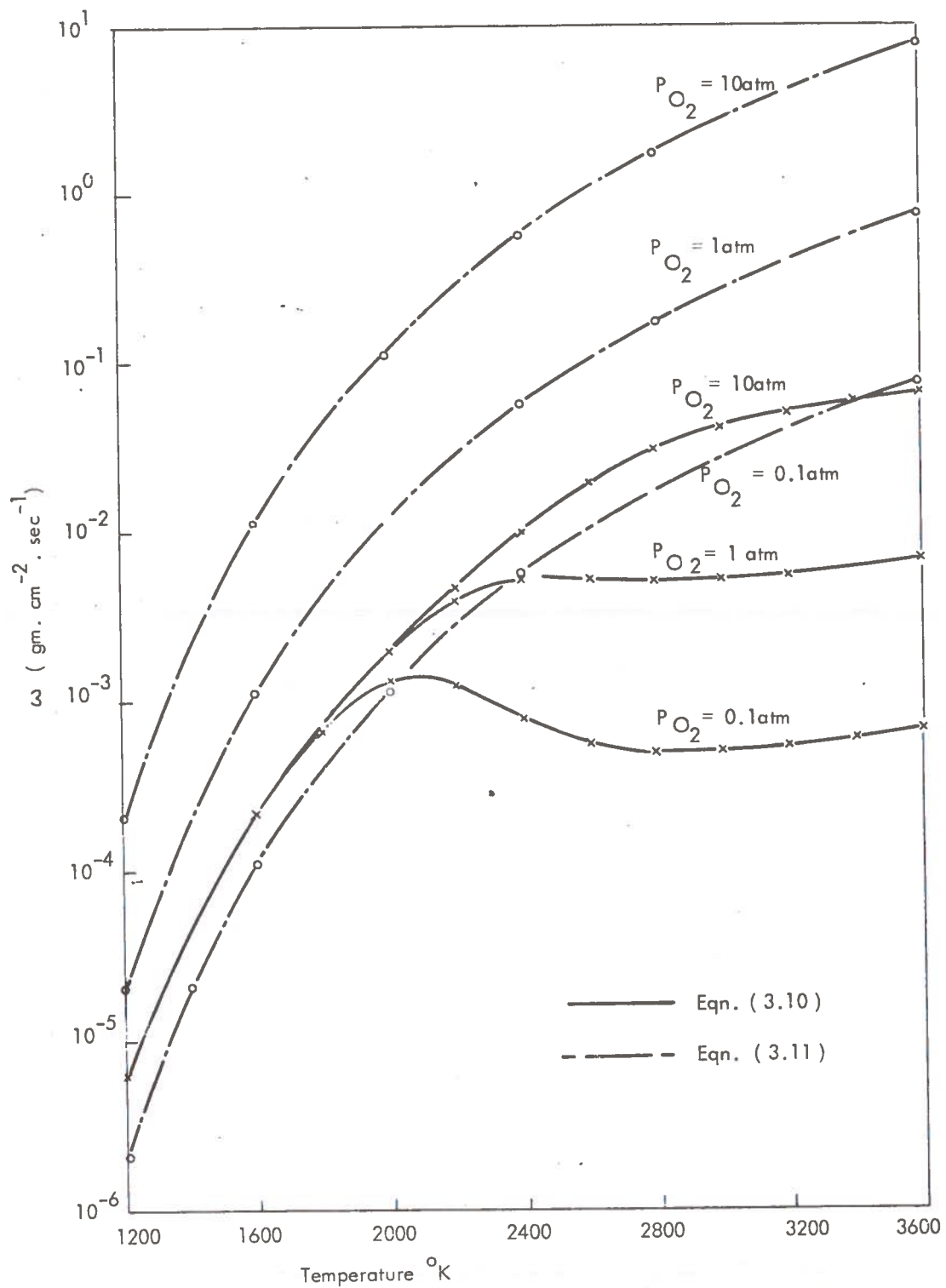
FIGURE 3.20. COMPARISON OF SOOT OXIDATION RATE GIVEN BY THE EQUATION OF NAGLE AND STRICKLAND – CONSTABLE (EQU. 3.10) AND OF LEE, THRING AND BEER (EQN. 3.11), AS A FUNCTION OF TEMPERATURE AND O_2 PARTIAL PRESSURE.

In view of these two criticisms, it is felt that the results of Khan et al. would repay further investigation.

3.3 Exhaust Smoke Measurements at Southampton

3.3.1 Engines and Methods

Diesel engines were tested for exhaust smoke at Southampton according to the procedure recommended by B.S. AU 141 (3.83). The equipment used for these smoke tests was a Hartridge light obscuration meter. The details of the engines tested are shown in Table 2.3. The results are for rated engine speed and load conditions.

3.3.2 Results and Discussion

The results of the tests are shown against converted Bosch Units in Figure 3.21 and compared with B.S. limits in Figure 3.22. It can be seen that the experimental unmatched turbocharged engine B produces smoke in excess of both the limits and all other engines. The matched turbocharged engines A and E as well as the IDI engine G show lower smoke levels than the other DI engines tested. All the production engines have been developed for performance without optimisation for minimal emissions. The designs have been such that the legal smoke requirement was just satisfied (Figure 3.22). The lower smoke levels with matched turbocharged and suise engines are attributed to improved fuel-air mixing, even though associated with slightly retarded fuel injection timing in the two designs. The increased smoke level from the unmatched turbocharged engine B is due to the higher specific fuel consumpton of this set up. The higher specific fuel consumpton is close to that characteristic of the indirect combustion system.
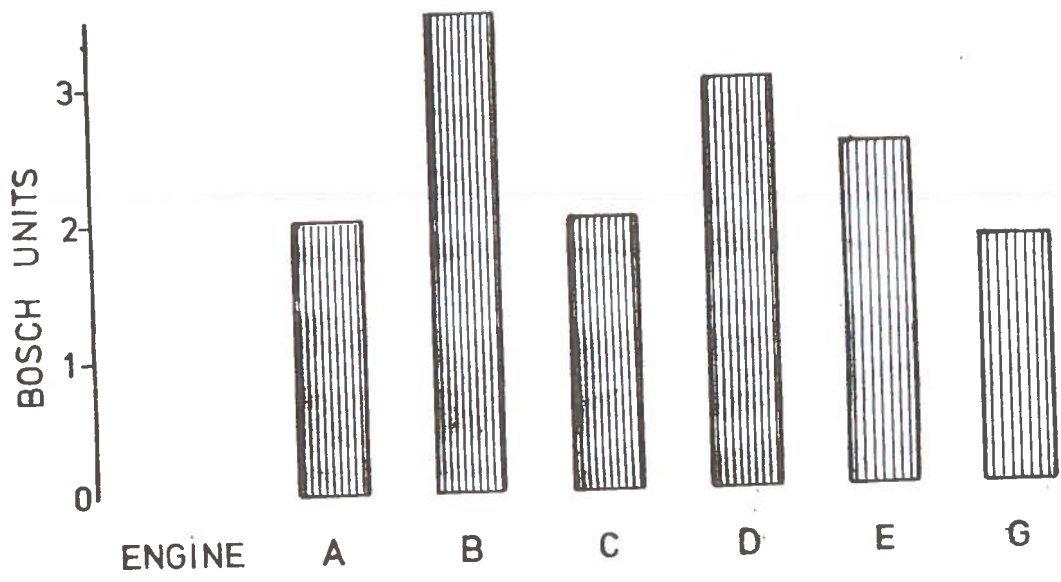
(From Anderton et al 3.84, 3.85)

FIGURE 3.21. SMOKE EMISSIONS IN BOSCH SMOKE UNITS AT RATED ENGINE SPEED AND LOAD
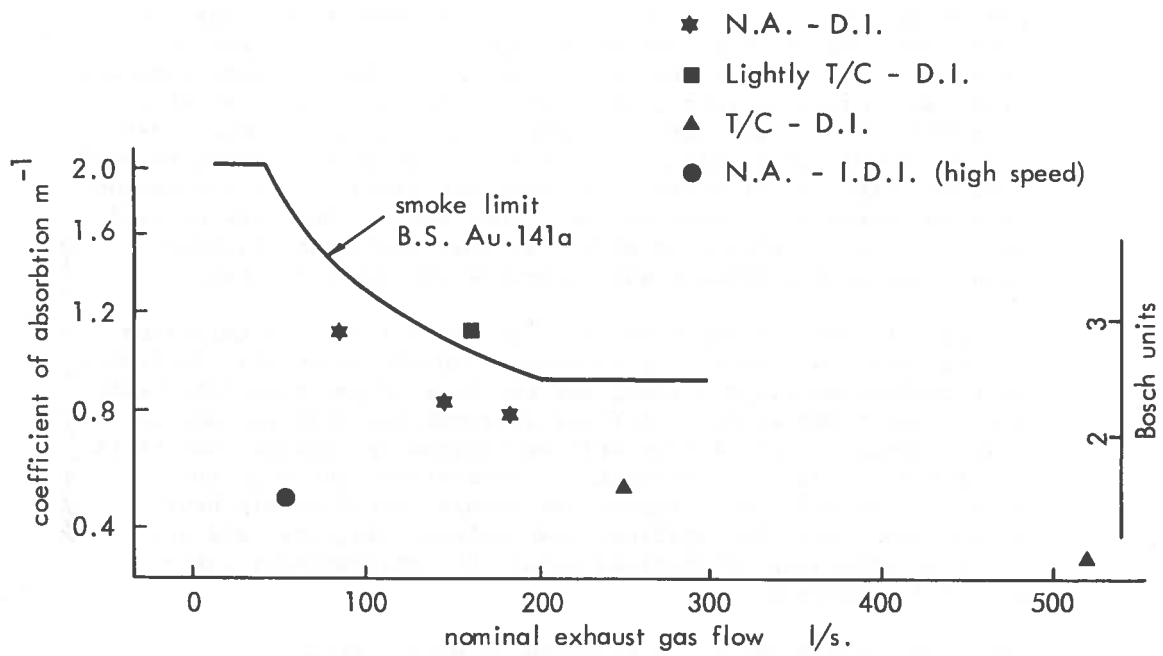
FIGURE 3.22. SMOKE EMISSIONS FROM ENGINES TESTED AND RELATION TO B.S. AU141a.

4. REVIEW OF DIESEL ENGINE EMISSIONS MODELLING

4.1 Introduction

Experimental measurements of cylinder pressure versus crank angle give an insight into the thermodynamics of the processes occuring during Diesel combustion. Thus the early work of, for example, Lyn, 1963 (4.1) assumed the cylinder contents to consist of a homogeneous charge with specific heat a function of the overall equivalence ratio and mean temperature. This allows the calculation of an "apparent rate of heat release" by application of the first law of thermodynamics, from the cylinder pressure diagram and a knowledge of cylinder geometry.

The inverse problem of assuming a rate of heat release diagram, and using this to calculate a cylinder pressure-time diagram has also been studied (e.g. Austen and Lyn (4.2)). This has been followed up by attempts to produce empirical heat release diagrams from fuel injection rates, which will reproduce experimentally measured cylinder pressure diagrams (e.g. Lyn (4.1), Whitehouse and Way (4.3), Shipinski et al. (4.4)). It must be borne in mind however, that all of these approaches are based on the assumption of a homogeneous cylinder charge. They cannot therefore be used as the basis for emissions models because only mean cylinder conditions of temperature and concentration are predicted.

In order to predict experimentally measured levels of emissions it has been found necessary to develop models which will determine peak combustion temperatures, and the mass of gas associated with these peak temperatures. A first approach has been to take an 'experimental' rate of heat release diagram and assume that it is the result of local stoichiometric combustion (see e.g. the Backhouse model). More recent and sophisticated models have broken away from the empirical heat release diagrams, and are based on modelling assumptions about the heterogeneous fuel-air mixing process.

The models which are to be reviewed in detail are;

> Bastress, Chng and Dix, 1971 (4.5)
> Khan, Greeves and Probert, 1971 (4.6)
> Backhouse, 1973 (4.7)
> Hodgetts and Shroff, 1975 (4.8)
> Shahed, Chiu and Lyn, 1975 (4.9)
> and Baluswamy, 1976 (4.10).

A detailed analysis of the models of Bastress et al., and of Khan et al., has been carried out previously by Wilson et al., 1974 (4.11).

Appendix II lists the remaining Diesel emissions models for completeness.

62

4.2 Model B

4.2.1 Summary

This model (ref 4.5) is based on an empirical mixing model which
was chosen to give a realistic heat release rate. Following an
empirically specified ignition delay, fuel is assumed to shift
instantly from the pure fuel state to combustion product when
mixed with air. Subsequently the product mixes with more air
during a specified mixing time. Nitric oxide formation is
assumed to occur in the post combustion products as given by a
six-equation extended Zeldovich mechanism.

The model is primarily designed to simulate the direct injection
process, but has also been modified to model the indirect injection
engine (4.12).

4.2.2 Description of the Model

Fluid within the cylinder is considered to be uniform in pressure
and to consist of a set of systems of variable mass:

1) Air and residual gas mixture – one system designated by
    subscript 'a'

2) Liquid fuel – one system, subscript 'f'

3) Vaporized fuel – one system, subscript 'fg'

4) Burned mixture (combustion products and excess air) – i
    systems (or elements), subscript 'bm,i'.

The model does not take into account the physical location of these
systems within the chamber. The burned mixture system 'i' is
assumed to contain all of the product formed during the ith crank
angle increment.

Mixing between fuel and air is patterned after Lyn's "preparation
to burn" process (4.1). Prior to mixing the fuel can be thought
of as liquid, and the mixing occurs due to vaporization. An
element of liquid fuel, injected during crank-angle interval, j,
is assumed to vaporize at a rate:

$$\frac{d(m_{f1,j})}{d\theta} = -C \frac{(\theta - \theta_{in,j})}{C_1^2} \cdot \exp\left[-\frac{(\theta - \theta_{in,j})}{C_1} \right], \quad (4.1)$$

where C = a constant related to the mass of fuel injected during
crank angle interval j,

C_1 = a vaporization rate constant,

and $(\theta - \theta_{in,j})$ = the time since injection of the element.

Ignition delays is specified by an empirical correlation developed by Tsao et al. (4.13), and is a function of the cylinder pressure and temperature at start of injection, and of engine speed. Following the ignition delay, the mixture prepared (or premixed) is assumed to burn at a rate described by a triangular-shaped burning function, with a base of C_2 $^{\circ}$CA (figure 4.1). Following this initial burning period the fuel burning and vaporization rates are assumed equal. During the second period of heat release, burning occurs at a specified mixture ratio, F_m, assumed to be stoichiometric. During the initial burning period, the fuel mass fraction at combustion, F°_{bm}, is allowed to diverge from F_m by an amount ΔF, according to an arbitrarily specified equation.

The rate of mixing of air with the burned mixture systems is specified by a parameter C_3 ($^{\circ}$CA).

Total heat transfer between the cylinder contents and chamber walls is expressed as

$$Q = C_4 \cdot A(T_h - T_w), \tag{4.2}$$

where A = surface area of the chamber

   T_h = mean temperature of fluid in chamber

   T_w = mean wall temp,

and C_4 = constant of heat transfer.

The total heat transfer is apportioned between each system according to the volume of the system.

In order to determine chamber pressure at each crank angle step, it is assumed that the mixture within the chamber is homogeneous and in thermodynamic equilibrium.

4.2.3 Nitric Oxide Kinetics

Nitric oxide formation is modelled by a six-equation extended Zeldovich mechanism (4.14):

(i) $N + NO \rightleftharpoons N_2 + O$

(ii) $N + O_2 \rightleftharpoons NO + O$

(iii) $N + OH \rightleftharpoons NO + H$

(iv) $H + N_2O \rightleftharpoons N_2 + OH$

(v) $O + N_2O \rightleftharpoons N_2 + O_2$

(vi) $O + N_2O \rightleftharpoons NO + NO$
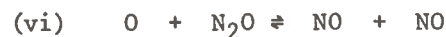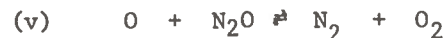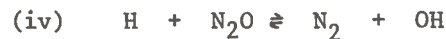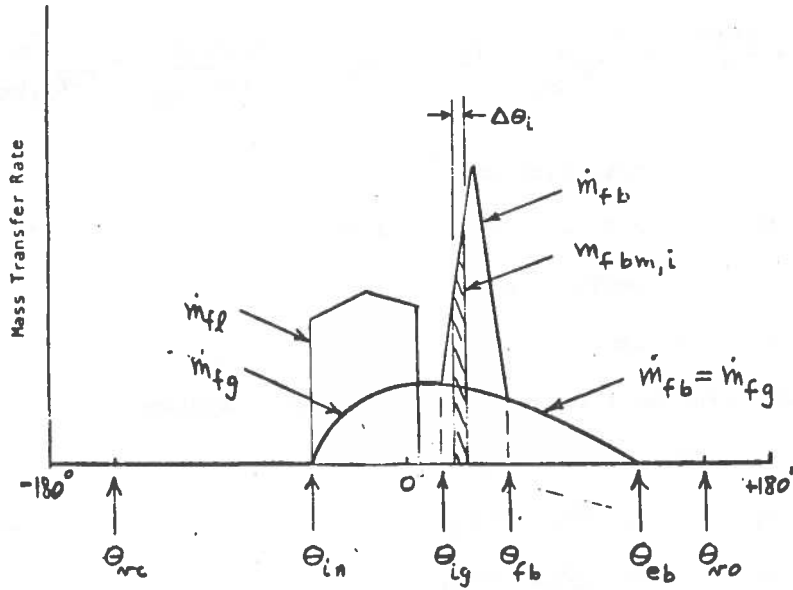
FIGURE 4.1. MODEL ENGINE COMBUSTION CYCLE AND MASS TRANSPORT PROCESSES
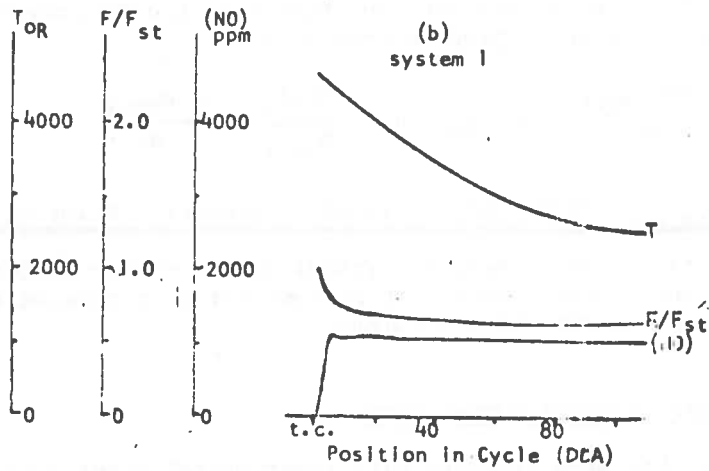
FIGURE 4.2. PREDICTED CONDITIONS IN BURNT ELEMENT SYSTEMS VS. CRANK ANGLE

On the assumpton that the hydrocarbon – oxygen reactions go rapidly to completion, to give equilibrium concentrations of N_2, O_2, O, OH, and H, and assuming steady state values for the concentration of N_2O and N, the above scheme gives, for the mass fraction of NO formed in system i, per degree crank angle;

$$\dot{r}_{bm,i} = \frac{d(NO)}{d\Theta} = \frac{2 \cdot M_{NO}}{6 \cdot N\rho_{bm,i}} \quad (1 - \alpha^2_{bm,i}) \quad (\frac{R_1,bm,i}{1+\alpha K_{1,bm,i}} + \frac{R_6}{1+K_{2,bm,i}}),$$

(4.3)

where ( ) = mass faction

$\quad M_{NO}$ = molecular weight of NO

$\quad N$ = engine r.p.m.

$\quad \rho$ = density

and subscript bm,i refers to burned product system 'i'.

$\quad \alpha$ = $[NO] / [NO]_e$

$\quad R_1$ = $k_{1f} [N]_e [NO]_e$

$\quad R_6$ = $k_{6f} [O]_e [N_2O]_e$

$\quad [\ ]$ = molar concentration

$\quad K_1$ = $R_1/(R_2 + R_3)$

$\quad K_2$ = $R_6/(R_4 + R_5)$

and R_2 to R_5 are defined similarly to R_1 and R_6.

It is assumed that NO reactions do not proceed in the air system, so that $(NO)_a$ is a constant, and therefore the NO conservation relation for a burnt product system is

$$\frac{d(NO)_{bm,i}}{d\Theta} = \dot{r}_{bm,i} + \frac{(NO)_a}{m_{bm,i}} \frac{d\ m_{bm,i}}{d\Theta} , \qquad (4.4)$$

where $m_{bm,i}$ = total mass of system i (product + diluting air).

Figures (4.2 – 4.4) indicate typical burned system histories, showing that, once formed, the NO concentration freezes at very nearly the maximum value attained.

4.2.4 Experimental Comparisons

The model has been compared with experimental results by Wilson et al (4.11). A single cylinder direct injection engine was used
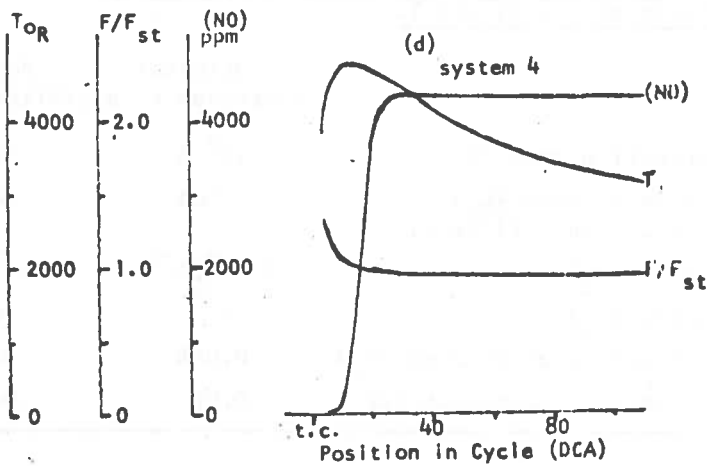
(From Bastress et al. (4.5))

FIGURE 4.3. PREDICTED CONDITIONS IN BURNT ELEMENT SYSTEMS VS. CRANK ANGLE
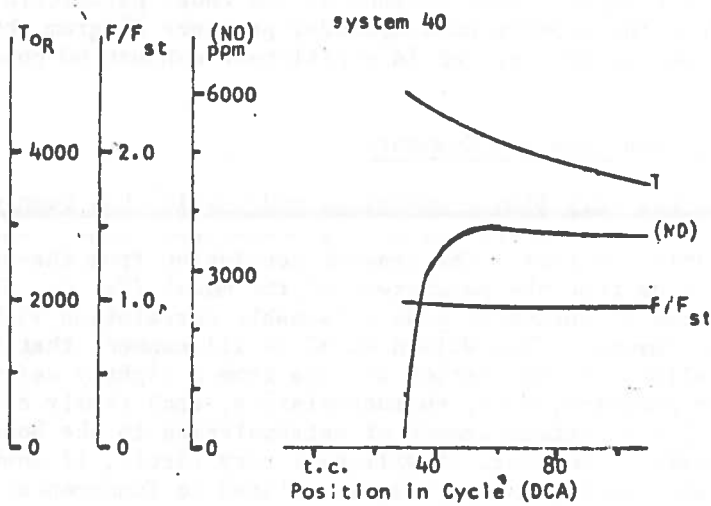
(From Bastress et al. (4.5))

FIGURE 4.4. PREDICTED CONDITIONS IN BURNT ELEMENT SYSTEMS VS. CRANK ANGLE

67

for the comparison, with 140mm (5.5in.) bore, 152mm (6 in.) stroke and at engine speeds of 1500 - 2100 r.p.m. The authors found that in order to obtain reasonable agreement between the model and their experimental results, the values of the model parameters required adjustment as indicated in the table. Wilson et al also suggested that the model could be further adjusted by assigning

---

Values of the parameters for the model of Bastress et al. (after Wilson et al. (4.11)).

	Original (Bastress et al)	Adjusted (Wilson et al)
Fuel vaporization rate (C_1)	$10^{\circ}CA$	$17^{\circ}CA$
Fuel gas burning rate (C_2) (base of "premixed" triangle)	$10^{\circ}CA$	$10^{\circ}CA$
Dilution rate (C_3)	$0.05^{\circ}CA^{-1}$	$0.01^{\circ}CA^{-1}$
Heat transfer (C_4)	10^{-3}	10^{-3}
Mean fuel fraction at burning (F_m)	0.066	0.066
Fuel mass fraction increment (ΔF)	0.01	0.003

---

individual values of C_1 and C_2 to each fuel element. With the adjusted parameters shown in the table, the model simulated "reasonably well" the emissions behaviour with changes in load, timing and turbocharging. However, the effects of air temperature, compression ratio, engine speed and rate of injection were not adequately predicted.

Bennethum et al. (4.15) have also mentioned their attempts to compare the predictions of this model with engine test data. They found that several combinations of the model parameters could reproduce the experimental cylinder pressure diagram, but that each combination resulted in a different exhaust NO concentration.

4.2.5 Discussion and Comments

This is the only Diesel emissions model which has been used by, and has had results published by, researchers other than the originating authors. The general conclusion from these comparisons seems to be that the parameters of the model (C_1, C_2, C_3, C_4, F_m and ΔF) can be chosen to give reasonable correlation with the results of experiments. Thus Wilson et al (4.11) comment that the model "will allow the correlation of data from a tightly defined (similar chamber geometry, swirl characteristics, etc) family of engines and will allow a certain amount of extrapolation to the boundaries of this family. However, it will tell very little, if anything about how engine design parameters are related to fundamental combustion and pollution formation phenomena."

In spite of these criticisms, with which the present authors agree , the model is extremely valuable in indicating which processes might be rate controlling in a more realistic Diesel model, and hence which processes must be studied more closely, and modelled more carefully. Bastress et al. conducted an extensive investigation into the effects of the various parameters on the results of the model. This showed, inter alia, that the predicted NO emitted is very sensitive to all of the parameters except the dilution rate parameter, C_3. The fuel consumption, and power predictions were only sensitive to the fuel vaporization rate parameter, C_1, and the heat transfer coefficient, C_4.

Finally, the model as it stands cannot be used as a basis for soot formation modelling since no account is taken of the rich fuel vapour zones at high temperature prior to combustion.

4.3 Model C

This model (4.6) has been reviewed by Wilson et al (4.11), though no details of experimental comparisons were published in the review.

4.3.1 Summary

This emissions model is a four zone extension of an earlier two zone heat release model. Mixing rates between the fuel and ambient gas are modelled using an empirical jet penetration equation, including a modification for wall impingement, and a diffusion rate equation. The zones considered are a fuel rich core, micromixed combustion zone, product-air mixing zone and an ambient air zone.

Nitric oxide formation is modelled in the micromixed combustion zone by a simple semi-empirical equation derived from the Zeldovich mechanism. Soot formation is modelled in the fuel rich core by an empirical equation, and the coagulation and oxidation of soot have also been investigated.

4.3.2 Description of the Model

Details of this model and of the investigations carried out using it have appeared in many publications (4.6, 4.16 - 4.18). It is an extension of an earlier two zone heat release model developed by Grigg and Syed (4.19).

Four zones are considered in the emissions model (figure 4.5);

        1) fuel rich zone, subscript u
        2) micromixed combustion zone, subscript b (NO formation zone)
        3) product-air mixing zone
and   4) ambient air zone, subscript a.

The rate of mixing between the fuel jet and ambient air is based on the macromixing model of Grigg and Syed (4.19) which was derived from the results of the jet penetration experiments of Schweitzer (4.20). Jet tip penetration is given by (figure 4.6);

69

4) Ambient zone

1) Fuel rich core of spray
(soot fomation zone,
T_u, ϕ_u)

3) Product/air
mixing zone

2) Micromixed reaction
zone (heat release and
NO fomation zone
T_b, ϕ_b)

Wall (piston bowl)
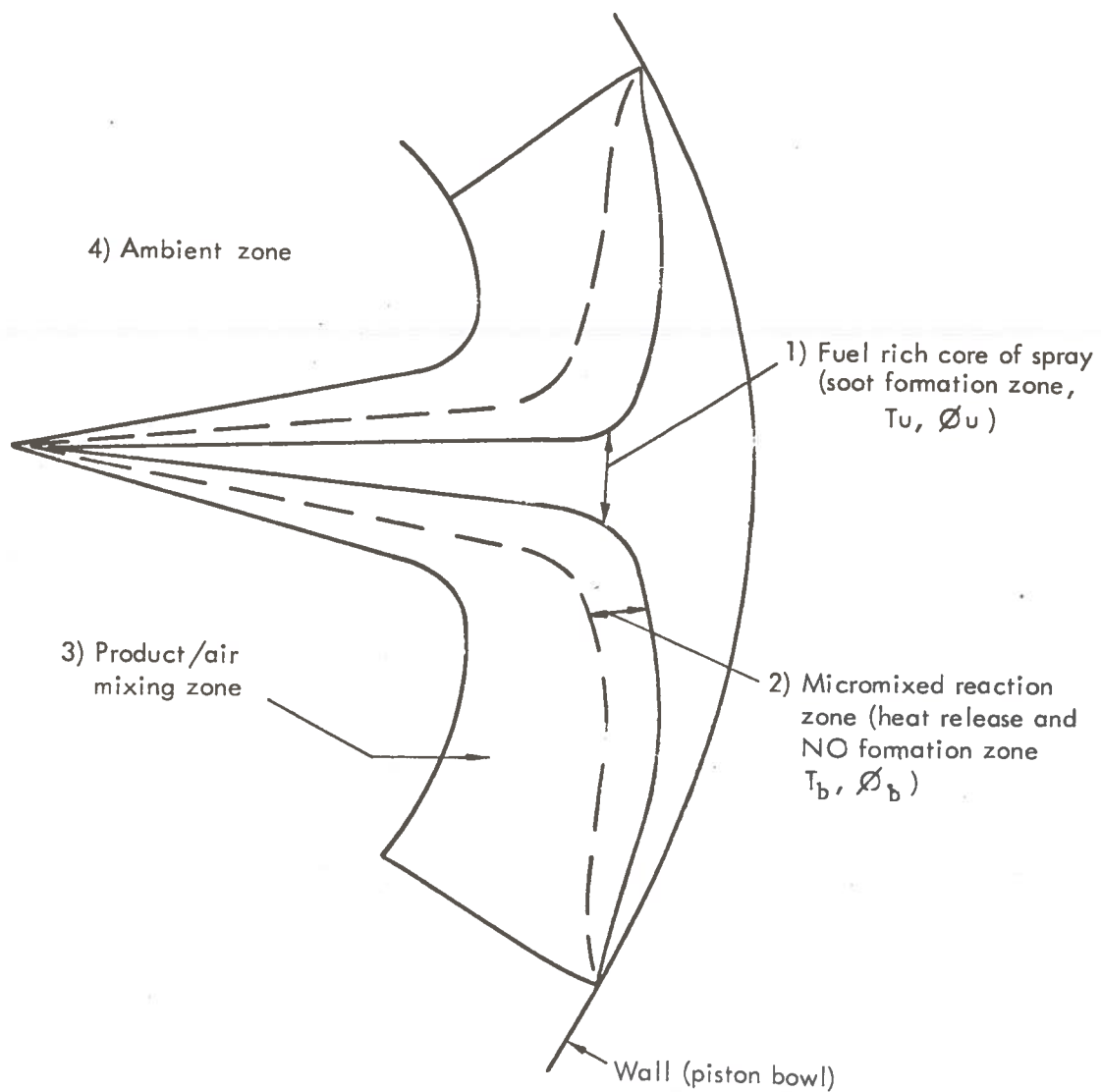
(After Khan et al. (4.16))

FIGURE 4.5.   ZONES OF HEAT RELEASE, SOOT FORMATION AND NO FORMATION
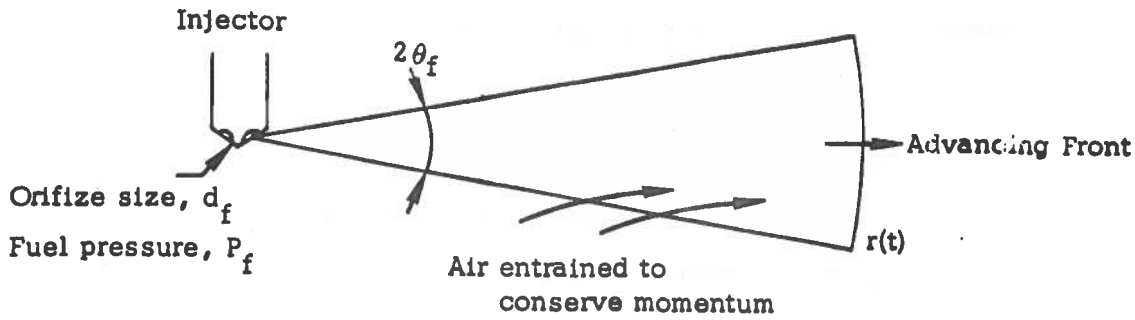
(From Wilson et al. (4.1))

FIGURE 4.6.   CONICAL JET PENETRATION
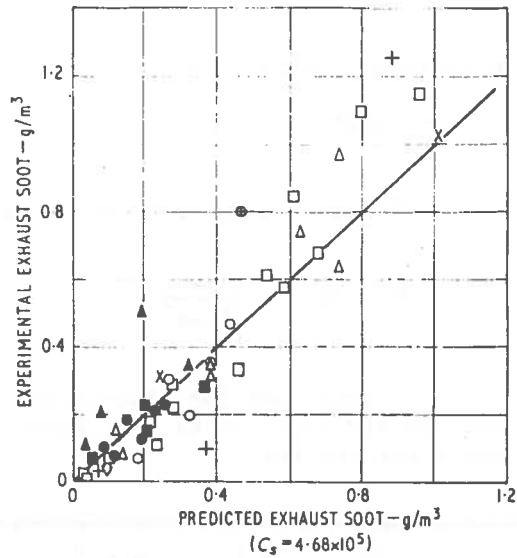
Injection timings of 35°, 30°, 20°, 10°, 5°, and 0° b.t.d.c. are included.

○ 2700 rev/min, 51·5 mm³/stroke ⎫ normal rate
⊔ 2000 rev/min, 30, 50, 60, 70, 75 mm³/stroke ⎬ injection.
△ 1100 rev/min, 60 mm³/stroke ⎭
● 2700 rev/min, 51·5 mm³/stroke ⎫
■ 2000 rev/min, 60 mm³/stroke ⎬ fast rate injection.
▲ 1100 rev/min, 60 mm³/stroke ⎭
+ High swirl ⎫
× Medium swirl ⎬ 1100 rev/min, 60 mm³/stroke.
⊕ Low swirl ⎭

(From Khan et al. (4.6))

FIGURE 4.7.   EXPERIMENTAL EXHAUST SOOT VS. PREDICTED VALUES FOR A SMALL DIRECT INJECTION ENGINE

71

$$r^2 = 1.042 \times 10^6 \cdot d_f \cdot p_f^{\frac{1}{2}} \cdot t \cdot \left(\frac{\rho_{NTP}}{\rho_a}\right), \qquad (4.5)$$

where r =   jet tip penetration, cm.

          d_f =   nozzle-hole diameter, cm.

          p_f =   injection pressure, atm.

          t =   time since start of injection, sec.

       ρ_{NTP} =   air density at NTP

and ρ_a =   ambient zone density.

The rate of air entrainment ("macromixing") is assumed to keep the plume density constant, so that

$$\frac{d(m_a)_j}{dt} = E_r \cdot \frac{\pi}{3} \frac{\rho_a \cdot \tan^2\Theta_f \cdot r^3}{t \cdot \left(\frac{\rho_a}{\rho_{NTP}}\right)} \qquad (4.6)$$

where E_r =   entrainment coefficient

and Θ_f =   jet semi angle.

Assuming conservation of momentum along the free jet axis gives the semi angle,

$$\tan^2\Theta_f = 1.09 \times 10^{-3} \cdot \left(\frac{\rho_a}{\rho_{NTP}}\right) \qquad (4.7)$$

A similar model has been developed for post-impingement macromixing. The macromixed fuel and air (eqn. (4.6)) is assumed to micromix by turbulent diffusion according to:

$$\frac{d(m_a)_b}{dt} = \varepsilon_D \frac{dr}{dt} \cdot \left[(m_a)_j - (m_a)_b \right], \qquad (4.8)$$

where ε_D is a diffusivity constant. Experimental data on ignition delay is used for the engine under consideration, and following ignition, the rate of heat release is assumed to follow a triangular rate law with an arbitrarily specified based of 6°CA. After this initial rapid process, further heat release is mixing controlled by equation (4.8), so that as the fuel and air micromix, they are assumed to shift to equilibrium products instantly.

72

The equivalence ratio of the fuel rich zone is assumed to be given by

$$\Phi_u = \frac{(m_f)_{inj}}{(m_f)_b} \cdot \Phi_u, \text{ mean} \tag{4.9}$$

where $\quad \Phi_u$, mean $= \dfrac{((m_f)_{inj} - (m_f)_b)}{((m_a)_j - (m_a)_b)} \cdot 15,$

$\qquad (m_f)_{inj} \quad = \quad$ mass of fuel injected

and $\qquad (m_f)_b \quad = \quad$ mass of fuel micromixed with air.

The temperature of the fuel-rich zone, T_u, is taken to be the thermodynamic mean temperature of the whole jet. The ambient air zone is assumed to undergo isentropic compression, thus

$$T_a = T_i \left(\frac{p}{p_i}\right)^{\frac{\gamma - 1}{\gamma}} \tag{4.10}$$

where subscript 'i' refers to conditions at ignition. The equivalence ratio of the micromixed zone (or NO formation zone) is given by

$$\Phi_b = \frac{15 \cdot x}{(m_a)_b} \tag{4.11}$$

where $x \quad = \quad$ mass of fuel burned,

and $(m_a)_b = $ mass of micromixed air.

The temperature of this zone is calculated from the heat release and the thermodynamics of the product and air zones.

The model assumes that heat transfer from the micromixed combustion zone accounts for all the heat loss to the walls. The consequences of this assumption are discussed later.

73

4.3.3 Nitric Oxide Kinetics

Khan et al (4.16) consider the Zeldovich mechanism to describe the kinetics of NO formation;

(i) $N_2 + O \rightleftharpoons NO + N$

(ii) $N + O_2 \rightleftharpoons NO + O$

Assuming a steady state concentration of N (4.14), and equilibrium concentrations of N_2, O_2 and O yields the following expression for the rate of change of NO mass fraction;

$$\frac{d(NO)}{dt} = \frac{p}{41.0.T_b} \cdot \frac{k_1 \, [N_2]_e \, [O]_e \cdot (1 - \frac{[NO]^2}{[NO]_e^2})}{1 + (\frac{k_{-1} \, [NO]}{k_{-2} \, [O_2]_e})} \qquad (4.12)$$

where k_1, k_{-1} = forward and reverse rate constant for reaction (i), and $[\ ]_e$ = molar concentration at equilibrium

Also, by assuming that

$$\frac{k_{-1} \, [NO]}{k_2 \, [O_2]_e} \quad \ll \quad 1,$$

equation (4.12) reduces to the simple form

$$\frac{d(NO)}{dt} = \frac{p}{41.0.T_b} \cdot k_1 \, [N_2]_e \, [O]_e \, (1 - \frac{[NO]^2}{[NO]_e^2}) \cdot \qquad (4.13)$$

Equilibrium concentrations of N_2, O and NO are obtained from the data of Vickland et al. (4.21) as a function of temperature and pressure. The rate constant for reaction (i) was modified from a literature value of (4.14).

$$k_1 = 1.36 \times 10^{14} \quad \exp \, (-75,400/R.T) \ cm^3/mole.s$$

to $$k_1 = 7.30 \times 10^{14} \quad \exp \, (-75,400/R.T) \ cm^3/mole.s,$$

i.e an increase of 5.4 times. The reasons for this modification are discussed later.

4.3.4 Soot Kinetics

Soot formation is assumed to occur in the fuel-rich zone, and is given by

$$\left(\frac{dm_s}{dt}\right)_{form.} = C_s \frac{V_u}{V_{NTP}} \cdot \Phi_u^n \cdot P_u \cdot \exp\left(\frac{-E_s}{RT_u}\right), \qquad (4.14)$$

where C_s = soot formation pre-exponential constant (mg/Nm.s),

$\quad\quad\quad E_s$ = soot formation activation energy (cal/mole),

$\quad\quad\quad V_u$ = volume of fuel rich zone (m^3),

$\quad\quad V_{NTP}$ = volume of cylinder contents at NTP (m^3),

$\quad\quad\quad \Phi_u$ = equivalence ratio of the fuel rich zone,

$\quad\quad\quad T_u$ = temperature of the fuel rich zone,

and P_u = partial pressure of unburned fuel (kN/m^2).

Values of E_s = 40,000 cal/mole and n = 3 were chosen to give the best fit to a range of experimental data.

After formation, the soot is assumed to exist in the form of spherical particles of 250 $\overset{o}{A}$ diameter which then undergo coagulation and oxidation.

Particle coagulation is assumed to obey the equation

$$\frac{dN}{dt} = -C_{coag} N^2, \qquad\qquad\qquad (4.15)$$

where N = particle number density $(part./cm^3)$.

The constant C_{coag} was chosen to fit experimental results at one engine test condition (4.17), and is assumed constant throughout the coagulation period with value 1.4×10^{-4} cm^3/part.sec.(4.18).

Soot oxidation is assumed to occur by surface attack of the soot particles by oxygen, at a rate given by the equation of Lee et al. (4.22)

$$\left(\frac{dm_s}{dt}\right)_{oxid.} = C_{ox} \cdot \frac{\pi d^2}{T^{\frac{1}{2}}} \cdot \exp\left(\frac{-E_{ox}}{RT}\right) \cdot P_{O_2} \qquad (4.16)$$

where d = soot particle diameter (cm)

$\quad\quad P_{O_2}$ = local partial pressure of oxygen (atm)

$\quad\quad E_{ox}$ = activation energy for soot oxidation (=39300 cal/mole, (4,17, 4.22))

and C_{ox} = soot oxidation constant (= 7.5×10^4 gm. $^{o}K^{\frac{1}{2}}$/atm.s.cm^2).

4.3.5 Experimental Comparisons

The model has been compared with a large amount of experimental data by the original authors, some of which has been used to determine the model parameters. Published data (4.16) includes comparison of the results of three direct injection engines of sizes; 98 - 130 mm bore, and 120 - 142 mm stroke, over a range of load, speed, injection timing, injection rate and swirl rate. The model seems to correlate the trends of emissions with these five variables rather than the absolute values. Figure 4.7 gives results of the comparison between model and experimental results on exhaust smoke.

4.3.6 Discussion and Comments

The model attempts to use simple equations, based on physical insight and experimental results of jet penetration into air, to describe the mixing process between the fuel spray and ambient air. However, the number of empirical constants required by the model is somewhat large, and reflects the many simplifications introduced. The empirical constants include;

E_r, an 'entrainment' coefficient for macromixing, fitted as a function of engine speed and swirl to data on soot emission,

ε_D, a diffusion constant for micromixing, determined by matching calculated and experimental heat release data as a function of engine speed and load,

E_s, activation energy for soot formation (equation (4.14) determined from experiments in which the cycle temperature was varied while holding other conditions constant, by varying the intake air temperature,

n, equivalence ratio exponent for soot formation, determined from experimental engine data in which large changes in the ϕ_u history were permitted.

The value to be assigned to C_s (equation (4.14)) has been investigated under conditions in which soot oxidation was neglected, and also where this effect was included (4.18). The results of calculations including the effects of soot coagulation and oxidation (equations (4.15) and 4.16)) gave agreement with observed exhaust soot concentration with a value of $C_s = 1.376 \times 10^6$ mg/Nm.s. Khan et al. (4.18) indicate that according to the model an approximately constant fraction of the soot formed is oxidised in the Diesel cylinder over a range of fuel injection timings (Figure 4.8). In the light of this result, they suggest a simplified model in which soot oxidation is neglected, so that the soot exhausted is entirely controlled by equation (4.14). In this case, the value of C_s required for agreement between the model and experiment is $C_s = 4.68 \times 10^5$.

The pre-exponential constant, C_{ox} in the soot oxidation equation (4.16) was obtained from experiments in which exhaust soot from one cylinder of a Diesel engine was recycled through a motored

76
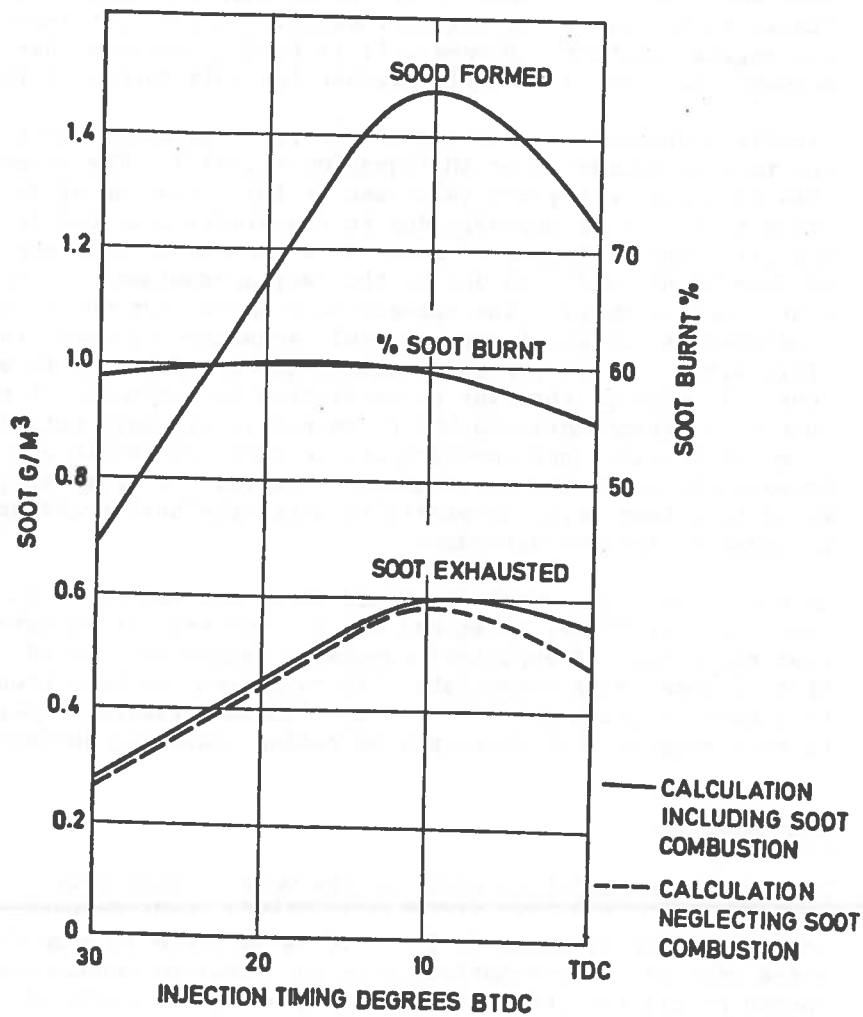
(From Khan et al. (4.18))

FIGURE 4.8. CALCULATION OF THE EFFECT OF INJECTION TIMING ON EXHAUST SOOT;
ENGINE SPEED = 2000 R.P.M.; FUELLING = 60 MM^3/STROKE

cylinder, and the weight change of the soot particles was measured. This experiment gave a higher value of the constant (C_{ox} = 7.5 x 10^4g. $^{o}K^{\frac{1}{2}}$/atm.s.cm^{-2}) than the work of Lee et al. (4.22) on soot oxidation in atmospheric pressure laminar diffusion flames (C_{ox} = 1.085 x 10^4). It should be noted, however, that the validity of Lee's equation at the pressures and temperatures of relevance to Diesel combustion is doubtful (see sections 3.1.4e and 3.2).

The coagulation rate constant (equation (4.15)) required to match the model results to experimental Diesel exhaust particle sizes is very high (C_{coag} = 1.4 x 10^{-4}) compared to experimental values of the constant for aerosols (C_{coag} of the order of 5 x 10^{-8} cm^3/ part.sec. (4.17)). Khan et al. state that the high value is likely to be due to the high air velocities and turbulence within the engine cylinder. However, it is hard to believe that fluid mechanic effects alone could account for this factor of 10^4.

Finally a change was required in the pre-exponential factor for the rate of formation of NO (equation (4.13)). The effect of this is shown in figures (4.9) and (4.10). Khan et al (4.16) argue that this is probably due to the simplifications in modelling the NO formation zone (i.e. the use of only one zone for NO formation), and also due to the very approximate nature of the heat transfer model. The authors have shown that the NO emissions predicted by the model are extremely sensitive to heat transfer (fig. 4.9), i.e. to the temperature history of the NO formation zone. In view of the many uncertainties in any model of this nature, it seems unreasonable to adjust fairly well established chemical kinetic rate coefficients in order to obtain agreement between the model and experimental results. In this case, it would have been more acceptable to alter the heat transfer model, in order to improve agreement.

In conclusion, the model is a good first attempt to produce a comprehensive Diesel emissions model. However, it is unfortunate that the number of empirical constants cannot be reduced, and that in some cases established literature values have been altered to produce a reasonable fit to experimental results. These factors suggest that there may be hidden modelling deficiencies.

4.4 Model D

This emissions model is based on the work of Backhouse (4.7) extended to include the kinetics of nitric oxide formation, and soot oxidation by Raine (4.23). It is outlined in some detail, since many of the assumptions made and problems encountered are common to all the other Diesel emissions models reviewed, and this model has yet to be published in the open literature.

4.4.1 Summary

The model requires heat release data as input (i.e. the presence of unburnt liquid and evaporated fuel is neglected). At each
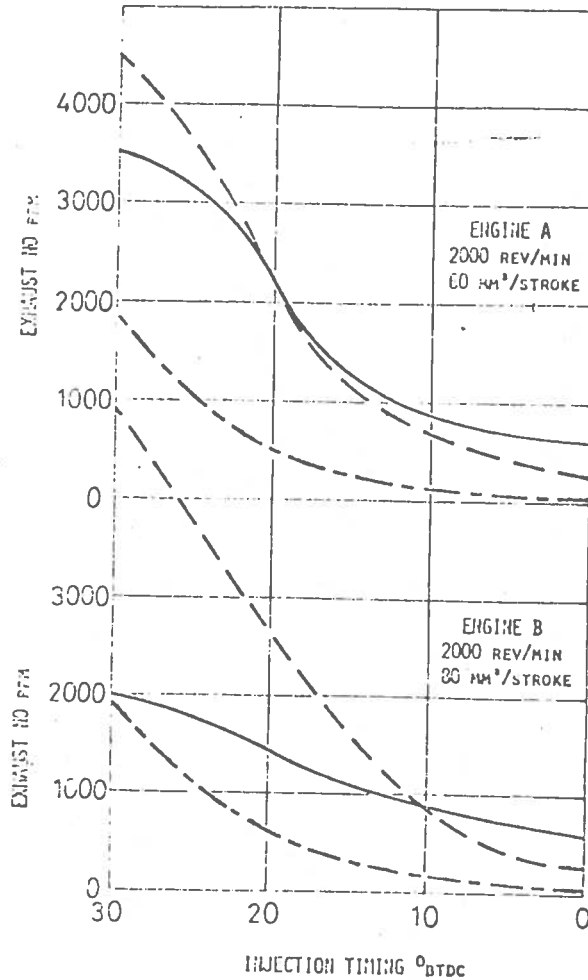
(From Khan et al. (4.16))

FIGURE 4.9.   CALCULATED EXHAUST NO WITH ZONE HEAT LOSS EQUAL TO WALL HEAT LOSS;
THE PERCENTAGE OF HEAT LOSS TO WALLS IS BASED ON EXPERIMENTS AND IS 16, 14, 12
AND 11% FOR TIMINGS OF 30, 20, 10, AND 0 DEG. BTDC RESPECTIVELY

SOLID LINE = EXPERIMENTAL VALVES
DOT-DASH = CALCULATED VALUES USING
k_1 = 1.36 x 10^{14} EXP (-75 400/RT)
EVEN-DASH LINE = CALCULATED VALUES USING
k_1 = 7.30 x 10^{14} exp (-75 400/RT)
(FROM KHAN ET AL (4.16)

79
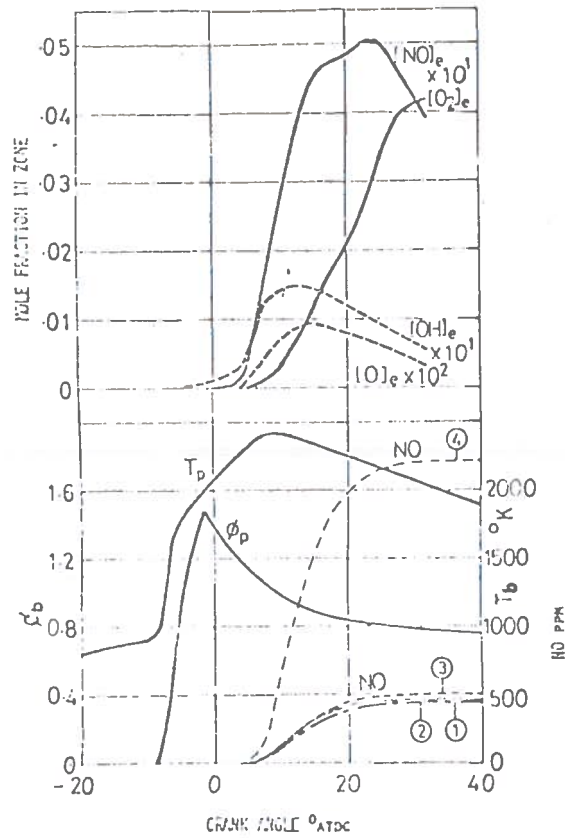
(From Khan et al. 4.16))

FIGURE 4.10. CONDITIONS IN NO FORMATION ZONE FOR DIFFERENT EXPRESSIONS OF THE NO RATE EQUATION

1. EXTENDED ZELDOVICH MECHANISM,
2. ZELDOVICH MECHANISM,
3. EQUATION (4.13) WITH $k_1 = 1.36 \times 10^{14}$ EXP $(-7500/RT)$
4. EQUATION (4.13) WITH $k_1 = 7.30 \times 10^{14}$ EXP $(-75400/RT)$

calculation step, a 'parcel' of stoichiometric fuel-air mixture
burns, of sufficient mass to give the required heat release for
that crank angle interval. This burning is assumed to occur at
adiabatic conditions.

Two systems are assumed to be present in the combustion chamber:-

1) unburnt air, and

2) 'parcels' of homogeneous burnt mixture - one sub-system for
    each calculation step during the heat release period.

Each 'parcel' of burnt mixture corresponds to many physically
separated elements of fuel-air mixture all burning within the
same crank angle increment.

To simulate post-combustion mixing, the temperature of each parcel
decays to the thermodynamic mean temperature of the cylinder
contents after a specified mixing time. However, no dilution is
allowed for so that, once formed, the parcels remain at the
stoichiometric equivalence ratio.

Nitric oxide formation is described by a three reaction extended
Zeldovich mechanism, and soot oxidation is modelled using a simple
surface reaction scheme. Both of these chemical kinetic processes
are assumed to occur only in the post-combustion parcels.

4.4.2 Description of the Model

At each crank angle step pressure is assumed constant throughout
the combustion chamber - this is a basic assumption of all the
models reviewed. At the start of the calculation, corresponding
to the crank angle of inlet valve closure, the cylinder is assumed
full of air at a temperature and pressure which are supplied as
input data.

Engine geometry, which includes cylinder bore, crank radius,
connecting rod length and compression ratio are also supplied as
input data. This allows the calculation of the cylinder volume
as a function of crank angle.

Considering a general crank angle step j; from the state of the
cylinder contents at the beginning of the step, the program makes
a first estimate of the values at the end of the step (subscript j)
by assuming isentropic compression with no heat release. An
iteration procedure based on maintaining energy balance (including
the required heat release) then adjusts the estimated values until
a specified accuracy of the energy balance is achieved (fig. 4.11).
Account is taken of heat transfer between the cylinder contents
and walls, of work done on the piston and of heat release during
each step of the calculation.

Calculation of Masses - The mass of air in the cylinder at the
start of compression is calculated from the pressure and temperature
by applying the ideal gas law, and calculating the cylinder volume

Input Data

Conditions at beginning of step

$j + 1$

Calculate:
$1. V_j$ at end of step
$2. m_{bm,j}, m_{a,j}, m_{tot,j}$

Estimate:
$T_{mean,j}, T_{a,j}$
(using $TV^{\gamma-1} = const$)

Calculate $T_{bm,j}$

$T_{a,j} = T_{a,j} (1 + \frac{error}{T_{mean,j}})$

If
$$T_{mean,j} = \left[\frac{m_a \cdot T_a}{m_{tot}}\right]_j + \sum_k^j \frac{m_{bm,k}}{m_{tot,j}} \cdot T_{bm,j}$$

large error

small error

$T_{mean,j} = T_{mean,j} (1 + \frac{error}{T_{mean,j}})$

Estimate P_j
$$P_j = (m_{a,j} R_{a,j} T_{a,j} + \sum_k^j m_{bm,k} \cdot R_{bm,k} \cdot T_{bm,k,j}) \frac{1}{V_j}$$

First law:
$dU_j = (Ht. release)_j - dW_j - Heatloss$

$error = \frac{U_j(1) - U_j(2)}{U_j(1)}$

Calculate U_j
$1. U_j = U_{j-1} + dU_j$
$2. U_j = m_{a,j} u_{a,j} + \sum_k m_{bm,k} u_{bm,k,j}$

large error

if
$U_{j(1)} = U_{j(2)}$

small error

Store or print values of T, p etc make NC formation rate calculation and soot oxidation rate calculation.

From Backhouse (4.7)

FIGURE 4.11.   BLOCK DIAGRAM OF THE STEP CALCULATION

82

from geometry. The mass of gas within the cylinder is assumed unchanged during the cycle apart from the addition of fuel (i.e. leakage past piston rings, valves and gaskets is neglected).

At any crank angle step, j, the mass of the stoichiometric fuel-air parcel that burns at that step is given by:-

$$m_{bm,j} = \frac{(heat\ release)_j}{(\ LCV\ of\ fuel)} \cdot (S + 1), \tag{4.17}$$

where   S = stoichiometric air-fuel mass ratio,

LCV = lower calorific value (J./kg)

and (heat release)$_j$ = heat released during crank angle step j(J.), supplied as input data.

The mass of unburnt air (m_a) is adjusted when heat release occurs to allow for the amount involved in the combustion process.

$$m_{a,j} = m_{a,j-1} - m_{bm,j} \cdot \frac{S}{(S+1)} \tag{4.18}$$

Calculation of Temperatures – Figure 4.12 illustrates the temperature profile of a typical parcel of combustion product. A mean temperature ($T_{mean,j}$) is defined by

$$m_{total,j} \cdot T_{mean,j} = m_{a,j} \cdot T_{a,j} + \sum_{k=1}^{j} m_{bm,k} \cdot T_{bm,k,j}. \tag{4.19}$$

Subscript 'a' refers to the unburnt air system and 'bm,k' refers to a parcel of combustion product formed at crank angle k (k ≤ j).

There is also a relation between $T_{bm,j}$ and $T_{a,j}$ defined by the assumptions made regarding combustion. These assumptions are;

1) that combustion is adiabatic and instantaneous,

2) that the temperature of the fuel-air mixture just prior to combustion is the same as that of the unburnt air, and

3) that the specific heat of the burnt products is the same as that of the unburnt mixture.

Thus, heat release during step j,

$$(heat\ release)_j = \int_{T_{a,j}}^{T_{bm,j}} (Cp_{bm} \cdot m_{bm,j})\ dT. \tag{4.20}$$

Cp_{bm} is a function of temperature for semi-perfect gases (and also of pressure for non-ideal gases), but for simplicity a constant
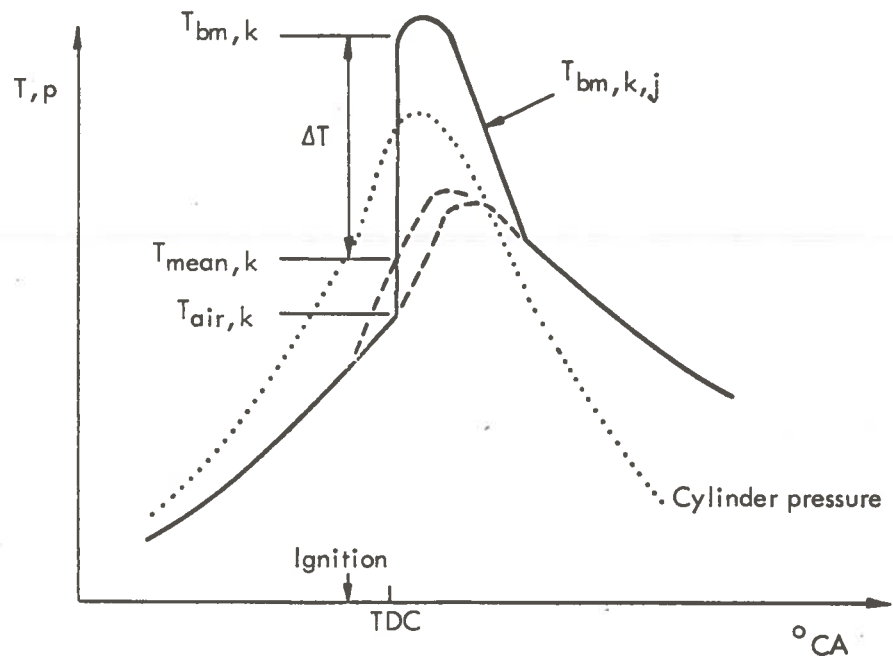
(From Backhouse (4.7))

FIGURE 4.12. TEMPERATURE PROFILE OF A TYPICAL SUB-SYSTEM OF FUEL/AIR MIXTURE

value is assumed so that equation (4.20) reduces to;

$$T_{bm,j} = T_{a,j} + dT_{bm,j},$$ (4.21)

where $dT_{bm,j} = \dfrac{(\text{heat release})_j}{m_{bm,j} \cdot C_{p_{bm}}}$

= constant for a given fuel and fuel-air ratio.

Whenever the value $T_{mean,j}$ is altered, a test is made on the validity of (4.19). The value of $T_{a,j}$ is altered in proportion to any error found unless this error is less than a specified fraction of $T_{mean,j}$ ($\sim$ 1%).

The subsequent parcel temperature history is given by;

$$T_{bm,k,j} = T_{mean,j} + (\ (MX + k - j)/MX).dT_{bm,k},$$ (4.22)

where MX is a characteristic mixing time divided by the step length. Equation (4.22) is a very simple attempt to take account of the 'cooling' of parcels subsequent to combustion, but it is to be noted that no attempt is made to consider parcel dilution (i.e. no equation similar to (4.22) for $\Phi_{bm,k,j}$ is at present incorporated in the program).

The value chosen for MX has a noticeable effect only on the emissions calculations, and several values were investigated for this parameter. It was found that nitric oxide emissions levels were not very greatly affected by MX, and so MX = 20°CA has been chosen as a reasonable value. Further details of this investigation are discussed later.

Energy Balance - At the heart of the calculation procedure is the conservation of energy equation as applied to the entire cylinder contents (fig. 4.11). In finite difference form it is:-

$$\delta Q = \delta W + dU$$ (4.23)

where   U = the total internal energy of the cylinder contents,

δQ = heat release minus heat lost to the coolant, and

δW = pressure work done on the piston.

From a knowledge of conditions at the beginning of a step and using the heat release specified for that step, the program proceeds to calculate U_j at the end of the step by two routes:-

1) $U_j = U_{j-1} + dU_j.$ (4.24)

Substituting from eqn. (4.23), $U_j = U_{j-1} + \delta Q_j - \delta W_j.$

U_{j-1} is known, and δQ_j and δW_j are calculated from the estimated mean temperature and pressure during the step.

2) Summing the internal energies of all the sub-systems forming the cylinder contents at the end of the step using the estimated values for temperature and pressure:

$$U_j = m_{a,j} \cdot u_{a,j} + \sum_{k=1}^{j} m_{bm,k} \cdot u_{bm,k,j}, \qquad (4.25)$$

where $u_{bm,k,j} = u_{bm}(T_{bm,k,j}, P_j)$.

The two values for U_j are compared. If the difference between the two values of U_j is larger than a specified fraction of U_j ($\sim 1\%$), then the estimate of $T_{mean,j}$ is revised to bring the two values of U_j into closer agreement.

Heat Loss to Coolant - Radiative heat loss and the effects on convective heat transfer of swirl velocity, surface temperature variation and gas density are neglected. Convective heat transfer is considered in two parts;

1) Heat transfer to the cylinder walls (where the surface area varies with crank angle):

$$\text{Heat loss} = \frac{4k(\Delta CA)}{6 \cdot RPM \cdot Bore} \cdot \left\{ \tfrac{1}{2}(T_{mean,j} + T_{mean,j-1}) - T_{wall} \right\} \cdot$$
$$\tfrac{1}{2}(V_j + V_{j-1}) \quad (4.26)$$

where T_{wall} = time-averaged mean wall temperature ($= 455^{\circ}K$, input data),

k = heat transfer coefficient ($= 450$ watts $m^{-2}({}^{\circ}K)^{-1}$)

and ΔCA = crank angle increment.

2) Heat transfer to the remaining combustion surfaces:

$$\text{Heat loss} = \frac{\pi}{2} \cdot k \cdot (Bore)^2 \cdot \frac{(\Delta CA)}{6 \cdot RPM} \cdot \left\{ \tfrac{1}{2}(T_{mean,j} + T_{mean,j-1}) - T_{cylhd} \right\} \quad (4.27)$$

where T_{cylhd} = time-averaged temperature for these surfaces ($= 530^{\circ}K$).

The Diesel combustion model as formulated by Backhouse (4.7) has been extended by Raine (4.23) to include the kinetics of nitric oxide formation, and a preliminary model for soot oxidation. It should be noted that in its present form the model cannot be used to consider soot formation, since no attempt has been made to model the history of fuel prior to combustion.

4.4.3 Nitric Oxide Formation Model

An extended Zeldovich mechanism (4.24) is assumed,

(i) $O + N_2 \underset{k_{-1}}{\overset{k_1}{\rightleftarrows}} NO + N$

(ii) $N + O_2 \underset{k_{-2}}{\overset{k_2}{\rightleftarrows}} NO + O$

(iii) $OH + N \underset{k_{-3}}{\overset{k_3}{\rightleftarrows}} NO + H$.
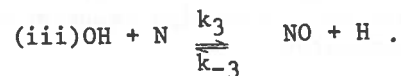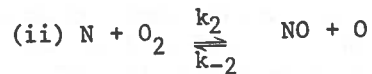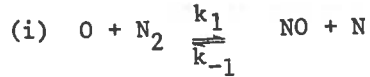
The rates chosen for these reactions are accepted literature values (4.24).

$$k_1 = 3.1 \times 10^{13} \exp(-0.344/RT) \quad cm^3/sec.gm\text{-}mole$$

$$k_2 = 6.4 \times 10^9 \, T \exp(-6.25/RT) \quad cm^3/sec.gm\text{-}mole$$

$$k_3 = 4.1 \times 10^{13} \quad\quad\quad\quad\quad cm^3/sec.gm\text{-}mole,$$

where the activation energies are in units of kcal/gm-mole.

Equilibrium conditions were assumed to exist for all the controlling species except N which was assumed to be in steady-state with the NO concentrations (4.14). These assumptions lead to the following overall NO reaction rate equation

$$\frac{d(NO)}{dt} = \frac{2 \, M_{NO}}{\rho} \cdot (1 - \alpha^2) \cdot \frac{R_1}{1 + \alpha K_1} \quad , \tag{4.28}$$

where

$\quad\quad (NO) =$ nitric oxide mass fraction,

$\quad\quad M_{NO} =$ molecular weight of NO,

$\quad\quad \rho =$ gas density,

$\quad\quad \alpha = [NO]/[NO]_e$ where 'e' indicates the equilibrium conditions,

$\quad\quad R_1 = k_1 \, [N]_e \, [NO]_e,$

$\quad\quad R_2$ and R_3 are similarly defined for equations (ii) and (iii),

and $\quad K_1 = R_1/(R_2 + R_3).$

The rate of change of nitric oxide mass fraction is therefore a function of local pressure, temperature and chemical species composition.

Equilibrium species concentrations are supplied to the program as input data in the form of a two dimensional array for pressures and temperatures of interest. The extension of the program to include equivalence ratios other than stoichiometric would involve a three dimensional array for species concentrations.

4.4.4 Soot Oxidation Rate

A preliminary attempt has been made to incorporate soot oxidation kinetics into the combustion model. This is based on a mechanism originally proposed for pyrolytic graphite oxidation by Nagle and Strickland-Constable (4.25) and more recently shown by Appleton (4.26) to be applicable to soot oxidation in the high temperature and pressure regime of gas turbine combustors.

The equations developed are:

specific surface reaction rate $(gm.cm^{-2}, sec^{-1})$

$$\omega = M_c \cdot x \cdot \left[\frac{k_A \cdot P_{O_2}}{(1 + k_Z \cdot P_{O_2})} \right] + M_c \cdot k_B \cdot P_{O_2} \cdot (1-x) \qquad (4.29)$$

where M_c = molecular weight of carbon

P_{O_2} = local partial pressure of oxygen, atm,

k_A = 20 exp (-30/RT), $gm.cm^{-2} \cdot sec^{-1} atm^{-1}$,

k_B = $4.46.10^{-3}$ exp (-15.2/RT), $gm.cm^{-2} \cdot sec^{-1} \cdot atm^{-1}$,

k_Z = 21.3 exp (4.1/RT) atm^{-1},

$$x = \left[1 + \frac{k_T}{P_{O_2} \cdot k_B} \right]^{-1},$$

and k_T = 1.51×10^5 exp (-97/RT) $gm.cm^{-2} \cdot sec^{-1}$.

Soot oxidation rate is thus a function of the local temperature, pressure and oxygen concentration only. This model can be used to determine whether a soot particle of an assumed initial size will be consumed during the post-combustion part of the Diesel cycle.

4.4.5 Experimental Comparison

The nitric oxide predictions of the model have been compared with a limited number of experiments. Bearing in mind the many simplifying approximations incorporated into the model, the results are very encouraging. The experiments (4.27) were carried out on a single cylinder direct injection engine, details of which are given in the following table.

Technical data for experimental, single-cylinder direct-injection engine (4.27).

Bore	80mm.	(3.15 ins)
Stroke	110mm.	(4.33 ins)
Power and Speed	3 b.h.p. @ 1000 r.p.m. to 6.5 b.h.p. @ 2000 r.p.m.	
Cubic capacity per cylinder	553 cm^3.	(33.7 cu.in.)
Compression Ratio	16.5 : 1	

Figure 4.13a illustrates the effect of load on nitric oxide emissions. The predicted levels are high at zero and half load, which is possibly due to the use of a constant value of specific heat resulting in calculated burnt mixture temperatures ($T_{bm,k}$) being somewhat high under these conditions.

A second series of experiments were carried out in which nitric oxide was added to the intake air of the engine. The amount of NO added was varied from 0 to about 6000 ppm, and the NO emissions were measured. It was felt that this experiment would prove a good test of the emissions model. Results at one speed and injection timing are plotted in figure 4.13b. As can be seen, there is considerable scatter of the experimental points at half load, and the experimental points at zero load may be fitted to a smooth curve. The model predictions are in surprisingly good agreement with the experimental results, and it is felt that this type of experiment would repay further investigation.

4.4.6 Discussion and Comments

The major criticism of this model is the need for 'experimental' heat release data as input, and work is in progress to remove this limitation. It should be stressed that the 'experimental' heat release data supplied to the program is based on the assumption of homogeneous combustion, whereas it is used in the model to generate a non-homogeneous charge.

Post-combustion mixing is represented only as a temperature decay of the burned parcels to the cylinder mean temperature over a specified mixing time, MX. The effect of the mixing time on nitric oxide formation has been investigated (fig. 4.14, 4.15) for MX = 10, 20 and 40°CA. In all cases, NO is initially formed very rapidly, reaching approximately the local equilibrium level in 0.5 - 5°CA ($\sim$ 50 - 500 µsec), depending upon the local temperature. Once

89
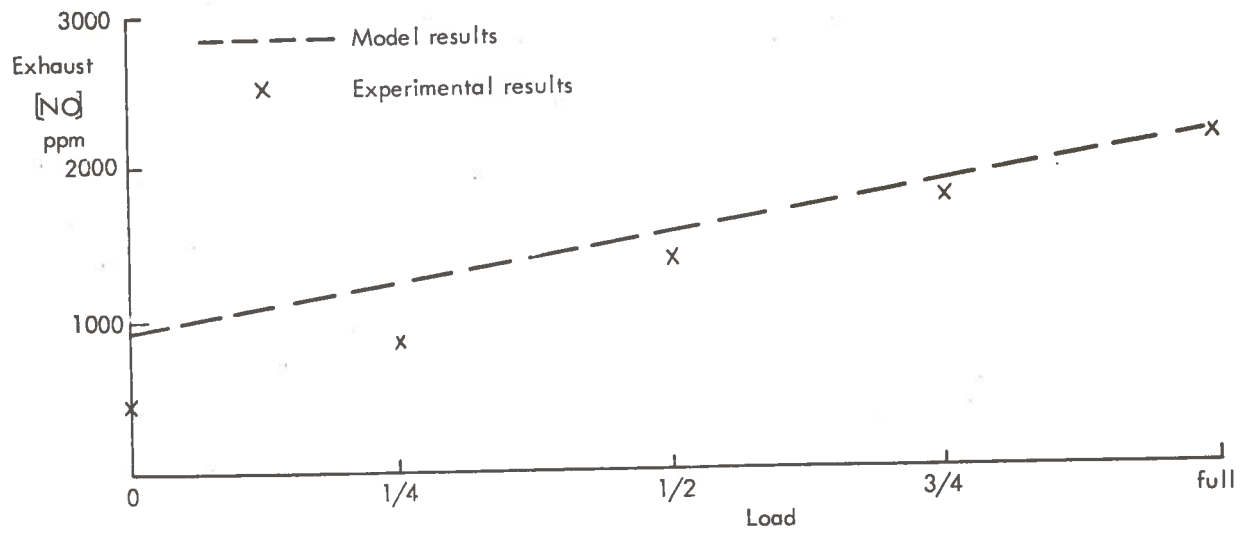
FIGURE 4.13a. COMPARISON BETWEEN EXPERIMENTAL AND MODELLED EXHAUST NO
CONCENTRATION VS LOAD
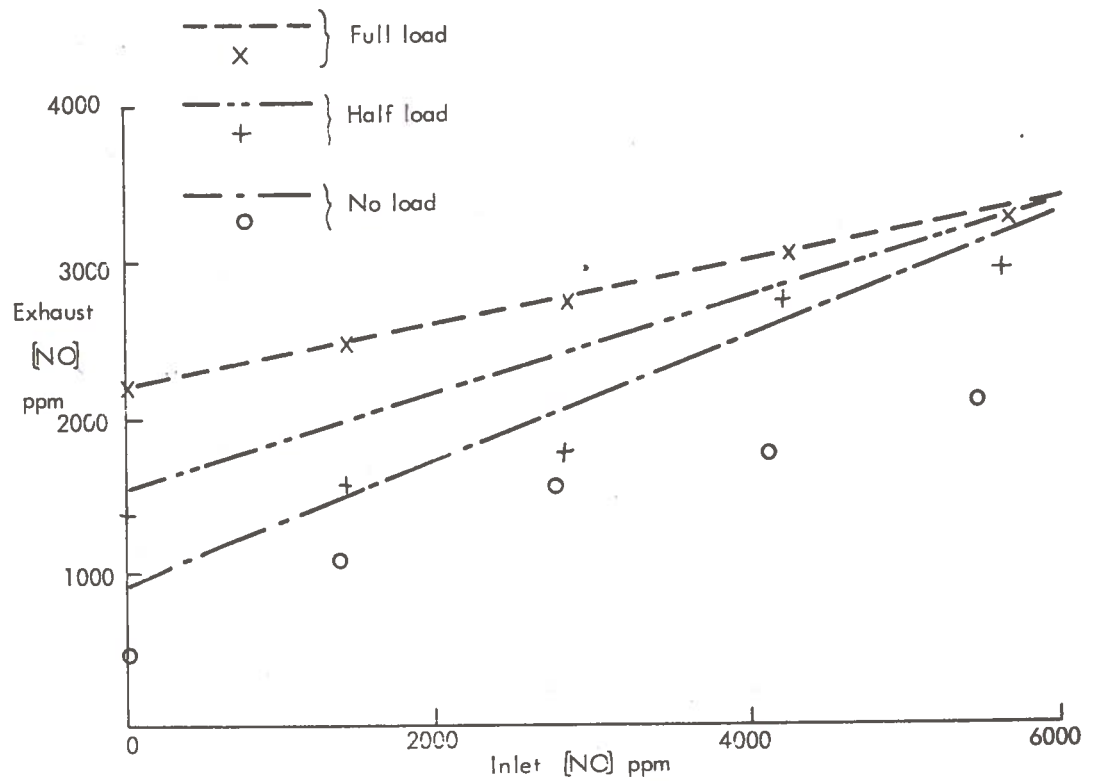
FIGURE 4.13b. COMPARISON BETWEEN EXPERIMENTAL AND MODELLED RESULTS. EFFECT OF
ADDING NO TO INTAKE AIR ON EXHAUST NO CONCENTRATION.

90
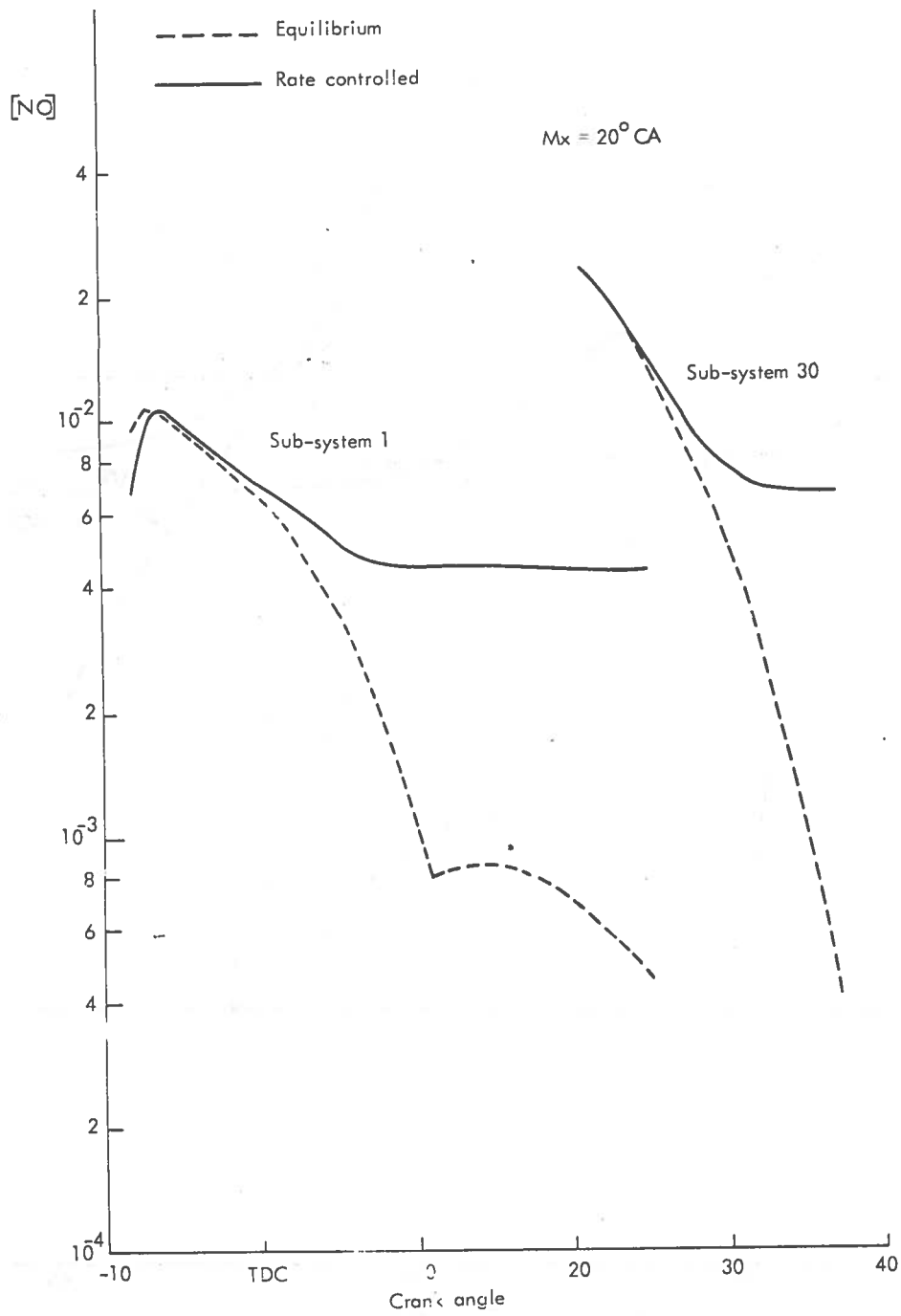
FIGURE 4.14. NITRIC OXIDE CONCENTRATION (MOLEFRACTION) IN TYPICAL SUB-SYSTEMS,
WITH A MIXING TIME OF 20° CA
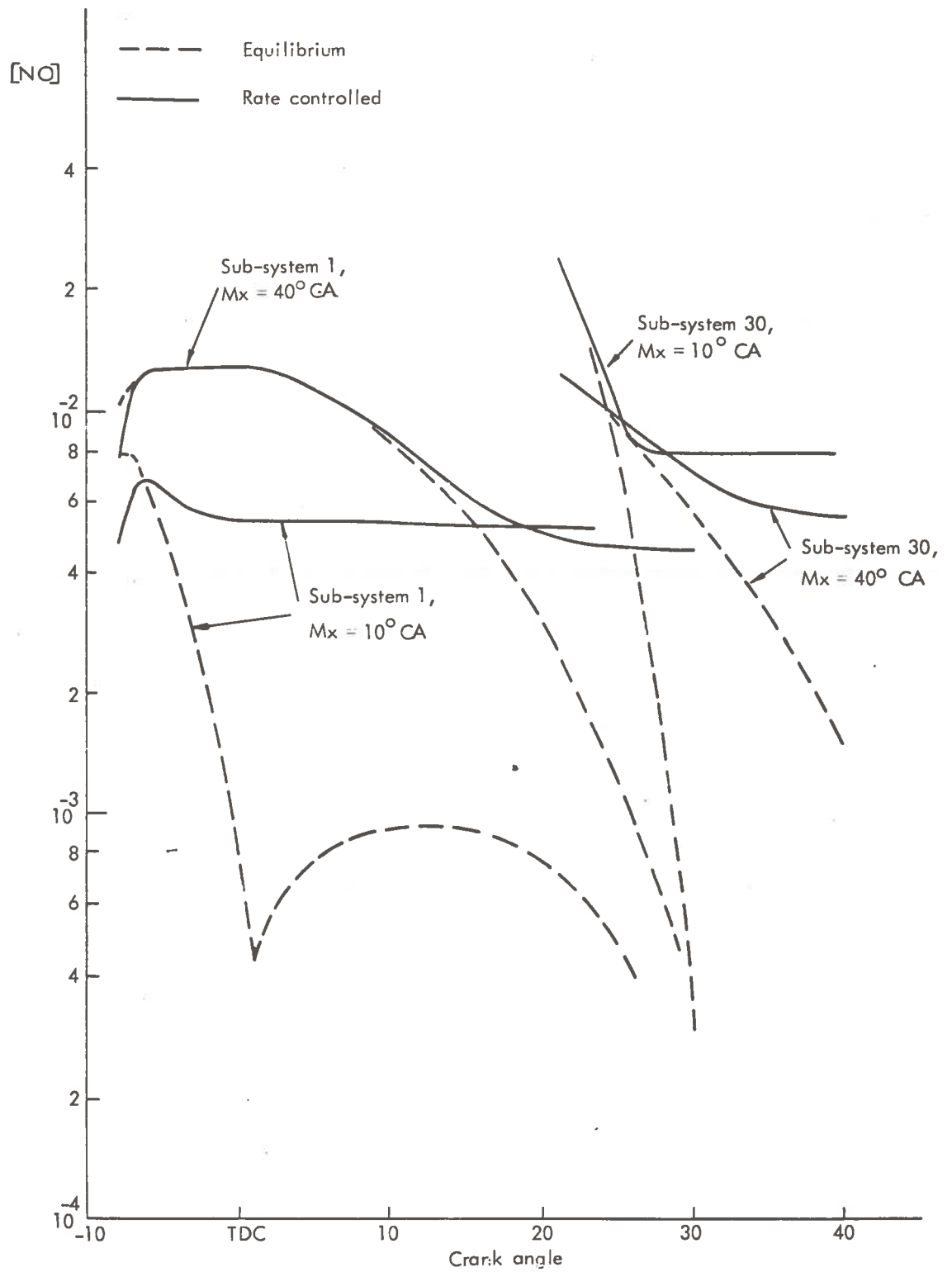
FIGURE 4.15. NITRIC OXIDE CONCENTRATION (MOLEFRACTION) IN TYPICAL SUB-SYSTEMS, SHOWING THE EFFECT OF CHANGING THE MIXING TIME FROM 10°CA to 40°CA.

92

formed, the NO is slow to dissociate, and is therefore frozen at a high concentration as the parcels cool. Note that for cases with a short mixing time, the equilibrium NO concentration in a parcel may have a second peak, due to continued compression of the parcel when it has attained the mean cylinder conditions. This second peak does not influence the kinetic calculations however, as the NO composition has frozen earlier than this.

The model does not consider parcels to change their composition following combustion. It is known that in many combustion situations, the effect of composition on NO kinetics is secondary to temperature effects (see section 2.2), and for this reason it is felt that this omission will not influence the general conclusions of the model.

Figure 4.16 illustrates the effect of the temperature mixing time, MX, on the integrated soot oxidation rate, and indicates that this parameter is not of great importance in determining the amount of soot which is oxidized in the post-combustion parcels.

We conclude that in spite of the many simplifying assumptions, the model is able to elucidate the role of various parameters in the modelling of Diesel engine emissions. Thus the effect of temperature, mixing time, engine load, and the addition of NO to the intake air, have been investigated.

4.5   Model E

4.5.1   Summary

The model (4.8) takes account of jet penetration into the combustion chamber and the interference of air swirl and the chamber wall. The burnt and unburnt fuel is divided into a number of zones. Each zone has a separate history of temperature and equivalence ratio as a consequence of evaporation and burning of the fuel, and air entrainment as it moves across the combustion chamber. Nitric oxide kinetics are modelled in each zone by a six equation scheme.

4.5.2   Description of the Model

During the combustion cycle any of the following three processes is assumed to be rate-limiting;

1)   macromixing between air and fuel - based on a simplified jet model,

2)   micromixing "at the surface of droplets", based on a modified Whitehouse and Way model (4.3),

3)   rate of burning of fuel assuming an Arrhenius form of kinetic equation.
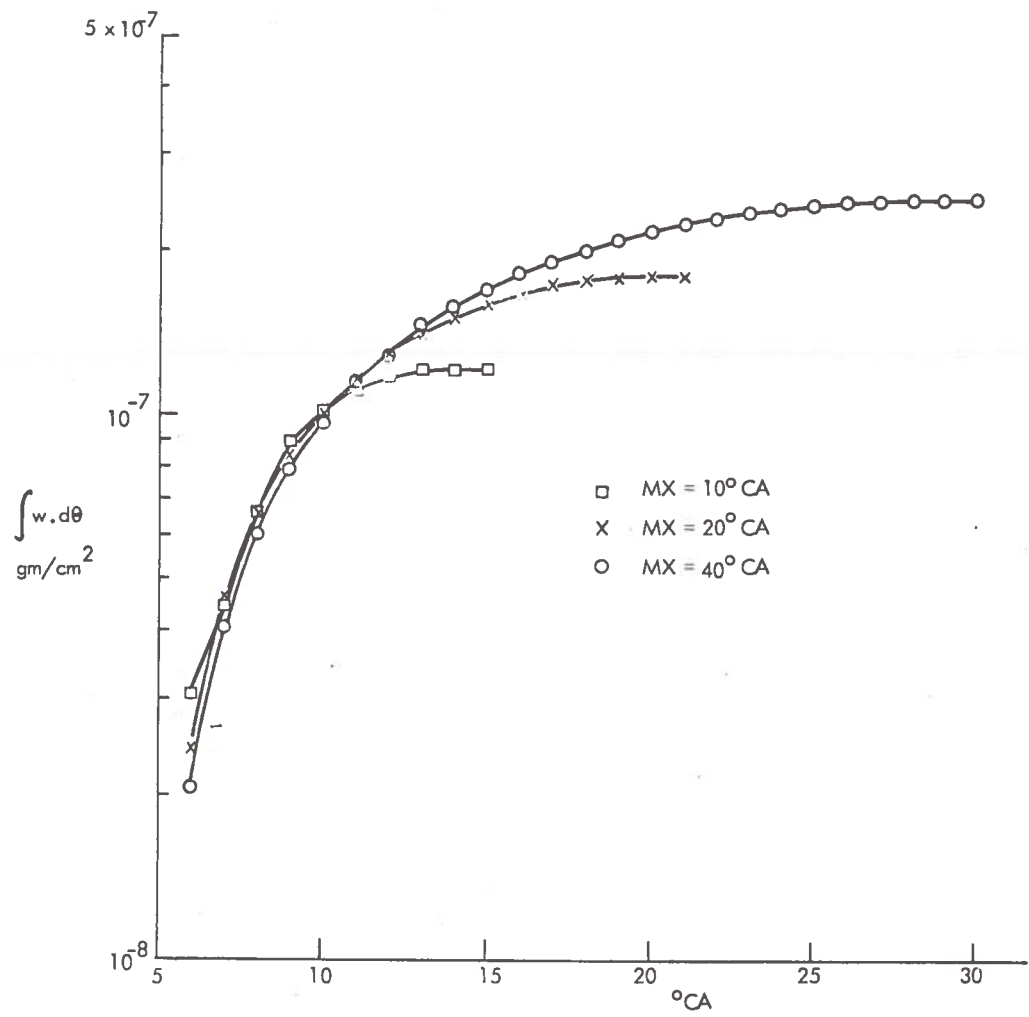
FIGURE 4.16. SOOT OXIDATION VS CRANK ANGLE FOR A SUB—SYSTEM BURNING AT 5°ATDC.

94

Macromixing

As fuel is injected it is divided between a specified number of
zones, each zone acquiring an approximately equal mass of fuel.
The method of allocating the fuel to the zones is illustrated
in figure 4.17. The velocity of each zone is determined by its
distance from the axis of the free jet (determined by the zone
number) and by its distance of travel from the nozzle.

Thus to describe the velocity profile across the jet,

$$U_{xi} = U_{ax} + C_{fi} \ (\hat{U}_x - U_{ax}), \qquad\qquad (4.30)$$

where U_{xi} = velocity of zone 'i' in the x- direction,

U_{ax} = component of swirl velocity in the x- direction,

$\hat{U}_x$ = centre line velocity of the jet,

and C_{fi} = velocity factor for zone 'i' to account for the
velocity profile across a free jet (supplied as
input data).

Assuming that the velocity at the jet axis varies in inverse
proportion to the relative distance travelled,

$$\frac{\hat{U}_x - U_{ax}}{U_j} = \frac{L}{S} \quad \text{for} \quad L > S, \qquad\qquad (4.31)$$

where U_j = nozzle exit velocity,

L   = potential core or mixing length

and   S   = relative displacement of the zone in the x-
direction.

A rate of mixing is obtained from equation (4.30) by assuming the
conservation of momentum in the x- direction for each zone, thus

$$m_{fi} \ U_j = (m_{ai} + m_{fi}) \ . \ (U_{xi} - U_{ax}) \qquad\qquad (4.32)$$

where m_{fi} and m_{ai} refer respectively to the mass of fuel and air
in zone 'i'.

Combining equations (4.30), (4.31) and (4.32), a mixing rate
equation is derived,

$$\frac{dm_a}{dt} = (\frac{S}{C_{fi} \cdot L} - 1) \ \frac{dm_f}{dt} + \frac{m_{fi}}{C_{fi} \cdot L^2} \ (\ L . \frac{dS}{dt} - S . \frac{dL}{dt} \ )$$

$$(4.33)$$

95
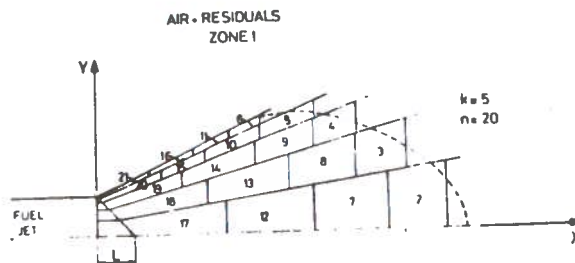
(From Hodgetts and Shroff (4.8))

FIGURE 4.17.   DIAGRAM OF FREE JET SHOWING FORMATION OF 'N' ZONES.
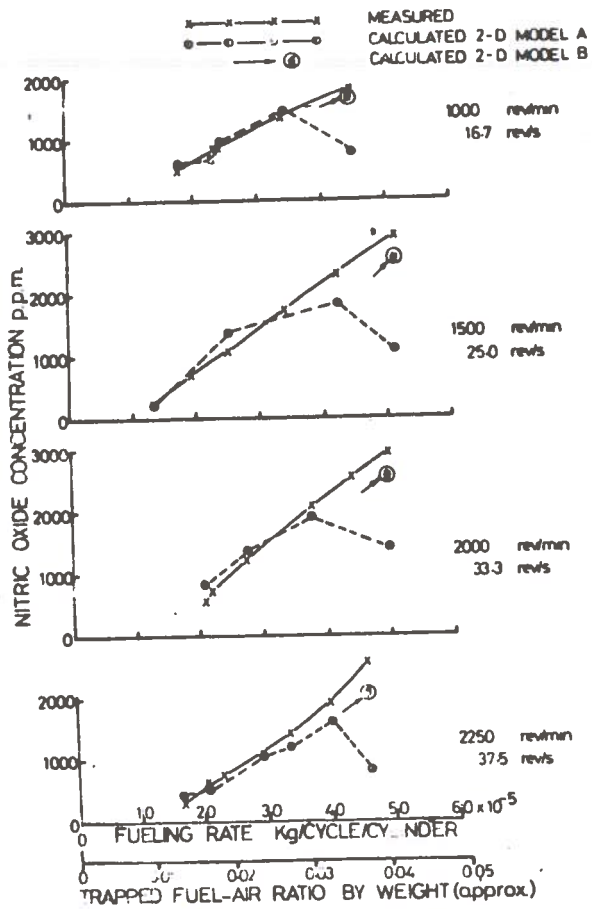
(From Hodgetts and Shroff (4.8))

FIGURE 4.18.   COMPARISON OF MEASURED AND CALCULATED EXHAUST NO CONCENTRATIONS VS LOAD

96

This equation determines the air-fuel ratio within a zone at any time after injection. When a zone hits the wall, it is arbitrarily assumed that the rate of air entrainment is reduced to 50% of that of a free jet.

Micromixing

Once air is entrained into a zone, micromixing with the fuel is assumed to occur by a process analogous to droplet vaporization. This is based on the formulation of Whitehouse and Way (4.3), with the inclusion of a "turbulence factor";

$$\frac{dm_{ev}}{dt} = \frac{K_7}{B} \cdot \zeta \cdot m_f^{1/3} (m_f - m_{ev})^{2/3} \left(\frac{m_a}{m_a + m_f}\right)^{0.4}$$

(4.34)

where m_{ev} = mass of fuel evaporated (or micromixed)

B = cylinder bore

ζ = turbulence factor $\Big\}$

and K_7 = constant $\Big\}$ supplied as input data

Arrehenius Burning Rate

With the evaporated fuel, m_{ev}, available for combustion, the rate of burning is assumed to be controlled by an Arrhenius form of kinetic equation, thus

$$\frac{dm_b}{dt} = K_9 \ p^{0.757} \cdot \Delta m \cdot \exp\left(\frac{-5500}{T_i}\right)$$

(4.35)

where p = cylinder pressure,

T_i = temperature of zone 'i'

K_9 = constant (supplied as input data).

Δm = $m_{ev} - m_b$, if $\{m_{ev} - m_b\} > \{m_a - \left(\frac{A}{F}\right)_s \cdot m_b\}$

or Δm = $\{m_a - \left(\frac{A}{F}\right)_s \cdot m_b\} \cdot \frac{1}{(A/F)_s}$ if $\{m_{ev} - m_b\} <$

$\{m_a - \left(\frac{A}{F}\right)_s \cdot m_b\}$.

where $\left(\frac{A}{F}\right)_s$ = stoichiometric air-fuel mass ratio.

97

An equation is also used to determine the ignition delay, τ, of each zone;

$$\int_0^\tau \frac{dt}{\Delta} = 1$$

where $\quad \Delta = K_8 \cdot p^{-0.757} \quad \exp\left(\frac{5500}{T_i}\right)$ $\qquad$ (4.36)

Heat transfer from the combustion zones to the cylinder walls is modelled as a convective process by the equation

$$\frac{dQ_i}{dt} = K_{10} \cdot \zeta^{0.8} \cdot B^{-0.2} \cdot p^{0.8} \, T_i^{-0.53} \, A_s \, (T_i - T_w) \, \frac{V_i}{\sum\limits_{i=1}^{n} V_i} \qquad (4.37)$$

where $\quad A_s \;=\;$ surface area of the walls,

$\qquad\quad B \;=\;$ cylinder bore,

$\qquad\quad T_w \;=\;$ temperature of the walls,

and $\qquad V_i \;=\;$ volume of zone 'i'.

The first law energy equation, and an ideal gas equation of state is assumed for each zone.

4.5.3 Nitric Oxide Kinetics

An extended Zeldovich mechanism (4.14) is used to model nitric oxide kinetics, with rate data taken from Baulch et al. (4.28);

$N + NO \;\rightleftharpoons\; N_2 + O \qquad k_f = 5.2 \times 10^{-11} \exp(-0.334/RT)$

$N + O_2 \;\rightleftharpoons\; NO + O \qquad k_f = 1.1 \times 10^{-14} \exp(-6.25/RT)$

$N + OH \;\rightleftharpoons\; NO + H \qquad k_f = 7 \times 10^{-11}$

$H + N_2O \;\rightleftharpoons\; N_2 + OH \qquad k_f = 5 \times 10^{-11} \exp(-10.8/RT)$

$O + N_2O \;\rightleftharpoons\; N_2 + O_2 \qquad k_f = 6 \times 10^{-11} \exp(-24.0/RT)$

$O + N_2O \;\rightleftharpoons\; No + NO \qquad k_f = 8 \times 10^{-11} \exp(-24.0/RT)$
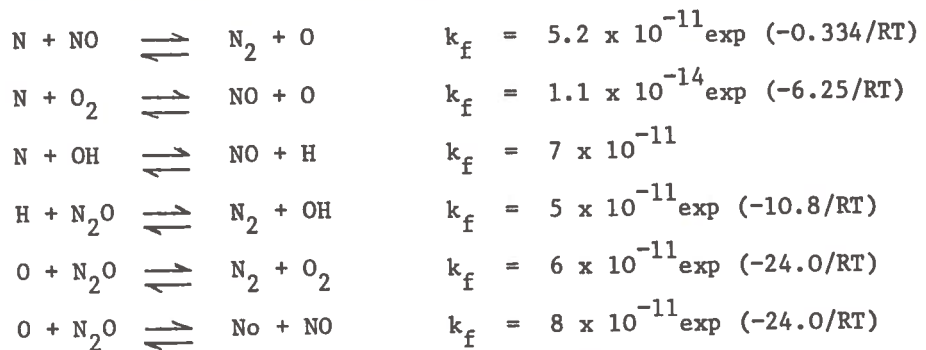
where rate constants are in units of cm^3/part.sec. and activation energies are in kcal/gm-mole.

Equilibrium concentrations are assumed for O, O_2, OH and N_2, with steady state concentrations for N and N_2O.

98

4.5.4 Experimental Comparison

Results have been published (4.8) comparing the model to a limited number of experiments. The tests were carried out on a six cylinder, water cooled, four stroke, direct injection engine, with bore and stroke of 98mm x 127mm (3.85 x 5.0 ins.). The results of the comparison are shown in figure 4.18. As is discussed later, the basic model (A) with $n = k = 8$ gives good correlation at all speeds and at loads below 60 - 70% of full load. However, in order to give good correlation with full load experiments, a "full load" model (B) had to be introduced, with $n \simeq 40$.

4.5.5 Discussion and Comments

The parameters which must be specified for the model are;

   k the number of zones across the jet

   n the total number of zones formed

   ζ turbulence factor in equations (4.34) and (4.37)

   K_7 constant in equation (4.34) for micromixing

   K_8 constant in the ignition delay equation (4.36)

   K_9 constant in the rate of burning equation (4.35)

   K_{10} constant in the rate of heat transfer equation (4.37)

   K_{11} constant determining the potential core or mixing length of the jet.

An extensive series of experiments would be required to determine how these constants varied from one engine to another, and whether any correlation could be deduced between the constants and fundamental parameters such as swirl rate, valve lift or fuel type.

Hodgetts and Shroff state that the number of zones n is critical to the solution for the nitric oxide concentration, since it has a considerable effect on the temperature of the entrained air. The authors indicate that a reasonable correlation with low and medium load experimental results was achieved with $n = k$ (model A in figure 4.18), and the assumption that 60% of the entrained air is received from the zone of unburnt air, and the remaining 40% by lateral transfer from the trailing edge of the jet towards the leading edge.

However, these values for the parameters gave less than 50% of the measured NO concentration at high to full load conditions (figure 4.18). It is suggested that the reason for this is that at high fuelling rates, all the air from the air zone is drawn into the fuel jet early in the process. Air for further combustion can then be obtained only by lateral transfer within the jet. Under these conditions, the zones with a high velocity fail to obtain sufficient

air to complete the combustion of the fuel. A "full load" model
(B of figure 4.18) which assumes a less structured jet, with more
rapid decay of velocity for the leading edge zones, gave good
correlation with the full load experimental results. In this
model, between 40 and 50 zone were required.

In conclusion, this model is one of the most sophisticated at
present available, with much scope for development, e.g. in
assigning values to the many parameters of the model.

4.6   Model F

4.6.1   Summary

This model (4.9) is based on spray mixing and combustion. The
evolution of "n" combustion zones within the spray, formed as a
result of fuel-air mixing, is modelled. An ambient and an
unburnt rich mixture zone are also considered. Conservation
equations applied to these zones yield local composition,
temperature and cylinder pressure. A simplified nitric oxide
kinetic calculation is carried out.

4.6.2   Description of the Model

Model calculations begin at "incipient" ignition. Experimental
data is used for the cylinder pressure just prior to ignition,
and the temperature, assumed uniform throughout the chamber, is
calculated from the ideal gas law.

At incipient ignition, the contents of the chamber are considered
to be divided into $(n + 2)$ zones (figure 4.19);

1)   zone "A" is the ambient medium (air + recirculated exhaust,
     if any),

2)   zone "C" forming the rich core of the spray,

3)   zones "B_i" $(i = 1,n)$ of combustible mixture of varying fuel-
     air ratios.

Further fuel injection causes entrainment of medium A into zones B_i
and into the core zone C. As a result of this entrainment, some
of the rich mixture in zone C is diluted, crosses the rich limit
of combustion, and becomes a new zone B_j. The rate at which fresh
mixture crosses the rich limit of combustion is termed the mixture
preparation rate, $\frac{dm_{mp}}{d\theta}$. Crank angle increments are chosen to give
approximately equal fuel mass in all zones B_i. The burning of
zones B_i is not considered to be chemically rate controlled. Thus
prepared mixture, as it crosses the rich limit from zone C into
zone B_j, is considered to instantaneously shift to burned
equilibrium at the local fuel-air ratio.

Subsequently the zone maintains chemical equilibrium as the fuel-
air ratio changes due to further air entrainment. The effect of

100
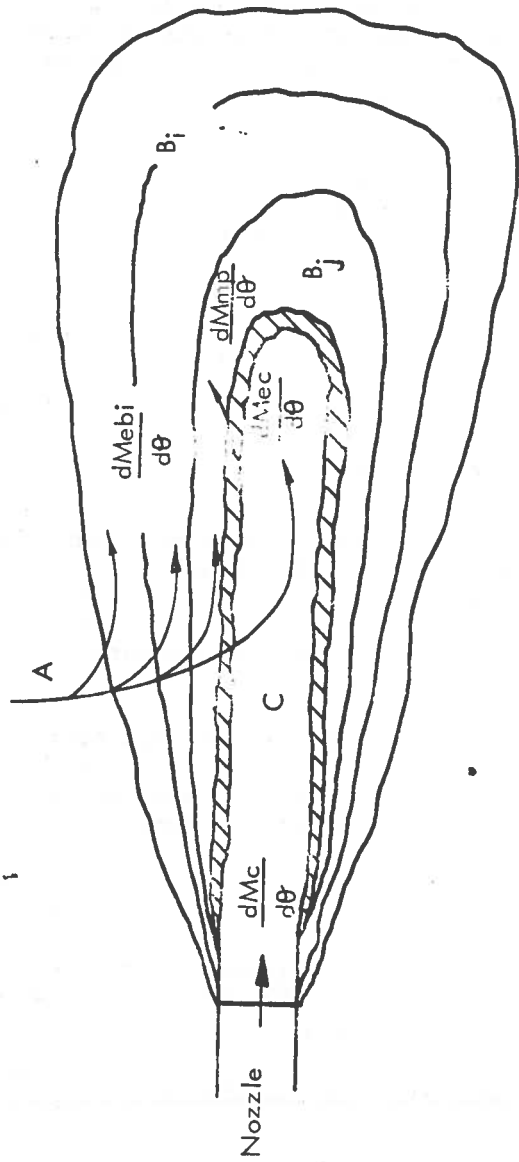
$\dfrac{dMf}{d\theta}$ = Fuel injection rate

$\dfrac{dMmp}{d\theta}$ = Mixture entrainment rate into new zone B_j = mixture preparation rate in zone C

$\dfrac{dMebi}{d\theta}$ = Medium entrainment rate into zone B_i

$\dfrac{dMec}{d\theta}$ = Medium entrainment rate into core.

(From Shahed et al. (4.9))

FIGURE 4.19.   SCHEMATIC REPRESENTATION OF THE COMBUSTION ZONES AND ENTRAINMENT RATES

this instantaneous shift to burned equilibrium in the premixed
zones when ignition occurs is discussed later.

Medium entrainment rates and fresh fuel-air preparation rates
are critical to this combustion model. These were derived from
experimental measurements of fuel injection into a constant
volume, high pressure chamber equipped with observation windows
and a fast response sampling valve (4.29), on the assumption
that combustion does not affect mixing rates.

Mixing Rate

Reference (4.29) gives details of the mixing rate equations used
in the model. The jet tip penetration into a quiescent
environment is given by

$$x_t = \frac{450d^{0.5} \; (\rho_f/\rho d)^{0.4}}{(1 + \rho_a/\rho_{amb})^{0.85}} \cdot (\frac{\rho_a}{\rho_{amb}})^{0.5} \cdot (p_{inj} - p_a)^{0.25} \cdot t^{0.6}$$

$$(4.38)$$

where $\quad$ d = nozzle diameter,

$\rho_a, \rho_{amb}, \rho_f, \rho_d \quad$ = density of air, ambient zone (zone "A"),
$\qquad\qquad\qquad\qquad$ reference fuel and Diesel fuel
$\qquad\qquad\qquad\qquad$ respectively,

$P_a, P_{inj} \qquad\qquad$ = chamber and injection pressure
$\qquad\qquad\qquad\qquad$ respectively,

and $t \qquad\qquad\qquad$ = time since the start of injection.

Following the end of fuel injection, the tail of the jet is assumed
to penetrate at a fraction of the tip velocity. Thus tail
penetration,

$$x_1 = a. \; x_t \qquad\qquad\qquad (4.39)$$

where $\qquad$ a = a constant, with a suggested value of 0.5,
and $\qquad\quad$ x_t is given by equation (4.38), but with t now the
$\qquad\qquad\quad$ time since end of injection.

A study was made (4.29) of the effect of varying 'a' from 0.25 to
1.0 and showed very little effect on the mixing rate.

The rate of growth of jet width is expressed as

$$\frac{db}{dx} = \frac{k}{2} \; (1 + \frac{\rho_{amb}}{\rho_j}) \qquad\qquad (4.40)$$

where $\quad$ k = a constant, with value 0.24

and $\qquad$ ρ_j = density at the jet axis, a function of x.

Various modifications to equations (4.38) to (4.40) are introduced if swirl is present on the assumption of solid body rotation within the chamber.

By analogy with steady jet concentration distributions, the fuel mass fraction along the jet axis,

$$c_m = \begin{cases} \dfrac{1}{\alpha(t) \cdot x + 1} & \text{for } x_1 < x < x_t \\ 0 & \text{for } x < x_1 \text{ and } x > x_t \end{cases} \tag{4.41}$$

where $\alpha(t)$ is a function of time only, and the fuel mass fraction across the jet is given by

$$\frac{c(x,y,t)}{c_m(x,t)} = 1 - \left(\frac{y}{b}\right)^{0.5}. \tag{4.42}$$

In order to determine $\alpha(t)$ in equation (4.41) the equation for the conservation of fuel mass is introduced;

$$\int_0^t \frac{dm_f}{dt} \cdot dt = 2\pi \int_{x_1}^{x_t} \int_0^b c \cdot \rho \cdot y \cdot dy \cdot dx, \tag{4.43}$$

where $\dfrac{dm_f}{dt}$ is the fuel injection rate. The local density ρ, for the fuel-air mixture is assumed to be given by

$$\rho = \frac{P_a}{\left[(1-c) R_a + c R_f\right] T_a}, \tag{4.44}$$

where R_a and R_f are gas constants for air and fuel vapour respectively, and T_a is the chamber temperature. Note that the local temperature T within the jet should be used in equation (4.44), but the use of T_a instead allows great simplification of subsequent calculations.

The solution of equations (4.41) to (4.44) by an iteration procedure (figure 4.20) yields $\alpha(t)$, from which equations (4.41) and (4.42) give the fuel-air ratio distribution in the entire spray.

Figure 4.21 shows the way in which $\alpha(t)$ varies as a function of time, and clearly demonstrates the unsteady nature of a Diesel spray. Note that typically, for a steady gas jet flame (4.30) $\alpha = \text{constant} \simeq 01$ for the conditions of figure 4.21.

The continuous fuel-air distribution as calculated above is divided into 'n' discrete combustion zones. The equivalence ratio boundaries of each zone are calculated from the conservation of fuel mass equation assuming an approximately equal mass of fuel in each zone. The zone is then characterized by its average equivalence ratio which varies with time (figure 4.22).

103
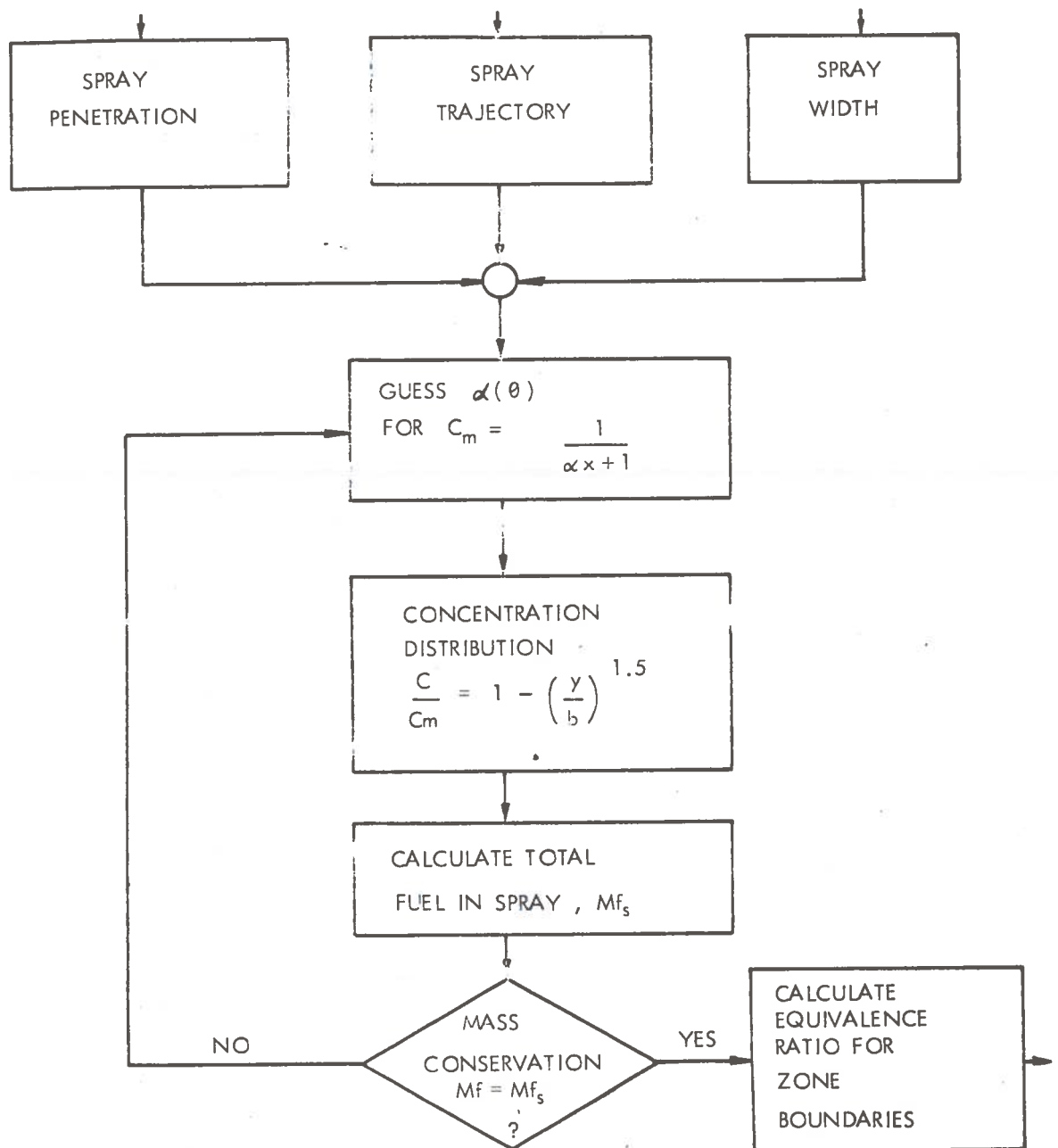
(After Chiu et al. (4.29))

FIGURE 4.20. FLOW CHART FOR ITERATION PROCEDURE TO SOLVE FOR $\propto$ (θ)
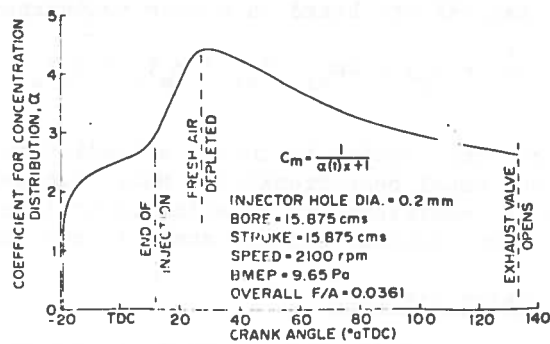
(From Shahed et al. (4.9))

FIGURE 4.21.   VARIATION OF α AS A FUNCTION OF TIME
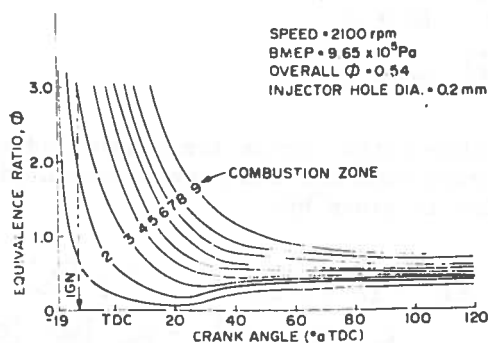
(From Shahed et al. (4.9))

FIGURE 4.22.   HISTORIES OF AVERAGE EQUIVALENCE RATIO OF DIFFERENT ZONES
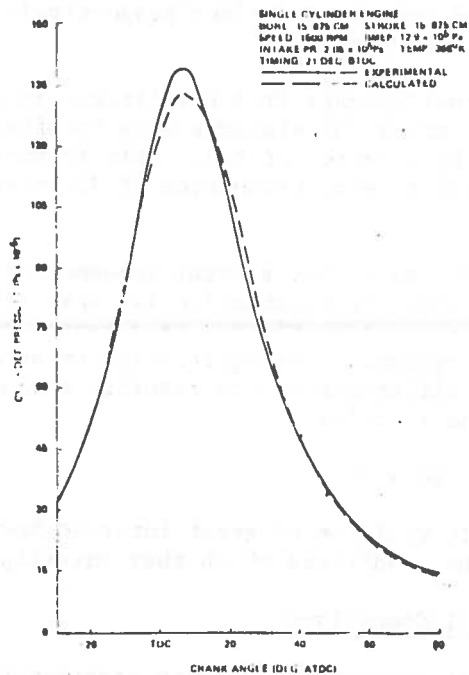
(From Shahed et al. (4.9))

FIGURE 4.23.   TYPICAL CALCULATED AND EXPERIMENTAL CYLINDER PRESSURE

105

Within the framework of the above mixing rate model, the equations of conservation of mass of air and of energy are solved. Heat transfer calculations are based on a mean temperature defined by;

$$T_{mean} \cdot (\Sigma m_{bi} + m_a + m_c) = \Sigma m_{bi} \cdot T_{bi} + m_a T_a + m_c T_c . \qquad (4.45)$$

An Annand (4.31) correlation including a 'radiation' term is used to calculate the total heat transfer. Heat transfer from the various zones is apportioned in relation to their mass and temperature. Heat transfer between zones is not modelled.

4.6.3 Nitric Oxide Kinetics

The Zeldovich mechanism is used to model nitric oxide kinetics:

$$N_2 + O \overset{k_{1f}}{=\!=} NO + N$$

$$N + O_2 \overset{k_{2f}}{=\!=} NO + O$$
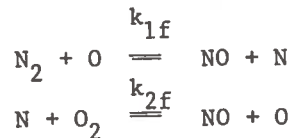
All species other than nitric oxide are considered to be at local equilibrium. For each zone B_i, the rate of production of NO due to chemical reaction is given by:

$$\frac{1}{V_{bi}} \cdot \frac{d}{dt} \left[NO\right] V_{bi} = k_{1f} \left[N_2\right]_e \left[O\right]_e + k_{2f} \left[O_2\right]_e \left[N\right]_e$$
$$- k_{1r} \left[NO\right] \left[N\right]_e - k_{2r} \left[NO\right] \left[O\right]_e , \qquad (4.46)$$

where V_{bi} is the volume of zone B_i; k_f, k_r are the rate coefficients for the forward and reverse reactions respectively, and $[\ ]_e$ = equilibrium molar concentration.

Established rate coefficients from the literature are used, though it was found that better correlations were obtained by increasing the reverse rates by a factor of two. This feature is discussed later. The chemical rate of production of NO in zones C and A is equal to zero.

Shahed et al. (4.9) state that several schemes for NO kinetics were investigated under representative isobaric, isothermal and constant fuel-air ratio conditions. As a result of this they conclude that the assumption of equilibrium or steady state N atoms made little difference to the results, and also that the contribution of the reaction.

$$N + OH \rightleftharpoons NO + H$$

was very minor. It would be of great interest however, to obtain more details of the conditions which they investigated.

4.6.4 Experimental Comparison

A limited number of comparisons between experimental results on a single cylinder direct injection engine and the model have been

106

published (4.9, 4.29). Figure 4.23 illustrates a typical comparison
for the pressure diagram, and figure 4.24 shows the effect of
injector hole configuration and air swirl on nitric oxide emissions.
More extensive comparisons with experiments, preferably from
independent sources, would be very useful in evaluating this model.

4.6.5 Discussion and Comments

The authors have chosen to use velocity data from experimental
measurements on unsteady jets as empirical input to the model. This
is combined with the assumption of a steady jet concentration
distribution. An obvious refinement of the model would be the use
of data on concentration distributions in unsteady jets, if this
were available.

Shahed et al. point out that the assumption of instantaneous chemical
equilibrium (except for NO) in the premixed zones B_i (i = 1,n) upon
ignition is questionable. This assumption causes a step increase in
pressure at the instant of ignition, with a similar effect on the
nitric oxide formation rate. A flame propagation rate, based on
chemical kinetics, could be introduced to allow the premixed portion
of the charge to burn more gradually. This would be analagous to
the Arrhenius burning rate expression of the Hodgetts model.

The model is sensitive to the total number of combustion zones 'n',
and n = 10 was found to be satisfactory. The choice of lean and
rich limits of combustion was another model parameter studied by
the authors. There was little effect on the initial rate of
pressure rise due to varying the lean limit from an equivalence
ratio of 0.3 to 0.7. However, the effect of the rich limit is more
noticeable. Figure 4.25 illustrates the effect of varying the rich
limit of combustion from Φ_R = 2.0 to 5.0. As the rich limit is
increased, more fuel is present in the premixed zones B_i (i = 1,n)
at incipient ignition, and hence the initial rate of pressure rise
increases. A value of Φ_R = 3 was adopted as the rich limit of
combustion.

The authors have also indicated that the model for heat transfer
should be improved. The total heat transfer is apportioned to
various zones in linear relation to their temperature, but radiation
is proportional to the fourth power of temperature. Hence the
temperature of the high temperature zones will be overestimated.
This was thought to have been the reason for requiring an increased
reverse rate for the nitric oxide reactions.

We conclude that this model has attempted to use experimental
results on unsteady jet penetration to derive mixing rates during
Diesel combustion. Further experiments of this type could be of
great use. It is encouraging that from this 'fundamental' approach,
a complex Diesel model has resulted which gives reasonable agreement
with experimental emissions measurements.

BORE = 15.875 cms
STROKE = 15.875 cms
SPEED = 2100 rpm
OVERALL ϕ = 0.54
FUEL RATE =
    265 mm 3/stroke

MEASURED
CALCULATED
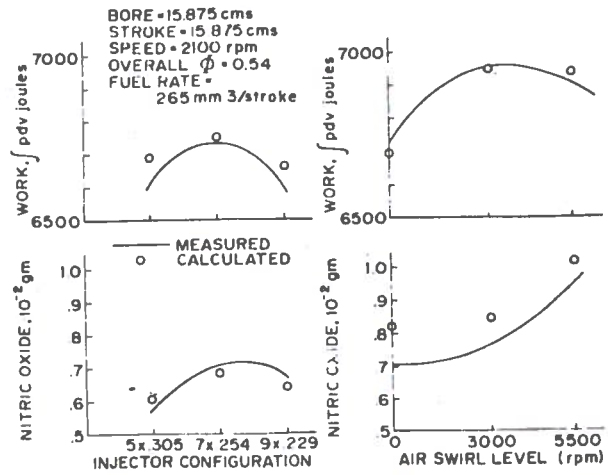
(From Chiu et al. (4.29))

FIGURE 4.24.   EFFECT OF INJECTOR HOLE CONFIGURATION AND AIR SWIRL ON PERFORMANCE
AND NO EMISSIONS OF A DIRECT INJECTION DIESEL ENGINE
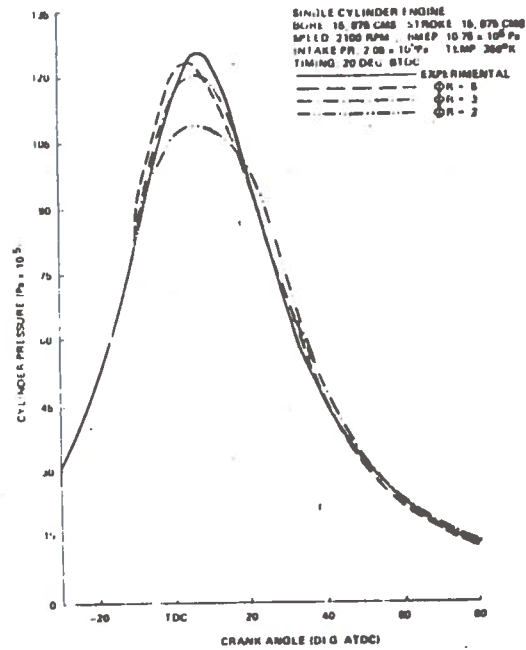
(From Chiu et al. (4.29))

FIGURE 4.25.   EFFECT OF RICH LIMIT OF COMBUSTION ON CALCULATED CYLINDER PRESSURE

4.7 Model G

4.7.1 Summary

This model (4.10) is a four-zone development of previous single-zone (4.3) and two-zone (4.32) Diesel combustion models from the University of Manchester. The four zones considered are a fuel zone, stoichiometric burning zone, product-air zone and a non-burning air zone. The earlier two-zone model, which is based on jet mixing, is used to generate a fuel burning rate and cylinder pressure diagram from the engine geometry and injection data. This fuel burning rate is then used in the four-zone model to calculate the mass of stoichiometric product formed during a crank angle increment.

Non-equilibrium nitric oxide chemistry is considered to occur in the stoichiometric combustion zone, and is modelled by a seven equation extended Zeldovich scheme. Stoichiometric product is allowed to mix with air from the non-burning zone at a specified rate, to form the product-air zone.

4.7.2 Description of the Model

The Diesel combustion chamber is assumed to be divided into four zones (figure 4.26);

1) fuel zone,

2) stoichiometric burning zone,

3) product-air mixing zone,

4) air or unburnt zone.

The model is based conceptually on the principles of jet mixing, although as the author points out, the geometry of the three zones forming the spray (zones 1, 2 and 3) as depicted in figure 4.26 are not intended to represent physical boundaries, but are a summation of the assumed zones whether existing around individual droplets of burning fuel or around a rich core of droplets in the burning spray.

In order to gain an understanding of the present emissions model it is necessary to have a knowledge of the earlier two-zone combustion model (4.32) from which mixing rates for product formation are obtained.

The Two-Zone Combustion Model (4.32).

The two-zone model, incorporating a non-burning zone and a burning zone, is used to calculate cylinder pressure and convective heat transfer from the non-burning zone; convective and radiative heat transfer from the burning zone and the fuel burning rate.

ZONE 1. FUEL ZONE
ZONE 2. STOICHIOMETRIC COMB ZONE
ZONE 3. PRODUCT/AIR ZONE
ZONE 4. AIR ZONE
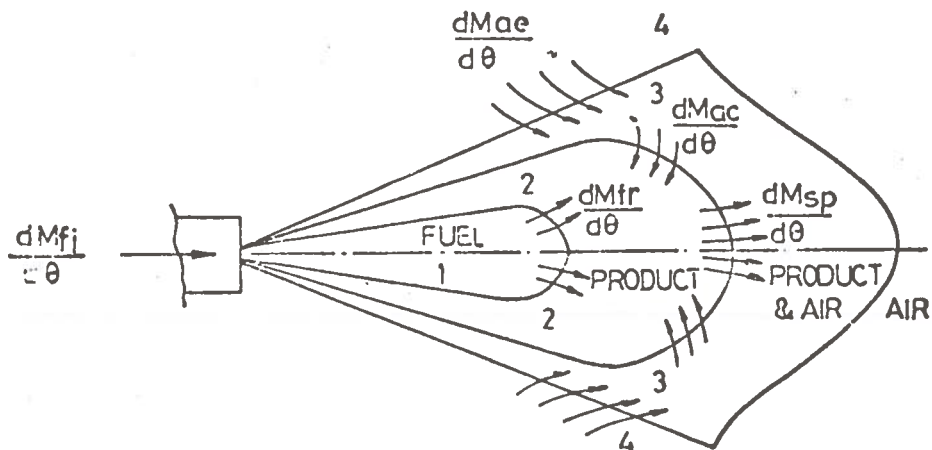
$$\frac{dM_{fi}}{d\theta} = \text{FUEL INJECTION RATE} \qquad \text{TO ZONE 1}$$

$$\frac{dM_{fr}}{d\theta} = \text{FUEL REACTION RATE} \qquad \text{FROM ZONE 1 TO ZONE 2}$$

$$\frac{dM_{ae}}{d\theta} = \text{AIR ENTRAINMENT RATE} \qquad \text{FROM ZONE 4 TO ZONE 3}$$

$$\frac{dM_{ac}}{d\theta} = \text{AIR CONSUMPTION RATE FOR}$$
$$\text{STOICHIOMETRIC BURNING} \qquad \text{FROM ZONE 3 TO ZONE 2}$$

$$\frac{dM_{sp}}{d\theta} = \text{PRODUCT MIXING RATE} \qquad \text{FROM ZONE 2 TO ZONE 3}$$

(From Baluswamy (4.10))

FIGURE 4.26.   SCHEMATIC REPRESENTATION OF THE FOUR ZONES

The rate of entrainment of air from the non-burning zone into the burning zone is calculated from the jet penetration rate. Jet penetration is based on the theory of steady free jets (4.33), modified by the use of an empirical "impulsive jet factor".

Steady jet penetration is given by

$$x_t = 2.42 \left[\frac{(\Delta p)^{\frac{1}{2}}}{\rho_a} \cdot d_{n.t} \right]^{\frac{1}{2}} \quad m., \qquad (4.47)$$

where d_n = nozzle diameter, mm.,

   Δp = injection pressure, bars,

   t = time, sec.,

and ρ_a = unburnt zone density, kg/m^3,

which is deduced from the steady jet centreline velocity. To obtain agreement between equation (4.47) and experiments on non-steady jet penetration, an empirically determined "impulsive jet factor" (= 0.685) is introduced. Jet penetration is allowed to take account of changing ambient density, ρ_a, due to both the combustion process and piston movement.

Conditions within the jet are used to calculate the rate of preparation of fuel based on a semi-analytical droplet vaporization process (Whitehouse and Way, (4.3)):

$$P = K^1 m_i^{(1-x)} m_u^x PO_2^L \qquad (4.48)$$

where P = rate of fuel preparation, kg/^{o}CA,

   K^1 = constant,

   m_i = mass of fuel injected,

   m_u = mass of fuel unburnt,

and PO_2 = partial pressure of oxygen (within the spray).

The coefficients x and L are empirical constants, with suggested values of

   x = 2/3

and L = 0.4.

A fuel reaction rate of the Arrhenius form is postulated:

111

$$R = K^{11} \frac{P_{O_2}}{N\sqrt{T}} \exp\left(-\frac{ACT}{T}\right) \cdot \int (P-R)dx \quad kg/^{o}CA, \quad (4.49)$$

where K^{11} = constant,

T = temperature, ^{o}K,

N = engine speed, r.p.m.,

ACT = index in reaction rate equation (effective activation temperature),

and $\int (P-R)dx$ = quantity of fuel in the cylinder that has been prepared but not yet burned.

At the high temperatures corresponding to the main period of combustion, the time taken for burning of the prepared fuel is negligible compared to the preparation time and therefore the fuel preparation rate (equation (4.48)) is the controlling process. The chemical kinetics of the combustion process, as represented by equation (4.49) are only important at the beginning of the burning period, when temperatures are low. The values of the constants in the reaction rate equation are chosen so that the initial period of low or negative heat release is identical to the measured ignition delay period, over a range of experimental conditions.

The four-zone emissions model of Baluswamy.

Fuel Zone (Zone 1).

This zone represents the central core of the spray and contains only fuel. The mass is determined by the rate of fuel injection $(\frac{dm_{fi}}{d\theta})$ and the rate of reaction of the fuel $(\frac{dm_{fr}}{d\theta})$. The fuel reaction rate is computed from the two-zone heat release model. The temperature of the zone is assumed equal to the average temperature of the burning zone of the two-zone model (figure 4.27). Baluswamy notes that the fuel zone is a potential source of soot due to pyrolysis.

Stoichiometric Burning Zone (Zone 2)

Fuel enters this zone at a rate $(\frac{dm_{fr}}{d\theta})$ computed from the two-zone model. Air required for stoichiometric combustion is entrained from zone 3 $(\frac{dm_{ac}}{d\theta})$. The zone temperature is calculated by apportioning the internal energy of the burning zone calculated with the two-zone model between the three sub-zones of the present model, and thence equilibrium species concentrations and rate calculations for nitric oxide formation are carried out. Mixing is allowed between this zone and the product/air zone at a rate $(\frac{dm_{sp}}{d\theta})$ specified empirically. Nitric oxide is formed only in zone 2, and nitric oxide carried by the diluting product into zone 3 (product/air zone) is assumed to freeze in that zone.

TEST CONDITIONS
SPEED = 500 RPM
BMEP = 9.3 BARS
INJECTION = 11° BTDC
NO. OF NOZZLE HOLES = 5
FUEL/CYLINDER/CYCLE = 0.00161 KG
PRODUCT MIXING FACTOR = 0.01
1 ———— CYLINDER MEAN TEMP
2 ----- UNBURNT TEMP (ZONE 4)
3 —-—- SPRAY MEAN TEMP (ZONE 1)
4 —-— PRODUCT/AIR ZONE TEMP (ZONE 3
5 —--— STOICHIOMETRIC COMBUSTION ZONE TEMP
                                    (ZONE 2)
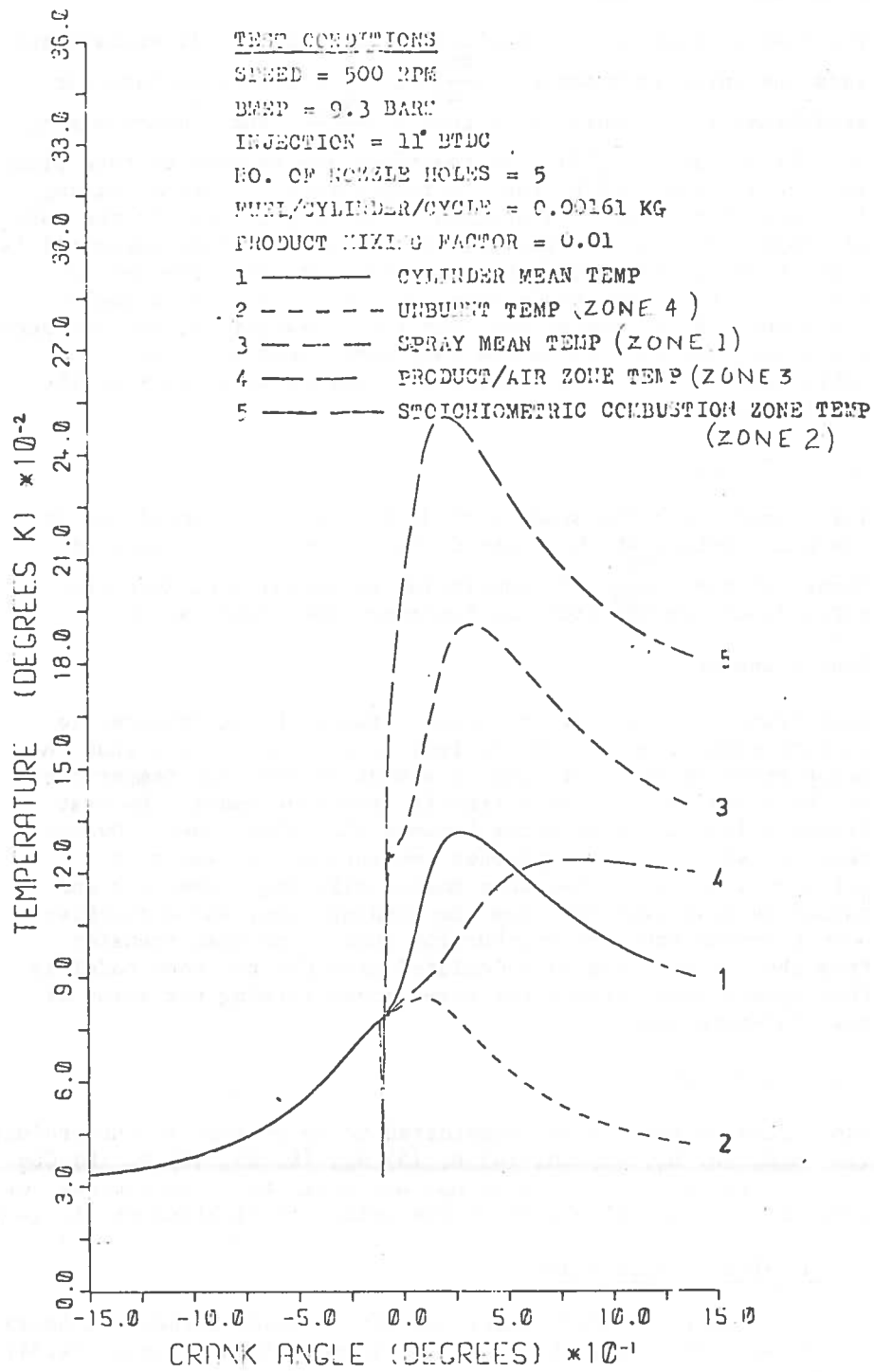
(From Baluswamy (4.10))

FIGURE 4.27.   COMPUTED TEMPERATURE HISTORIES OF THE FOUR ZONES AT TYPICAL
               ENGINE CONDITIONS.

113

Product/Air Zone (Zone 3).

The mass of zone 3 is controlled by the rate of air entrainment into the spray from ambient ($\frac{dm_{ae}}{d\Theta}$), air consumption rate for stoichiometric combustion in zone 2 ($\frac{dm_{ac}}{d\Theta}$), and product mixing rate from zone 2 ($\frac{dm_{sp}}{d\Theta}$). No reactions are assumed to take place in zone 3, justified by the low temperatures. Product mixing from zone 2 to zone 3 is assumed to be proportional to the mass of product in zone 2. The proportionality constant suggested is 0.01, that is, 1% of the stoichiometric product from zone 2 mixes into the product-air zone 3 during each crank angle increment. Baluswamy states that this constant has not yet been optimised, and that it is the only extra empirical factor introduced into the four zone model over those already in the two zone model.

Air or Unburnt Zone (Zone 4).

This constitutes the space outside the spray. Composition is assumed constant at the trapped charge conditions. Rate of change of mass ($\frac{dm_{ae}}{d\Theta}$) is controlled by entrainment into the spray as determined from the two-zone model calculations.

Heat Transfer

Heat transfer is assumed to occur between the stoichiometric burning zone (zone 2) and the fuel zone (zone 1) such that the temperature of the fuel zone is always at the mean temperature of the spray as calculated from the two-zone model. No heat transfer is assumed to occur between the other zones. Overall heat transfer from the cylinder contents to the walls is calculated using the two-zone model, allowing convective and radiative heat transfer from the burning zone, and convective heat transfer from the non-burning zone. The heat transfer from the burning zone as calculated from the two-zone model is then apportioned between the three zones forming the spray of the four-zone model.

Gas Properties

The following species are considered to be present in the product (1) H_2O, (2) H_2, (3) OH, (4) H, (5) N_2, (6) NO, (7) N, (8) CO_2 (9) CO, (10) O_2, (11) O, (12) A_r, and equilibrium conditions for these species are calculated by the method of Vickland et al. (4.21).

4.7.3 Nitric Oxide Kinetics

A seven equation kinetic model for nitric oxide formation, based on the work of Lavoie et al. (4.14) as modified by Baruah (4.34) is used:

114

(i) $N + NO \rightleftharpoons N_2 + O,$ $k_{1f} = 3.1 \times 10^{10} \exp\left(\frac{-160}{T}\right)$

(ii) $N + O_2 \rightleftharpoons NO + O,$ $k_{2f} = 6.4 \times 10^6 \times T \times \exp(-3125/T)$

(iii) $N + OH \rightleftharpoons NO + H,$ $k_{3f} = 4.2 \times 10^{10}$

(iv) $H + N_2O \rightleftharpoons N_2 + OH,$ $k_{4f} = 3 \times 10^{10} \exp(-5350/T)$

(v) $O + N_2O \rightleftharpoons N_2 + O_2,$ $k_{5f} = 3.2 \times 10^{12} \exp(-18900/T)$

(vi) $O + N_2O \rightleftharpoons NO + NO,$ $k_{6f} = k_{5f}$

(vii) $N_2O + M \rightleftharpoons N_2 + O + M,$ $k_{7f} = 10^{12} \exp(-30500/T)$

with the rates given in m^3/kg-mole.s.

Assuming OH, O_2, O and N_2 are at local equilibrium and 'steady state' values for N and N_2O, the above kinetic scheme is reduced to;

$$\frac{1}{V} \cdot \frac{d}{dt}\left[[NO] \cdot V\right] = 2(1 - \alpha^2)\left[\frac{R_1}{1 + \dfrac{\alpha R_1}{R_2 + R_3}} + \frac{R_6}{1 + \dfrac{R_6}{R_4 + R_5 + R_7}}\right]$$

$$(4.50)$$

where $\alpha = \dfrac{[NO]}{[NO]_e},$ $R_1 = k_{1f}[N]_e[NO]_e$

                             $R_2 = k_{2f}[N]_e[O_2]_e$

                          etc.

Figure (4.28) shows the result of the nitric oxide calculation for a typical engine condition.

4.7.4 Experimental Comparison

No direct comparison between the results of the model and experimental measurements have been published. The trends of the model are in qualitative agreement with generally accepted experimental results. Thus exhaust NO decreases with injection retard, increases with load, and is fairly insensitive to speed.

4.7.5 Discussion and Comments

This model is a development of an earlier two-zone heat release model, and incorporates all of the assumptions of the earlier work. The only extra parameter introduced here is a rate of mixing of product from the stoichiometric combustion zone to the product-air zone. Baluswamy states that this parameter has not yet been

TEST CONDITIONS
SPEED = 500 RPM
BMEP = 9.3 BARS
INJECTION = 11° BTDC
NO. OF NOZZLE HOLES = 5
FUEL/CYLINDER/CYCLE = 0.00161 KG
PRODUCT MIXING FACTOR = 0.01

1 - - - - - EQUILIBRIUM NO IN STOICHIOMETRIC
                             COMBUSTION ZONE
2 ――――― RATED NO IN STOICHIO. COMB. ZONE
3 ― ― ― NO IN THE SPRAY
4 ― ― ― NO IN THE CYLINDER
5 ― ― ― NO IN PRODUCT/AIR ZONE
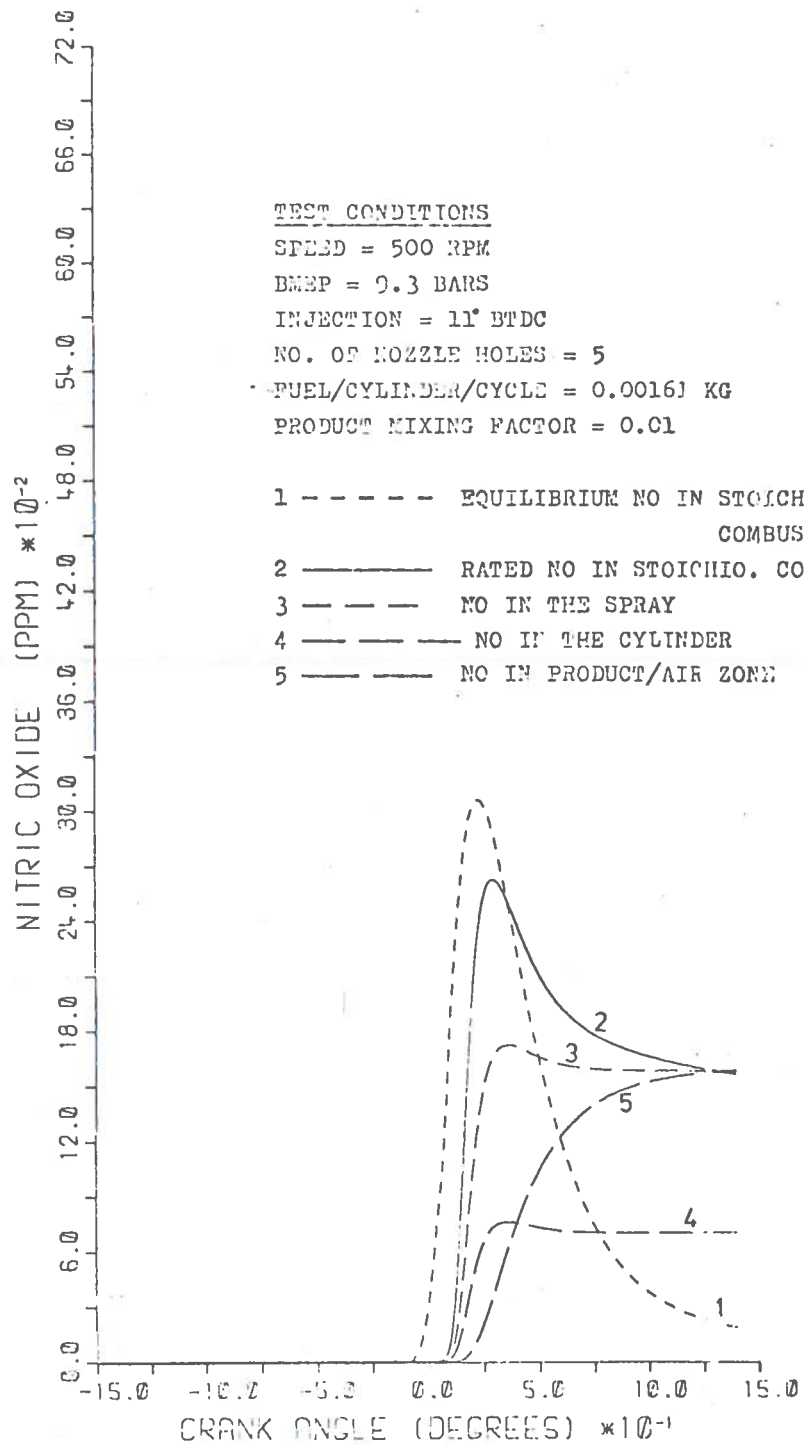
(From Baluswamy (4.10))

FIGURE 4.28.   COMPUTED NITRIC OXIDE LEVELS IN VARIOUS ZONES

116

optimised, and that many of the earlier model parameters should
be re-optimised. However, it is encouraging that the trends
predicted by the model are in agreement with generally accepted
experimental results.

The chemical kinetic model for nitric oxide formation seems over-
detailed in relation to many of the other model assumptions, for
example the use of only one NO formation zone.

In conclusion, this is another model which would repay detailed
comparison of the predictions with more experimental results,
both to optimise the model parameters, and to bring out any
shortcomings.

5. GENERAL DISCUSSION

5.1. The current status of diesel emissions modelling

5.1.1. Models

The ultimate goal of developing a model based entirely upon physical
and chemical laws free from empiricisim, with engine geometry specified a
priori, has not been achieved. The present best models (e.g. Kau et al
(5.1), Shahed et al (5.2) and Hodgetts and Shroff (5.3)) appear to be able
to provide reasonable correlations, at least for NO_x dependence on engine
parameters for a specific engine, using a minimum number of empirical con-
stants determined under one set of engine conditions. Nevertheless, the
effects of some engine variables, such as turbocharging on NO_x (for example)
are still poorly modelled. No current model appears to be able to incorporate
design factors explicitly - they remain hidden in the empirical constants -
and in consequence no model can yet be labelled "predictive" in the sense of
being applicable to a variety of combustion chamber designs without substantial
adjustment. Precisely how good or bad is the current modelling capability is
difficult to assess, principally because the models, with only one or two
exceptions (such as that of Bastress et al (5.4)), have not been compared to
test data from more than one engine design or, more importantly, to data from
more than one laboratory. This last factor represents a serious weakness and
is a hindrance to the successful development of more fundamentally based
models.

We illustrate some of the foregoing comments from the recent models of
Hiroyasu and Kadota (5.5), Shahed et al (5.2) and Hodgetts and Schroff (5.3).
These models all develop moreorless sophisticated descriptions of the mixing
process, a feature which we shall advocate for more detailed attention in
future developments of diesel combustion models.

Hiroyasu and Kadota develop a relatively sophisticated mixing model,
giving the equivalence ratio in different fluid packages, but then use a
simplistic net heat release calculation, incorporating heat loss based on a
mean cylinder temperature, to determine cylinder pressure and hence local
temperature (no details of how C_p and C_v have been calculated is included in
the published account of the model). No post-combustion mixing of packages
is permitted and they are assumed to remain at the adiabatic temperature.
The consequence is extremely high local temperatures (peaks~3300-3700 K); it
is surprising that this does not cause excessive NO concentrations to be
predicted.

Shahed et al (5.2) and Hodgetts and Schroff (5.3) incorporate the results
of free jet experiments. The former workers (5.2) assume a steady jet concen-
tration distribution, combined with empirical knowledge of the velocity of an
unsteady jet, whereas Hodgetts and Schroff (5.3) assume a steady jet velocity
distribution and invoke the principle of conservation of momentum to determine
a concentration distribution across the jet. It would be of great interest to
determine the effect of these two very different basic assumptions upon the
model results. Recent work (5.6) indicates that although steady jet analysis
(Abramovich (5.7)) may give general guidelines for some of the phenomena
occurring in non-steady diesel sprays (e.g. penetration correlations), it is
far from adequate to describe many of the high pressure non-steady combustion
phenomena occurring in such sprays. Many workers have not even mentioned the
effects of combustion on the Abramovich analysis. More data is needed of the

118

effects of high ambient temperature and pressure on, for example, the spreading angle of steady burning jets, before confident extension to the non-steady situation can be considered.

What is perhaps not sufficiently appreciated is that a successful diesel model must be, almost by definition, a much more complex and sophisticated animal than the present generation of successful S.I. engine models. To expect simple, empirical engineering approximations, in which much of the fundamental physics and chemistry is lost in empirical constants, to do more than provide the most obvious correlations between, say, NO_x and some engine variables, is no more than wishful thinking. Nor is it reasonable to expect a successful predictive diesel emissions model to appear overnight. A number of factors predicate against such an event, including such basic shortcomings as our present inability to properly describe the in-cylinder mixing pattern, or the influence of turbulence on the chemistry, or the mechanisms of NO production in a two phase diffusion combustion process.

All the models consider only 'laminar' chemical kinetics. If it is intended to make the models truly predictive, then it will be necessary to include the effects of turbulent temperature and composition fluctuations. The recent models which describe many elements, each with different temperature, equivalence ratio histories to make up the mixing/combustion zone (e.g. Raine (5.6), Kau et al (5.1), Shahed et al (5.2), Hodgetts and Schroff (5.3)) would appear to offer the best scope for incorporating turbulence effects into the individual elements. Similarly droplet vaporisation should be incorporated on a more discrete basis, as some modellers are now doing (Kau et al (5.1), Hiroyasu and Kadota (5.5)).

To date only Khan et al (5.8) and Hiroyasu and Kadota (5.5) have attempted to incorporate soot formation and oxidation kinetics and these efforts are best viewed as exercises in curve fitting.

5.1.2 NO_x chemistry and emissions

In the Introduction we suggested that, as NO_x emissions from diesels were reduced, a situation might be reached where NO formation from mechanisms other than the extended Zeldovich become important. Our present knowledge of diesel combustion is inadequate to make such a statement quantitative, although it must be emphasised that significant reduction can probably be achieved before the need to include the additional NO_x formation mechanisms becomes mandatory. The somewhat equivocal statements here are a reflection of a number of contirbutory factors. These include the evidence, from stratified charge engine studies (5.9), for prompt NO contributions to NO_x emissions under very lean engine conditions, and an inability to model NO formation under rich conditions even when 'prompt' NO is included (5.9, 5.10). The latter factor is also evident in attempts to model NO in droplet combustion under laboratory conditions (5.11). In addition there is the vexed problem of how to incorporate turbulence-chemistry interaction effects in a two-phase, unpremixed, unsteady combustion process.

In view of the foregoing remarks it is somewhat surprising that attempts to model NO_x formation and emission in diesels have progressed as far as they have. On closer inspection, however, as is indicated in Section 4, much of the 'agreement' obtained is little more than correlation and is certainly inadequate to be used predictively. In fact it might be said with some justification that, although the modelling had to start from a relatively simple beginning, it has now reached the stage where to continue with such simple ideas is likely to inhibit, rather than help, the future development of NO_x modelling.

119

The comparatively high NO_2 emissions found in idling diesels should be viewed in relation to high NO_2 measurements in the primary combustion zone of gas turbines, the almost 100 per cent NO_2 sampled under very lean low temperature flame conditions (5.12) and the chemical equilibrium shift in the NO_2/NO system (5.13). The two most obvious qualitative explanations of the measurements are

(i)   that recirculated combustion products are cooled adjacent to fuel-rich or pure fuel zones to temperatures at which NO_2 is the predominant oxide at equilibrium and which are sufficiently high for the $NO \rightarrow NO_2$ conversion to remain rapid, and

(ii)   that under very lean premixed combustion conditions the consequent lower temperatures cause the higher oxides to be preferred and to be either formed directly or to form rapidly from intermediate NO (5.12).

If such zones are subsequently frozen chemically, either by sampling or by further mixing to lower temperatures, then high NO_2 measurements may be expected. At this juncture attention should again be drawn to the inherent difficulties associated with quantitative determination of the nitrogen oxides in some circumstances (see Section 2.1.4.).

5.1.3. Smoke chemistry and emissions

Despite over half a century of research, our understanding of soot formation in combustion is still only rudimentary. The processes which are generally considered to control soot formation can be summarised as follows:

(1) Gas phase reactions which are responsible for the formation of soot precursors and of growth species.

(2) Nucleation of gas phase precursors to form soot nuclei.

(3) Surface growth of soot particles as appropriate gas phase molecules collide with the particles.

(4) Coagulation of soot particles to form larger particles and to form chains of particles.

(5) Surface oxidation of the soot particles as they come into contact with oxidising gas phase species.

The heterogeneous processes are not fully understood even under very idealised laboratory conditions. However, as indicated in Section (3.1.4), several attempts have been made to model certain aspects of the processes, with varying degrees of success. These models range in complexity from the chemical kinetic description of Jensen (5.14) (involving 10 gas phase reactions, and approximately 100 particle-particle reactions), to the semi-empirical approach of Gilyazet dinov (5.15), involving the solution of three simultaneous differential equations. None of the available models mentioned in the review have, however, considered the effects of turbulence on soot formation, which could be of major importance in the diesel situation. The first studies of turbulence effects on soot formation in idealised laboratory situations (5.16, 5.17) are only just beginning to be reported.

No satisfactory model of soot formation and oxidation, applicable to the diesel, appears to exist. Even the models developed by Khan et al (5.8) and Hiroyasu and Kadota (5.5), the only attempts to date, are empirical in the extreme. Inclusion of fluid mechanical-chemical kinetic interactions are evidently further in the future than in the case of NO_x production.

5.2 Summary of shortcomings and suggestions for remedial action

We now summarise the more important shortcomings in both the emissions models and fundamental data, as revealed by the foregoing review, and indicate in general terms the directions in which we believe progress should be sought.

Our main criticism of the modelling efforts to date is that they are too empirical and in consequence they have proven non-predictive. There has been an unfortunate tendency on the part of some modellers, to obtain a 'fit' between experiment and model at the expense of almost any sacrifice in the fundamentals. In one instance this has even extended to substantially modifying well-established rate coefficients in the NO_x chemistry. The result has been to obscure the underlying reasons for failure to obtain predictive capability and to hinder model development and comparison between models and data from different laboratories. What is in effect a corollary of the foregoing concerns the large number of empirical coefficients which are incoporated in many of the models.

We advocate less empiricism, even though, initially, this will almost certainly result in poor comparisons between model and experiment. This approach should be coupled with a deliberate attempt to compare the models with data from several laboratories - on a co-operative basis - and with data from carefully designed experiments. Examples of such experiments include adding NO to the engine air supply, making detailed turbulence and other property measurements, and tracing the flow history of a marked fraction of the fuel charge in each cycle. The latter can be accomplished by addition of a trace species to part of the fuel and monitoring the result either by in-cylinder probe sampling or by an in situ optical technique. Direct sampling has the drawback of introducing some element of time averaging whereas the optical techniques, whilst capable in principle of instantaneous local property measurements, suffer from a much greater "degree of difficulty" in the diesel context. Considerably more insight should be gained from such experiments, which will be necessary in any case to exploit fully the potential of the recent trend towards more realistic modelling of the flowfield and mixing processes.

A complementary excercise, which we should like to encourage, is for the different modellers to calculate a common 'test case' - perhaps a particular engine test or series of tests. The relative strengths and weaknesses of the various models would then be highlighted and sign posts to the improvements necessary made more obvious.

Addition of turbulence effects on the chemistry of the NO_x reaction and a more detailed model of soot formation, such as Jensen's, should be primary objectives in model improvement.

The effects of combustion chamber geometry are probably the most difficult features of the diesel to model and no successful attempt is known to us. In Section 2 we presented, apprently for the first time, an attempt to correlate NO_x emission levels with engine surface-to-volume ratio for a variety of engines. Undoubtedly such a simple parameter as the surface-to-volume ratio, with no account taken of compression ratio or flow pattern, is unlikely to succeed for such a wide range of engine types. Figure 2.5 does suggest, however, a degree of usefulness and insight which we feel should be exploited.

Spalding is undoubtedly correct in suggesting (1.18) that unsteady effects are important in the diesel; what is not clear is what priority inclusion of these effects should take, nor is the magnitude of the task. In principle,

solving the full Navier-Stokes equations is the proper course; unfortunately it is impractical, and likely to remain so for the foreseeable future, despite Anderson's recent publication (5.19) of a much simplified model of the S.I. engine using just this approach.

One feature of diesel combustion which should be removed from the realm of speculation as soon as possible is whether, and under what conditions, the diesel spray burns as a diffusion flame, and under what conditions, if any, it burns on a single droplet basis.

Another poorly modelled feature of diesel combustion is the heat transfer. The new generation of more detailed mixing models should permit a basic re-appraisal of the heat transfer, with potentially important consequences for the strongly temperature dependent rate processes which govern the emissions of both NO_x and smoke. This should also be an important early objective.

Finally, we turn to basic data requirements. Although we have said little about it, the ignition delay largely determines the extent of the premixed burn and thereby significantly affects both NO_x and, more especially, smoke production. There is surprisingly little data on ignition delays under carefully controlled laboratory conditions - as distinct from engine tests - for the higher hydrocarbons, such as diesel fuels, in the literature. Part of the problem is to separate out the purely chemical from the physical (mixing) components of the problem in the diesel. Both are important. More work is needed in this area.

Closely allied to the ignition delay problem is the production of soot in diesel combustion. A really major research effort is required here and should be directed particularly at the specific fuels of interest, rather than at the simpler hydrocarbons as has been the tendency to date. A good example is the recent work of Gosling (5.20), who has studied the pyrolysis of kerosene using a shock tube.

We are also uneasy about the reliance which is placed on the Zeldovich mechanism to explain all the NO_x produced in a diesel. Whilst it is undoubtedly true that it is adequate for the S.I. engine under most conditions, the evidence quoted earlier (Section 5.1.2), relating to the stratified charge engine, suggests there is need to avoid complacency so far as the diesel is concerned. What is not clear is the solution, since neither is the mechanism of NO production from reaction between hydrocarbon fragments and atmopsheric nitrogen known, nor are the concentrations of such fragments predictable.

6. CONCLUSIONS

1. Existing diesel engine emissions models have been reviewed (Section 4). The models show considerable variability in their capacity to correlate emissions with engine variables for a given engine design. None of the models has shown any predictive capability. NO_x has been modelled with more fundamental insight than has soot. Combustion chamber geometry effects have not been modelled to date.

2. The following deficiencies in basic data and understanding have been identified: flowfield and mixing processes; turbulence-reaction rate interactions; soot formation kinetics; chemical ignition delays; and NO_x chemistry involving hydrocarbon fragments.

3. Further work is required to remove model shortcomings and basic data deficiences.

(a) Models: we advocate development of the multi-element combustion/mixing zone models. This approach should prove amendable to the inclusion of turbulence-reaction rate interactions, improved soot kinetics, and other basic data improvements as these become available.

(b) Engine studies: in-cylinder studies, either by sampling probe or optical technique are necessary to characterize the macroscopic properties of the flowfield, the mixing patterns and, hopefully, the turbulence properties.

(c) Basic data: as listed in Conclusion 2.

The three components (a)-(c) should be viewed as contributing interactively to the development of diesel emissions model predictive capabilities.

123

7. <u>REFERENCES</u>

1.1 WILSON R P, WALDMAN C H and MUZIO L J,
     "Foundation for modelling NO_x and smoke formation in diesel flames"
     EPA-460/3-74-002a, Jan 1974 (CRC Report APRAC CAPE 20 71 1)

1.2 HENEIN N A,
     "Analysis of pullutant formation and control and fuel economy
     in diesel engines"
     Progr Energy Combust. Sci 1, 165-207 (1976)

1.3 KHAN I M, GREEVES G and WANG C H T,
     "Factors affecting smoke and gaseous emissions from direct
     injection engines and a method of calculation"
     SAE Paper 730169 (1973)

1.4 BECKER H A and YAMAZAKI S,
     "Soot concentration field of turbulent propane/air diffusion
     flames"
     16th Symposium (International) on Combustion, The Combustion
     Institute, in press.

     MAGNUSSEN B F and HJERTAGER B H ,
     "On mathematical modelling of turbulent combustion with special
     emphasis on soot formation and combustion"
     16th Symposium (International) on Combustion,
     The Combustion Institute, in press.

1.5 HIROYASU H and KADOTA T,
     "Models for combusion and formation of nitric oxide and soot in
     direct injection diesel engines"
     SAE Paper 760129, (1976).

1.6 "Summary of Legislation on Pollution from Diesel Engined Vehicles"
     - prepared by Diesel Sub Group of British Technical Council of
     Motor and Petroleum Industries - Feb 1975.
     Updated from Federal Register, EPA - Heavy duty engines, May 24 1976.

1.7 ECE Regulation 24, 11th March 1970.

1.8 SPIERS J, VULLIAMY N M F,
     "Diesel Engine Smoke and Pollutants" - Publication No 342, June 1971;
     Diesel Engineers and Users Association.

1.9 KHAN I M,
     "Diesel engines as a Power Plant for the future" Power Plants
     and future fuels Conference 1975, I Mech E, London.

2.1   BOWMAN C T
      "Kinetics of pollutant formation and destruction in combustion"
      Progr. Energy Combust. Sci. 1, 33-45 (1975)

2.2   ZELDOVICH Ya B, SADOVNIKOV P Ya and FRANK-KAMENETSKII D A ,
      "Oxidation of nitrogen in combustion" (transl by M Shelef)
      Academy of Sciences of USSR, Institute of Chemical Physics
      Moscow-Leningrad (1947).

2.3   BAULCH D L, DRYSDALE D D, HORNE D G and LLOYD A C,
      "Evaluated Kinteic data for high temperature reactions"
      Vol 2 Butterworths (1973)

2.4   LAVOIE G A, HEYWOOD J B and KECK J C
      "Experimental and theoretical study of nitric oxide formation
      in internal combustion engines"
      Combust. Sci. Technol. 1, 313-326 (1970)

2.5   SHAHED S M and NEWHALL H K
      "Kinetics of nitric oxide formation in propane-air and hydrogen
      -air-diluent flames"
      Combust. Flame 17, 131-137 (1971)

2.6   FENIMORE C P,
      "Formation of nitric oxide in premixed hydrocarbon flames"
      13th Symposium (International) on Combustion, pp 373-380,
      The Combustion Institute, (1971)

2.7   LIVESEY J B, ROBERTS A L and WILLIAMS A

      Combust. Sci. Technol. 4, 9 (1971)

2.8   SAROFIM A E and FLAGAN R C,
      "No$_x$ control for stationary combustion sources"
      Progr. Energy Combust, Sci. 2, 1-25 (1976).

2.9   MALTE P C and PRATT D T
      "The role of energy-releasing kinetics on NO$_x$ formation:
      fuel-lean, jet stirred, CO-air combustion"
      Combust Sci Technol 9, 221-231, (1974)

2.10 HOMER J G and SUTTON M M,
      "Nitric Oxide formation and radical overshoot in premixed hydrogen
      flames"   Combust. Flame 20, 71-76 (1973)

2.11 ANNAND W J D
      "Effects of simplifying kinetic assumptions in calculating nitric
      oxide formation in spark-ignition engines"
      Proc. Inst Mech Engrs 188, 431-445, (1974).

2.12 BOWMAN C T
"Kinetics of nitric oxide formation in combustion processes"
14th Symposium (International) on Combustion pp 729-738. The
Combustion Institute (1973).

2.13 ENGLEMAN V S, BARTOK W, LONGWELL J P and EDELMAN R B
"Experimental and Theoretical Studies of NO_x formation in a
jet-stirred reactor"
14th Symposium (International) on Combustion, pp 755-765,
The Combustion Institute (1973).

2.14 SAROFIM A F and POHL J H
"Kinetics of nitric oxide formation in premixed laminar flames"
14th Symposium (International) on Combustion pp 739-754,
The Combustion Institute (1973).

2.15 IVERACH D, KIROV N Y and HAYNES B S
"The formation of nitric oxide in fuel-rich flames"
Combust Sci Technol 8, 159-164 (1973).

2.16 HAYNES B S, IVERACH D and KIROV N Y,
"The behaviour of nitrogen species in fuel rich hydrocarbon flames"
15th Symposium (International) on Combustion pp 1103 - 1112,
The Combustion Institute (1975).

2.17 BACHMAIER F, EBERIUS K.H. and JUST Th,

Combust Sci Technol 7 77-   (1973).

2.18 BOWMAN C T,
"Investigation of NO formation kinetics in combustion processes;
the $H_2-O_2-N_2$ reaction"
Combust. Sci Technol 3, 37-45 (1971).

2.19 BOWMAN C T and SEERY D J
Emissions from continuous combustion systems, (Ed Cornelius
and Agnew) p.123-139, Plenum (1972).

2.20 THOMPSON D, BROWN T D and BEER J M,
"NO_x formation in combusion"

Combust Flame 19, 69-79 (1972).

2.21 EDELMAN R B and FORTUNE O F
"A quasi-global chemical kinetic model for the finite-rate
combustion of hydrocarbon fuels with application to turbulent
burning and mixing in hypersonic engines and nozzles"
AIAA Paper 69-86 (1969).

2.22 SCHOTT G L
     "Kinetic studies of hydroxyl radicals in shock waves.
     III The OH concentration maximum in the hydrogen-oxygen reaction".
     J Chem. Phys 32, 710-716 (1960).

2.23 IVERACH D, BASDEN K S and KIROV N Y
     "Formation of nitric oxide in fuel-lean and fuel-rich flames"
     14th Symposium (International) on Combustion, pp 767-775,
     The Combustion Institute (1973).

2.24 BOWMAN C T
     "Non-equilibrium radical concentrations in shock-initiated
     methane oxidation".
     15th Symposium (International) on Combustion pp 869-882,
     The Combustion Institute (1975).

2.25 McCREATH C G
     "The effect of fuel additives on the exhaust emissions from
     diesel engines".
     Combust Flame 17, 359-366 (1971).

2.26 FENMORE C P
     "Formation of nitric oxide from fuel nitrogen in ethylene flames"
     Combust Flame 19, 289-296 (1972).

2.27 DE SOETE
     "Overall reaction rates of NO and N_2 formation from fuel nitrogen"
     15th Symposium (International) on Combustion, pp 1093-1102,
     The Combustion Institute (1975).

2.28 DUXBURY J and PRATT N H
     "A shock tube study of NO kinetics in the presence of H_2 and fuel-
     N"
     15th Symposium (International) on Combustion pp 843-855, The
     Combustion Institute (1975).

2.29 BRADLEY J N and CRAGGS P
     "The reaction of hydrogen with nitric oxide at high temperatures."
     15th Symposium (International) on Combustion pp 833-842,
     The Combustion Institute (1975).

2.30 WESTENBERG A A
     "Kinetics of NO and CO in lean, premixed hydrocarbon- air flames"
     Combust Sci Technol 4, 59-64 (1971).

2.31 FENMORE C P
     "Reactions of fuel-nitrogen in rich flame gases"
     Combust Flame 26, 249-256 (1976).

2.32 FLAGAN R C, GALANT S and APPLETON J P
"Rate constrained partial equilibrium models for the
formation of nitric oxide from organic fuel nitrogen".
Combust Flame 22, 299-311 (1974).

2.33 HILLIARD J and WHEELER R W
"Catalysed oxidation of nitric oxide to nitrogen dioxide"
Combust Flame in press

2.34 TUTTLE J H, SHISLER R A and MELLOR A M
"Nitrogen dioxide formation in gas turbine; measurements and
measurement methods".
Combust Sci Technol 9, 261-271 (1974).

2.35 MERRYMAN E L and LEVY A
"Nitrogen oxide formation in flames; the roles of NO_2 and fuel
nitrogen"
15th Symposium (International) on Combustion pp 1073 - 1083,
The Combustion Institute (1975).

2.36 ALLEN J D
"Probe sampling of oxides of nitrogen from flames"
Combust Flame 24, 133-136 (1975).

2.37 FENIMORE C P
"The ratio NO_2/NO in fuel-lean flames"
Combust Flame 25, 85-90 (1975).

2.38 MELLOR A M
Emissions from continuous combustion systems
(Ed Cornelius and Agnew) pp 23-53, Plenum (1972).

2.39 CERNANSKY N P and SAWYER R F
"NO and NO_2 formation in a turbulent hydrocarbon/air diffusion
flame"
15th Symposium (International) on Combustion pp 1039-1050,
The Combustion Institute (1975).

2.40 LAURENDEAU N M,
"Fast nitrogen dioxide reactions: significance during NO decomposition
and NO_2 formation".
Combust Sci Technol 11, 89-96 (1975)

2.41 MOSS J B and BRAY K N C
"A statistical model of NO formation in pre-mixed turbulent flames"
Deuxieme Symposium sur la Combustion, pp 315-320, French Section,
The Combustion Institute (1975).

2.42 BILGER R W
     "Turbulent jet diffusion flames"
     Prog Energy Combust Sci 1, 87-109 (1976).

2.43 KENT J H and BILGER R W
     "The prediction of turbulent diffusion flame fields and nitric
     oxide formation"
     16th Symposium (International) on Combustion
     The Combustion Institute, in press.

2.44 LIBBY P A and WILLIAMS F A
     "Turbulent flows involving chemical reactions"
     Ann Rev Fluid Mech 8, 351-376 (1976).

2.45 HILL J C
     "Homogeneous turbulent mixing with chemical reaction"
     Ann Rev Fluid Mech 8, 135-161 (1976).

2.46 SPALDING D B

     Combust Sci Technol 13, No 1-6 (1976)

2.47 CARETTO L S
     "Mathematical modelling of pollutant formation" Progr Energy
     Combust Sci 1 47-71 (1976).

2.48 BRAY K N C, PRATT N H and KEWLEY D J,
     "Review of modelling problems in turbulent mixing chemical lasers"
     Symposium on Gasdynamic and Chemical Lasers, Cologne, Oct 1976.

2.49 BELLAN J R and SIRIGNANO W A,
     "Combustion and NO formation in a Stratfield-Charge engine:
     a two-turbulent equations model".
     Combust Sci Technol 12, 75-104 (1976)

2.50 SEMERJIAN H and VRANOS A,
     "NO_x formation in premixed turbulent flames"
     16th Symposium (International) on Combustion,
     The Combustion Institute, in press.

2.51 DAVIES P O A L and YULE A J,
     "Coherent structures in turbulence"
     J Fluid Mech 69, 513-537 (1975).

2.52 ACTON E,
     "The modelling of large eddies in a two-dimensional shear layer"
     J Fluid Mech 76, 561-592 (1976).

2.53 CHIGIER N A,
"The atomisation and burning of liquid fuel sprays"
Progr Energy Combust Sci 2, 97-114 (1976).

2.54 ONUMA Y, OGASAWARA M and INOUE T,
"Further experiments on the structure of a spray combustion flame"
16th Symposium (International) on Combustion
The Combustion Institute, in press.

2.55 WILLIAMS A
"Combustion of droplets of liquid fuels: a review"
Combust Flame 21, 1-31 (1973).

2.56 WILSON R P, WALDMAN C H and MUZIO L J,
"Foundation for modelling NO_x and smoke formation in diesel flames"
CRC Report APRAC CAPE 20 71 1, (1974).

2.57 LUDWIG D E, BRACCO F V and HARRJE D T,
"Nitric oxide and composition measurements within diffusion flames
around simulated ethanol and ethanol-pyridine droplets".
Combust Flame 25, 107-120 (1975).

2.58 BRACCO F V,
"Nitric oxide formation in droplet diffusion flames"
14th Symposium (International) on Combustion pp 831-842,
The Combustion Institute (1973).

2.59 BOWMAN C T and KESTEN A S,
"Kinetic modelling of nitric oxide formation in combustion processes"
Western States Section, The Combustion Institute, Fall Meeting (1971).

2.60 WILLIAMS A,
Comment on Ref 2.58
14th Symposium (International) on Combustion, p 841
The Combustion Institute (1973).

2.61 HART R, NASRALLA M and WILLIAMS A,
"The formation of oxides of nitrogen in the combustion of droplets
and sprays of some liquid fuels" Comb. Sci. Technol. II, 57-65, (1975)

2.62 DUGGAL V K and HOWARTH J S
"A preliminary study of the structure of diesel smoke"
J Inst of Fuel 48, 34-44 (1975)

2.63 ANDERTON D and DUGGAL V K,
"Diesel Engine Emissions and Noise" J. Inst of Fuel 49, 398 (1976)

2.64 ANDERTON D and DUGGAL V K,
"Effects of turbocharging on diedel engine noise, Emissions and
Performance"
SAE Paper 750797 (1975).

2.65 DUGGAL V K
"Diesel Combustion Sampling"
ISVR Memoranda Nos. 535, 543, 544, 550 (1974-75).

2.66 BRAY K N C and MOSS J B
"A Unified statistical model of the premixed turbulent flames"
AASU Report No 335, (1970).

2.67 MARSHALL W F and FLEMING R D
"Diesel emission as related to engine variables and fuel characteristics"
SAE Paper 710836 (1971).

2.68 MYERS P S, UYEHARA O A and NEWHALL H K,
"The ABCs of engine exhaust emissions"
SAE Paper 710481 (1971).

2.69 WILSON R P, MUIR E B and PELLICCIOTTI F A,
"Emissions study of a single cylinder diesel engine"
SAE Paper 740123 (1974).

2.70 DUGGAL V K, Ph D Thesis, University of Southampton,
(1976)- to be submitted.

2.71 WALDER C J,
"The reciprocating diesel engines"
Conference on Developments in Automotive power plants to reduce
fuel consumption, Air Pollution and Noise".
Queen Mary College, London, April 1973.

2.72 PISCHINGER R and CARTELLERI
"Combustion system parameters and their effect upon diesel engine
exhaust emissions"
SAE Paper 720756, (1972).

2.73 KHAN I M,
"Diesel engine as a power plant of the future"
Power Plants and Future Fuels Conference 1975
I Mech E. London.

2.74 FLOWER W L, HANSON R K andKRUGER C H,
"Kinetics of the reaction of Nitric oxide with Hydrogen"
15th Symposium (International) on Combustion, pp 823-832,
The Combustion Institute (1975).

3.1   PALMER H B and CULLIS C F,
      "The formation of carbon from gases"
      in Chemistry and Physics of Carbon (Ed P L Walker)
      1, 256 (1965).

3.2   HOMANN K H
      "Carbon formation in premixed flames"
      Combust Flame 11, 265 (1967).

3.3   HOMANN K H,
      "Carbon formation in premixed flames"
      in NBS-SP 357 "The Mechanisms of Pyroysis, Oxidation and Burning of
      Organic Materials", P 143 (1970).

3.4   FEUGIER A,
      "Carbon- soot in flames"
      Rev Inst Franc Petr 24 (11) 1374 (1969).

3.5   GAYDON A G and WOLFHARD H G,
      "Flames, their structure, radiation and temperature."
      3rd Edn (1970).

3.6   McARRAGHER J S and TAN K J,
      "Soot formation at high pressures: A literature review".
      Combust Sci Technol 5(5), 257 (1972).

3.7   BROOME D and KHAN I M,
      "The mechanics of soot release from combustion of hydrocarbon
      fuels with particular reference to the diesel engine."
      Lucas Eng Rev 6(2) 46(1973).

3.8   PALMER H B and SEERY D J,
      "Chemistry of pollutant formation in flames"
      Ann Rev Phys Chem 24, 235 (1973).

3.9   LAHAYE J and PRADO G,
      "Formation of carbon particles from a gas phase:
      nucleation phenomenon".
      Water, Air and Soil Pollution 3, 473 (1974).

3.10 VUK C T, JONES M A and JOHNSON J H,
      "The measurement and anlysis of the physical character of Diesel
      particulate emissions".
      SAE 760131, (1976).

3.11 KNORRE V G et al,
      "A study of the thermal decomposition of acetylene and the
      properties of the soot formed under the conditions of a constant
      volume bomb".
      Comb, Expl and Shockwaves 8(4) 437 (1972).

3.12 MINCHIN S T,
   "Luminous stationary flames"
   J Inst Petr Tech 17, 102 (1931).

3.13 CLARKE A E, HUNTER T G and GARNER F H,
   "The tendency to smoke of organic substances on burning (I)"
   J Inst Petr 32, 627 (1946).

3.14 MEIER ZU KOCKER H,
   "Kinetics of soot formation, investigations into the mechanism
   of soot formation in hydrocarbon diffusion flames".
   Combust Sci Technol 5(5) 219 (1972).

3.15 MEIER ZU KOCKER H and KLOSE W,
   "Assessment of gaseous and liquid fuels in view of their expected
   tendency towards soot formation in a diffusion flame."
   Chem-Ing-Tech 44 (1-2) 46 (1972).

3.16 GAY N R et al,
   "Thermochemical equilibrium in hydrocarbon-oxygen reactions involving
   polyatomic forms of carbon".
   Combust and Flame 5, 257 (1961).

3.17 STREET J C and THOMAS A,
   "Carbon formation in premixed flames"
   Fuel 34, 4 (1955).

3.18 DANIELS P H,
   "Carbon formation in premixed flames".
   Combust Flame 4, 45 (1960).

3.19 FENIMORE C P, JONES G W and MOORE G E,
   "Carbon formation in quenched flat flames at $1600^{\circ}K$"
   6th Symposium (International) Combust 242 (1956).

3.20 WRIGHT F J,
   "The formation of carbon under well-stitted conditions"
   12th Symposium (International) Combust 8, 67
   The Combustion Institute (1969).

3.21 RADCLIFFE S W and APPLETON J P,
   "Shock-tube measurements of carbon to oxygen atom ratios for incipient
   soot formation with C_2H_2, C_2H_4 and C_2H_6 fuels".
   Combust Sci Technol 3, 255 (1971).

3.22 DEARDEN P and LONG R,
   "Soot formation in ethylene and propane diffusion flames".
   J Appl Chem 18, 243 (1968).

3.23 WRIGHT F J,
     "Effect of oxygen on the carbon-forming tendencies of diffusion flames".
     Fuel 53 (4) 232 (1974).

3.24 McLINTOCK I S,
     "The effect of various diluents on soot production in laminar ethylene diffusion flames".
     Combust Flame 12(3) 217 (1968).

3.25 MACFARLANE J J, HOLDERNESS F H and WHITCHER F S E,
     "Soot formation rates in premixed C_5 and C_6 hydrocarbon-air flames at pressures up to 20 atm".
     Combust Flame 8, 215 (1964).

3.26 SJÖGREN A,
     "Soot formation by combustion of an atomized liquid fuel".
     14th Symposium (International) on Combust 919,
     The Combustion Institute (1972).

3.27 SCHALLA R L, CLARK T P, and MCDONALD G E,
     "Formation and combustion of smoke in laminar flames".
     NACA Rept 1186 (1954).

3.28 HOLDERNESS F H and MACFARLANE J J,
     "Soot formation in rich kerosine flames at high pressures".
     AGARD-CP-125, Paper 18, (1973).

3.29 BONNE U and WAGNER H GG,
     "Reactions in rich hydrocarbon-oxygen flames"
     Ber. Bunsenges phys Chem 69, 35 (1965).

3.30 MACFARLANE J J and HOLDERNESS F H,
     "Laboratory studes of carbon formation in fuel-rich flames at high pressures"
     Proc I Mech E 184J, Pt 3, 57 (1969-70).

3.31 JENSEN D E,
     "Prediction of soot formation rates: a new approach".
     Proc Roy Soc A338, 375 (1974).

3.32 GARDINER W C et al,
     "Rate and mechanism of methane pyrolysis from 2000 to $2700^{\circ}K$"
     15th Symposium (International) on Combust 857,
     The Combustion Institute, (1974).

3.33 BOWMAN C T,
     "Non-equilibrium radical concentrations in shock-initiated methane oxidation."
     15th Symposium (International) on Combustion 869,
     The Combustion Institute (1974).

3.34 GOSLING A J, LAMPARD D and FUSSEY D E,
    " A shock tube study of the formation of carbon particles during
    the pyrolysis of hydrocarbons".
    Combust Inst European Symp. 388 (1973).

3.35 ATEN C F and GREENE E F,
    "The high temperature pyrolysis of acetylene at 1400-2500°K"
    Combust Flame 5, 55 (1961).

3.36 HOOKER W J,
    "Shock tube studies of acetylene"
    7th Symposium (International) on Combust 949
    The Combustion Institute (1959).

3.37 JONES D G,
    Unpublished data - University of Southampton (1975).

3.38 D'ALESSIO A et al,
    "Optical and chemical investigation of fuel-rich methane- oxygen
    flames at atmospheric pressure".
    14th Symposium (Internation) on Combust 941
    The Combustion Institute (1972).

3.39 HOWARD J B
    "On the mechanism of carbon formation in flames"
    12th Symposium (International) on Combustion 877,
    The Combustion Institute (1968).

3.40 PORTER G,
    "Carbon formation in the combustion wave".
    4th Symposium on Combust 248, (1952).

3.41 PRADO G and LAHAYE J,
    "Association of nuclei during carbon black formation in thermal
    systems".
    12th Bien Conf Carbon, Extended Abs, 41 (1975).

3.42 GRAHAM S C, HOMER J B and ROSENFELD J L J,
    "The formation and coagulation of soot aerosols generated by the
    pyrolysis of aromatic hydrocarbons".
    Proc Roy Soc A344, 259 (1975).

3.43 VIRK P S, CHAMBERS L E and WOEBCKE H N,
    "Thermal hydrogasification of aromatic compounds".
    Adv Chem, Srs 131, 237 (1973).

3.44 HOMANN K H and WAGNER H GG,
    "Some new aspects of the mechanism of carbon formation in premixed
    flames"
    11th Symposium (International) on Combust 371
    The Combustion Institute, (1966).

3.45 PLACE E R and WEINBERG F J,
      "The nucleation of flame carbon by ions and the effeect of electric
      fields"
      11th Symposium (International) on Combust 245
      The Combustion Institute (1966).

3.46 JESSEN P F and GAYDON A G,
      "Estimation of carbon radical concentrations in fuel-rich
      acetylene-oxygen flames by absorption spectroscopy."
      12th Symposium (International) on Combust 481,
      The Combustion Institute, (1968).

3.47 D'ALESSIO A et al,
      "Soot formation in methane-oxygen flames",
      15th Symposium (International) on Combust 1427
      The Combustion Institute (1974).

3.48 TESNER P A, SNEGIRIOVA T D and KNORRE V G,
      "Kinetics of dispersed carbon formation".
      Combust Flame 17, 253 (1971).

3.49 TESNER P A,
      "Formation of soot particles"
      Faraday Symp 7 (1973) p 104.

3.50 GILYAZETDINOV L P,
      "Kinetics of the formation of a carbon black aerosol on incomplete
      combustion of hydrocarbons"
      Russ J Phys Chem 44 (7) 1032, (1970).

3.51 GOSLING A J,
      "Smoke formation in gas turbine combustion chambers -
      shock tube studies of induction times".
      Ph D Thesis, Nottingham Univ., (1974).

3.52 TESNER P A,
      "Formation of dispersed carbon by thermal decomposition of
      hydrocarbons".
      7th Symposium (International) Combust 546
      The Combustion Institute (1959).

3.53 DUGWELL R and FOSTER P J,
      "Carbon formation from methane in combustion products".
      Carbon 11(5) 455, (1973).

3.54 MAGARIL R Z,
      "The formation of soot on a carbon surface".
      Russ J Phys Chem 48 (2) 280 (1974).

3.55 TESNER P A, ROBINOVITCH H J and RAFALKES I S,
"The formation of dispersed carbon in hydrocarbon diffusion flames"
8th Symposium (International on Combust 801,
The Combustion Institute (1961).

3.56 GILYAZETDINOV L P,
"The kinetics and formation mechanism of carbon black during the
thermal decomposition of hydrocarbons in the gas phase".
Khim Tverd Topl 3, 103 (1972)
C E Trans 6106.

3.57 NARASIMHAN K S and FOSTER P J,
"The rate of growth of soot in turbulent flow with combustion
products and methane".
10th Symposium (International) on Combustion 253
The Combustion Institute (1965).

3.58 FUCHS N A,
The mechanics of aerosols
Pergamon Press (1964).

3.59 FENIMORE C P and JONES G W
"Coagulation of soot to smoke in hydrocarbon flames"
Combustion Flame 13, 303 (1969).

3.60 GILYAZETDINOV L P
"Coagulation growth of soot aerosol particles"
Adv Aerosol Phys 7, 49 (1972).

3.61 SAMKHAN I I et al,
"Theory of formation of carbon black"
Kolloid Zhur 33 (6) 885 (1971)

3.62 GRAHAM S C and HOMER J B
"Coagulation of molten lead aerosols"
Faraday Symp 7, 85 (1973).

3.63 GRAHAM S C, HOMER J B and ROSENFELD J L J,
"Shock tube study of the formation and growth of soot particles"
2nd European Comb Symp 374 (1975).

3.64 ESSENHIGH R H, FROBERG R and HOWARD J B,
"Combustion behavious of small particles"
Ind Eng Chem 57 (9) 32 (1965).

3.65 PARK C and APPLETON J P
"Shock tube measurements of soot oxidation rates"
Combust Flame 20 (3) 369 (1973).

3.66 APPLETON J P
"Soot oxidation kinetics at combustion temperatures"
AGARD - CP - 125, Paper 20, (1973).

3.67 WRIGHT F J
"The oxidation of soot by O atoms"
15th Symposium (International) Combustion 1449
The Combustion Institute (1974).

3.68 NAGLE J and STRICKLAND - CONSTABLE R F
"Oxidation of carbon between 1000 and 2000ºC"
Proc 5th Carbon Conf 1, 154 (1962).

3.69 LEE K B and THRING M W and BEER J M,
"On the rate of combustion of soot in a laminar soot flame".
Combust Flame 6, 137 (1962).

3.70 FEUGIER A
"Soot oxidation in laminar hydrocarbon flames"
Combust Flame 19, 249 (1972).

3.71 FEUGIER A
"Soot oxidation in laminar hydrocarbon flames"
in "Heat Transfer in Flames" Ch 33 (1974)
Ed Afgan and Beer.

3.72 TESNER P A and TSIBULEVSKY A M
"Kinetics of dispersed carbon gasification in diffusion flames
of hydrocarbons.
Combust Flame 11, 227 (1967).

3.73 DONNET J B and DEMENDI J F
"Relative rates of gas-carbon reactions"
10th Bien Conf on Carbon Abs p 256 (1971)

3.74 GOLOVINA E S and SAMSONOV V G
"The effect of elevated pressures on reaction rate for $C + CO_2$
at high temperatures".
10th Bien Conf on Carbon, Abs 254 (1971)

3.75 FENIMORE C P and JONES G W
"Oxidation of soot by hydroxyl radicals"
J Phys Chem 71, 593 (1967).

3.76 ROSNER D E and ALLENDORF H D
"Comparative studies of the attack of pyrolytic and isotropic
graphite by atomic and molecular oxygen at high temperatures."
AIAA J 6, 650 (1968).

3.77 DALZELL W H, WILLIAMS G C and HOTTEL H C
" A light scattering method for soot concentration measurements"
Combust Flame 14, 161 (1970).

3.78 MAGNUSSEN B F
"An investigation into the behaviour of soot in a turbulent
free jet C_2H_2 - flame".
15th Symposium (International) on Combust 1415
The Combustion Institute (1974).

3.79 KHAN I M, GREEVES G and WANG C H T
"Factors affecting smoke and gaseous emissions from direct
injection engines and a method of calculation".
SAE 730 169 (1973).

3.80 KHAN I M, WANG C H T and LANGRIDGE B E
"Coagulation and combustion of soot particles in diesel engines".
Combust Flame 17, 409 (1971).

3.81 KHAN I M, GREEVES G and PROBERT D M,
"Prediction of soot and nitric oxide concentration in diesel
engine exhaust".
I Mech E Symp., Paper C142 (1971).

3.82 KHAN I M and GREEVES G
"A method for calculating the formation and combustion of soot in
diesel engines".
in 'Heat Transfer in Flames' ed Afgan and Beer, Ch 25 (1974).

3.83 British Standard B S AU 141a, (1971)
(see Construction and Use Regulation 25B, 1972).

3.84 ANDERTON D and DUGGAL V K
"Diesel Engine Emissions and Noise"
J Inst Fuel 49, 398 (1976)

3.85 ANDERTON D and DUGGAL V K,
"Effects of turbocharging on diesel engine Noise, Emissions
and Performance".
SAE Paper 750797 (1975).

4.1 LYN W T
"Study of burning rate and nature of combustion in diesel engines"
9th Symposium (International) on Combust 1069
The Combustion Institute (1963).

4.2 AUSTEN A E W and LYN W T
"Relation between fuel injection and heat release in a direct injection engine and the nature of the combustion processes"
Proc I Mech E (AD) 47 (1960-61).

4.3 WHITEHOUSE N D and WAY R J B
" A simple method for the calculation of heat release rates in diesel engines based on the fuel injection rate"
SAE Paper 710 134 (1971).

4.4 SHIPINSKI J, UYEHARA O A and MYERS P S
"Experimental correlation between rate of injection and rate of heat release in a diesel engine".
ASME Paper 68-DGP-11, (1968).

4.5 BASTRESS E K, CHNG K M and DIX D M
"Models of combustion and nitrogen oxide formation in direct and indirect injection compression - ignition engines"
SAE Paper 719053 (1971).

4.6 KHAN I M, GREEVES G and PROBERT D M
"Prediction of soot and nitric oxide concentrations in diesel engine exhaust."
I Mech E Symp Paper C142 (1971).

4.7 BACKHOUSE R J
"Factors affecting NO formation in a direct - injection diesel engine with a computer model."
MSc Thesis, Univ of Southampton (1973).

4.8 HODGETTS D and SHROFF H D
"More on the formation of nitric oxide in a diesel engine".
I Mech E Paper C95/75 (1975).

4.9 SHAHED S M, CHIU W S and LYN W T
"A mathematical model of diesel combustion"
I Mech E Paper C94/75 (1975).

4.10 BALUSWAMY N
"Spatial and temporal distribution of gaseous pullutants in a diesel engine combustion chamber"
Ph D Thesis, Univ of Manchester (1976).

4.11 WILSON R P, WALDMAN C H and MUZIO L J
"Foundation for modelling NOx and smoke formation in diesel flames"
CRC Report APRAC CAPE 20 71 1 (1974)

4.12 BASTRESS E K, CHNG K M, DIX D M and MURAD R J
    "Control of Nitrogen Oxide emissions from diesel engines:
    A theoretical analysis"
    NREC Report No 1160-1   June 1971.

 4.13 TSAO K C, MYERS P S and UYEHARA O A,
    "Gas temperature during compression in motored and fired diesel engines"
    SAE Trans 70, 136 (1962).

4.14 LAVOIE G A, HEYWOOD J B and KECK J C
    "Experimental and theoretical study of nitric oxide formation in
    internal combustion engines".
    Comb Sci & Technol 1, 313 (1970).

4.15 BENNETHUM J E, MATTAVI J N and TOEPEL R R
    "Diesel combustion chamber sampling - hardware, procedures and data
    interpretation."
    SAE 750849 (1975).

4.16 KHAN I M, GREEVES G and WANG C H T,
    "Factors affecting smoke and gaseous emissions from direct
    injection engines and a method of calculation".
    SAE Paper 730169 (1973).

4.17 KHAN I M, WANG C H T and LANGRIDGE B E
    "Coagulation and combustion of soot particles in diesel engines".
    Combust Flame 17, 409 (1971).

4.18 KHAN I M and GREEVES G
    "A method for calculating the formation and combustion of soot in
    diesel engines".
    in 'Heat Transfer in Flames' ed Afgan N H Ch 25 (1974).

4.19 GRIGG H C and SYED M H
    "The problems of predicting rate of heat release in diesel engines".
    Proc I Mech E 184 (3J) 192 (1969-70).

4.20 SCHWEITZER P H
    "Oil sprays"
    Auto Engr   61-64 (1938).

4.21 VICKLAND C W et al
    "A consideration of the high temperature thermodynamics of internal
    combustion engines"
    in SAE Progress in Technology 7, 1(1964).

4.22 LEE K B, THRING M W and BEER J M
"On the rate of combustion of soot in a laminar soot flame"
Combust Flame 6, 137 (1962).

4.23 RAINE R R,
Ph D Thesis, University of Southampton (to be published)

4.24 FLETCHER R S
"The prediction of nitric oxide formation in combustion systems."
Comb Inst Europ Symp 445 (1973).

4.25 NAGLE J and STRICKLAND-CONSTABLE R F
"Oxidation of carbon between 1000 and $2000^{\circ}C$".
Proc 5th Carbon Conf 1, 154 (1962).

4.26 APPLETON J P
"Soot oxidation kinetics at combustion temperatures".
AGARD CP-125 Paper 20 (1973).

4.27 GONZALEZ J M
"A study of nitric oxide and its decomposition during diesel engine
combustion".
MSc Thesis, University of Southampton (1975).

4.28 BAULCH D L et al
"Critical evaluation of rate data for homogeneous gas phase reactions
of interest in high temperature systems".
Rept No 4 Dept Phys Chem, Leeds Univ (1969).

4.29 CHIU W S, SHAHED S M and LYN W T
"A transient spray mixing model for Diesel combustion".
SAE Paper 760128 (1976).

4.30 BEER J M and CHIGIER N A
"Combustion Aerodynamics"
App Sci Pub (1972).

4.31 ANNAND W J D
"Heat transfer in the cylinders of reciprocating internal
combustion engines"
Proc I Mech E 177 (36) 973 (1963).

4.32 WHITEHOUSE N D and SAREEN B K
"Prediction of heat release in a quiescent chamber diesel engine
allowing for fuel/air mixing".
SAE Paper 740084 (1974).

4.33 ABRAMOVICH G N
     "The Theory of Turbulent Jets"
     M I T Press (1963).

4.34 BARUAH P C
     "A generalised computer programme for internal combustion
     engines including gas exhange systems".
     Ph D Thesis UMIST (1973).

5.1 KAU C J, HEAP M P, TYSON T J and WILSON R P
     "The prediction of nitric oxide formation in a direct injection
     diesel engine".
     16th Symposium (International) on Combustion , 1976
     The Combustion Institute, in press.

5.2 SHAHED S M, CHIU W S and LYN W T
     "A mathematical model of diesel combustion"
     I Mech E Paper C94/75 (1975)

5.3 HADGETSS D and SHROFF H D
     "More on the formation of nitric oxide in a diesel engine"
     I Mech E Paper C95/75 (1975)

5.4 BASTRESS E K, CHNG K M and DIX D M,
     "Models of combustion and nitrogen oxide formation in direct and
     indirect injection compression - ignition engines"
     SAE Paper 719053 (1971).

5.5 HIROYASU H and KADOTA T,
     "Models for combustion and formation of nitric oxide and soot in direct
     injection diesel engines"
     SAE Paper 760129 (1976).

5.6 RAINE R R
     "A modelling study of soot and NO formation in diesel engines"
     Ph D Thesis, University of Southampton (1977)

5.7 ABRAMOVICH G N
     The theory of turbulent jets
     MIT Press (1963)

5.8 KHAN I M, GREEVES G and WANG C H T,
     "Factors affecting smoke and gaseous emissions from direct
     injection engines and a method of calculation"
     SAE Paper 730169, (1973)

5.9 LAVOIE G A AND BLUMBERG P N
     "Measurement of NO emissions from a Stratified Charge engine:
     comparison of theory and experiment"
     Combust Sci Technol 8 25-37 (1973)

5.10 HEYWOOD J B,
"Pollutant formation and control in spark-ignition engines"
Prog Energy Combust Sci 1, 135-164 (1976)

5.11 LUDWIG D E, BRACCO F V and HARRJE D T,
"Nitric oxide and composition measurements within diffusion flames
around simulated ethanol and ethanol-pyridine droplets"
Combust Flame 25, 107-120 (1975)

5.12 SCHEFER R W, and SAWYER R F,
"Lean premixed recirulating flow combustion for control of oxides
of nitrogen"
16th Symposium (International) on Combustion, 1976
The Combustion Institute, in press

5.13 LAURENDEAU N M,
"Fast nitrogen dioxide reactions; significance during NO
decomposition and NO_2 formation".
Combust Sci Technol 11, 89-96 (1975)

5.14 JENSEN D E,
"Prediction of soot formation rates: a new approach"
Proc Roy Soc A 338, 375 (1974)

5.15 GILYAZETDINOV L P,
"Coagulation growth of soot acrosol particles"
Adv Aerosol Phys 1, 49 (1972)

5.16 PRADO G P, FLAGAN R C and HOWARD J B,
"Soot and hydrocarbons formation in a turbulent diffusion flame"
16th Symposium (International) on Combustion 1976
The Combustion Institute, in press

5.17 BECKER H A and YAMAZAKI S
"Soot concentration field of turbulent propane/air diffusion flames"
16th Symposium (International) on Combustion, 1976
The Combustion Institute, in press

5.18 SPALDING D B,
"Mathematical models of turbulent flames: a review"
Imp Coll Sci Tech Report HTS/75/1, 1975

5.19 GRIFFEN M D, ANDERSON J D, AND DIWAKER R,
"Navier-Stokes solutions of the flowfield in an internal combustion
engine"
AIAA Paper 76-403 (1976)

5.20 GOSLING A J
"Smoke formation in gas turbine combustion chambers -
shock tube studies of induction times"
PH D Thesis, Nottingham University, 1974

APPENDIX I

NITRIC OXIDE CHEMISTRY EMPLOYED IN VARIOUS DIESEL COMBUSTION MODELS

Ia) BASTRESS, CHNG AND DIX

From Fletcher, R.S. and Heywood, J.B (A1AA, 71 - 123).

$$N + NO \rightleftharpoons N_2 + O \qquad (1)$$

$$N + O_2 \rightleftharpoons NO + O \qquad (2)$$

$$N + OH \rightleftharpoons NO + H \qquad (3)$$

$$H + N_2O \rightleftharpoons N_2 + OH \qquad (4)$$

$$O + N_2O \rightleftharpoons N_2 + O_2 \qquad (5)$$

$$O + N_2O \rightleftharpoons NO + NO \qquad (6)$$

This scheme was reduced to (for the mass fraction of NO)

$$\frac{d(NO)}{dt} = \frac{2M_{NO}}{\rho} (1 - \alpha^2) \left[\frac{R_1}{1+\alpha K_1} + \frac{R_6}{1+K_2} \right] ,$$

on the assumption that the species O, O_2, OH, H and N_2 are in equilibrium in the post flame gases; and that N is at steady state.

$$M_{NO} = \text{molecular wt. of NO}$$

$$\rho = \text{gas density}$$

$$\alpha = [NO]/[NO]_e$$

$$R_1 = k_1 [N]_e \cdot [NO]_e \qquad [\ ] \sim \text{concentration in molecules per unit volume.}$$

$$k_1 = \text{forward rate constant for reaction (1)}$$

$$K_1 = R_1/(R_2 + R_3)$$

$$R_6 = k_6 [O]_e [N_2O]_e$$

$$K_2 = R_6/(R_4 + R_5)$$

Rates $k_1 - k_6$ from established sources.

Ib) KHAN ET AL. (SAE. 730169)

Considered extended Zeldovich mechanism but then dismissed

$$N_2 + O \rightleftharpoons NO + O \qquad (1)$$

$$O_2 + N \rightleftharpoons NO + O \qquad (2)$$

$$OH + N \rightleftharpoons NO + H \qquad (3)$$

reaction (3). Using assumptions about equilibrium and steady state, and also assuming that lean mixtures are being considered, reduced NO production rate to

$$\frac{d[NO]}{dt} = \frac{P}{41.0T} k_1 [N_2] [O] \left(1 - \frac{[NO]^2}{[NO]_e^2}\right)$$

Then introduced $k_1 = 7.30 \times 10^{14} \exp(-75,400/RT)$ compared to the then accepted literature value of $k_1 = 1.36 \times 10^{14} \exp(-75,400/RT)$.

Ic) SHAHED ET AL. (1973)

Considered Zeldovich Mechanism

$$N_2 + O \rightleftharpoons NO + N \qquad (1)$$

$$N + O_2 \rightleftharpoons NO + O \qquad (2)$$
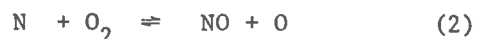
Assumed that for stocihiometric composition of a fuel-air package, the mole fractions of O_2 and N_2 may be considered constant over the range of temperatures and pressures of interest. The two rates can be simplified ... and all constants lumped together to obtain:

$$\frac{1}{V} \frac{d(NO)V}{dt} = A_3 \exp(-E/RT) \frac{P^{3/2}}{T^2} \left(1 - \frac{(NO)}{(NO)_e}\right)$$

The values of A_3 and E were determined by fitting experimental emissions to those calculated but were not given in the reference.

Id) HODGETTS AND SHROFF (1975)

Identical to Bastress et al.

I e) SHAHED ET AL. (1975)

Used

$$N_2 + O \rightleftharpoons NO + N \qquad (1)$$

$$O_2 + N \rightleftharpoons NO + O \qquad (2)$$

with all species other than NO in local equilibrium.
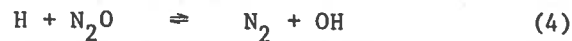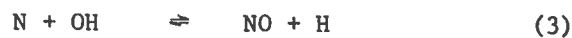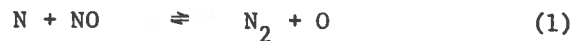
Also considered

$$N + OH \rightleftharpoons NO + H \qquad (3)$$

Tested "the various schemes with a simple NO kinetics program". "A range of representative isothermal, isobaric and constant F/A ratio conditions were used. It was found that assumptions of equilibrium or steady state N atoms made little difference".

Reaction rate constants from Schofield. "However, it was found that slightly better correlation obtained by increasing reverse rate constants by a factor of two". (Thought to compensate for heat transfer model used).

If) BALUSWAMY (1976) UMIST Ph.D.

$$N + NO \rightleftharpoons N_2 + O \qquad (1)$$

$$N + O_2 \rightleftharpoons NO + O \qquad (2)$$

$$N + OH \rightleftharpoons NO + H \qquad (3)$$

$$H + N_2O \rightleftharpoons N_2 + OH \qquad (4)$$

$$O + N_2O \rightleftharpoons N_2 + O_2 \qquad (5)$$

$$O + N_2O \rightleftharpoons NO + NO \qquad (6)$$

$$N_2O + M \rightleftharpoons N_2 + O + M \qquad (7)$$

Assumes H, OH, O, O_2 and N_2 in equilibrium.

Assumes N and N_2O at a steady state; $\dfrac{d[N]}{dt} = 0,\quad \dfrac{d[N_2O]}{dt} = 0$

Reduces to $\dfrac{1}{V}\dfrac{d}{dt}((NO)V) = 2(1-\alpha_e)^2 \left[\dfrac{R_1}{1+\alpha_e \cdot \dfrac{R_1}{R_2+R_3}} + \dfrac{R_6}{1+\dfrac{R_6}{R_4+R_5+R_7}} \right]$

Rates from Baruah (U.MIST Ph.D. (1973)

$$k_{1f} = 3.1 \times 10^{10} \exp(-160/T)$$

$$k_{2f} = 6.4 \times 10^6 \, T. \, \exp(-3125/T)$$

A. 3

$$k_3 = 4.2 \times 10^{10}$$

$$k_4 = 3.0 \times 10^{10} \exp(-5350/T)$$

$$k_5 = 3.2 \times 10^{12} \exp(-18900/T)$$

$$k_6 = k_5$$

$$k_7 = 10^{12} \exp(-30500/T)$$

All rates given in m^3/kg/mole.sec.

<u>Ig)</u> BACKHOUSE (incorporated by RAINE).

$$N_2 + O \rightleftharpoons NO + N \qquad (1)$$

$$O_2 + N \rightleftharpoons NO + O \qquad (2)$$

$$N + OH \rightleftharpoons NO + H \qquad (3)$$

Reduces to

$$\frac{d(NO)}{dt} = \frac{2M_{NO}}{p} (1 - \alpha^2) \cdot \frac{R_1}{1 - \alpha K_1}$$

Using rates $k_1 - k_3$ from Fletcher and Heywood.   See Ia for symbols.

<u>I$_h$) HIROYASU AND KADOTA (Hiroshima) SAE 760129</u>

Extended Zeldovich mechanism applied to combustion products of 400 <u>isolated</u> packages of fuel/air mixture each having a different temperature and temperature history.

<u>I$_i$) KAU, HEAP, TYSON AND WILSON 1976 (16th Combustion Symposium)</u>

Zeldovich mechanism, equilibrium radical concentration. Premixed pockets or droplet diffusion flames. Includes an analysis which treats the formation of NO in a confined spherical diffusion flame in a continuously variable environment.

ANNOTATED BIBLIOGRAPHY OF OTHER DIESEL

EMISSIONS MODELS

1.   BRACCO, F. V.

A theoretical model for Diesel combustion.

Paper No. WSCI 71-29, Comb. Inst. Central States Spring Meeting (1971)

No details of this model are known to the present author, but it
is believed to be based upon single droplet combustion.

2.   SHAHED, S. M., CHIU, W. S. and YUMLU, V. S.

A preliminary model for the formation of nitric oxide in direct
injection Diesel engines and its application in parametric studies.

SAE Paper 730083 (1973)

A heat release rate is simulated from a knowledge of the rate of fuel
injection. A fuel-air package is identified with each crank-angle
increment during the heat release period, of stoichiometric composition,
and containing sufficient fuel to account for the incremental heat
release. The package is assumed to reach the adiabatic flame temperature
and the subsequent temperature history is calculated from a burned gas
polytropic relationship. The post-combustion packages do not mix.
Nitric oxide formation is modelled in the post-combustion packages by
a simplified Arrhenius equation.

This model has been superseded by the model of Shahed, Chiu and Lyn
(1975) reviewed in detail in this report (Section 4).

3.   CAKIR, H.

Nitric oxide formation in Diesel engines.

Proc. I. Mech. E. 188 paper 46 (1974)

An 'experimental' heat release (mass fraction of fuel burnt) is
calculated from the experimental pressure-time diagram and engine
parameters. The air-fuel ratio of combusting elements is allowed
to vary during the cycle, according to an empirical equation. Nitric
oxide formation is assumed to occur by the Zeldovich mechanism in the
burnt elements.

4.   PACHERNEGG, S. J.

Efficient and clean Diesel combustion

SAE 750787 (1975)

A simplified model which attempts to correlate the squared mean
temperature profile of the cycle, integrated above a threshold
temperature, with NO_x emissions. This correlation is then used
to evaluate the effects of parameters like compression ratio,
ignition timing and heat release rate on emissions.

5.   NIGHTINGALE, D. R.

Fundamental investigation into the problem of nitric oxide for-
mation in Diesel engines.

SAE 750848 (1975)

A single zone (homogeneous) combustion model (Whitehouse and Way)
is used to generate a heat release diagram and cylinder pressure
diagram. The heat release diagram is then used to determine the
mass of stoichiometric elements involved in combustion at any crank
angle increment (as Backhouse, Section 4). Post-combustion elements
do not mix with fresh air or with other elements, and their temperature
is assumed to change only due to adiabatic compression or expansion.

6.   HIROYASU, H. and KADOTA

Models for combustion and formation of nitric oxide and soot in
direct injection Diesel engines.

SAE 760129 (1976)

A 'comprehensive' combustion and emissions model, received too late
for a detailed review. 'Macromixing' is based on an empirical jet
penetration equation and an entrainment rate determined from photo-
graphic observations. 'Micromixing' is based on single droplet
vaporisation. The jet is divided into many (400) fuel/air packages.
During heat release, the cylinder pressure is determined by assuming
that the cylinder contents can be described by a mean C_p and C_v.
Nitric oxide formation is described by a three equation, extended
Zeldovich mechanism. Soot formation and oxidation is described by
Arrhenius equations, with constants determined by matching calculations
to experiments (values of the pre-exponential factors are not given).

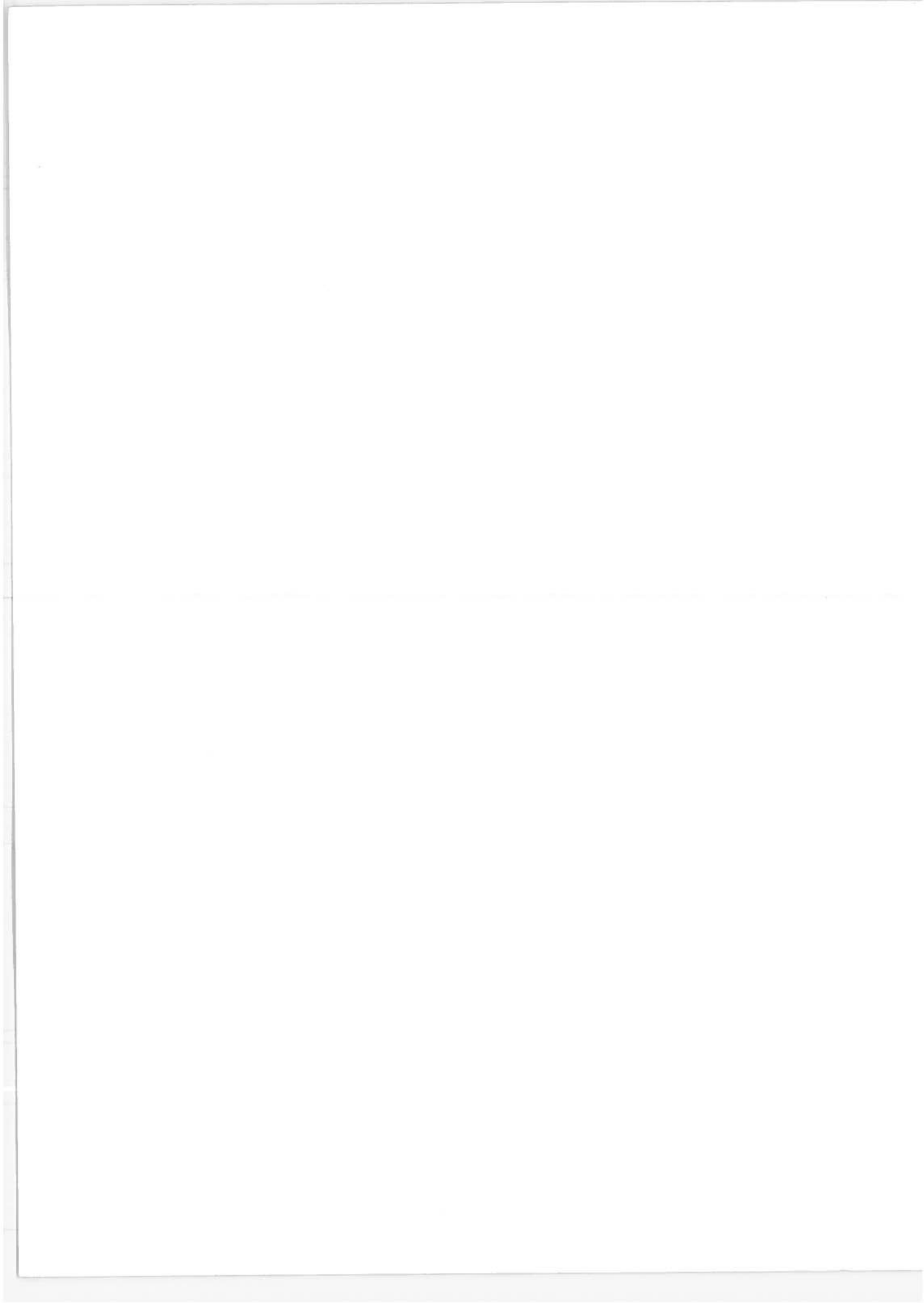7.   KAU, C. J., HEAP, M. P., TYSON, T. J. and WILSON, R. P.

The prediction of nitric oxide formation in a direct injection Diesel engine.

16th Combustion Symposium (1976)

A five-zone model incorporating a mixing description similar to that of Hiroyusa and Kadota (1976). NO production calculated using the Zeldovich mechanism applied to equilibrium combustion products in either premixed products, droplet diffusion flames or homogeneous mixing zones.

APPENDIX III

REPORT OF INVENTIONS

A diligent review of the work performed under this contract has revealed no innovations, discoveries, or inventions at this time. In addition, all methodologies employed are available in the open literature. However, improvements are provided for modeling of diesel NOx and smoke emissions in the area of a) chemical kinetic processes, b) incylinder experimental sampling techniques, and c) fundamental data acquisition.